

HYDROLOGIC ANALYSIS OF A STEEP FORESTED WATERSHED USING
SPATIALLY DISTRIBUTED MEASUREMENTS OF SOIL MOISTURE
AND SOIL INFILTRATION PROPERTIES

by

Gregory Charles Loscher

A thesis submitted in partial fulfillment
of the requirements for the degree

of

MASTER OF SCIENCE

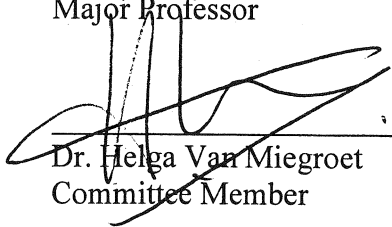
in

Civil and Environmental Engineering

Approved:



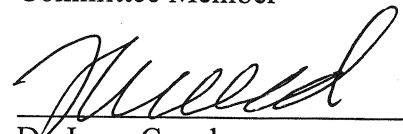
Dr. David G Tarboton
Major Professor



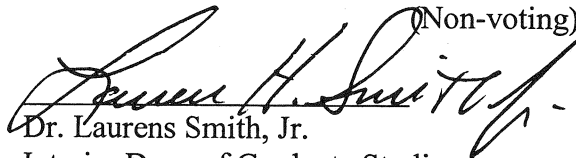
Dr. Helga Van Miegroet
Committee Member



Dr. David Chandler
Committee Member



Dr. Irena Creed
Committee Member
(Non-voting)



Dr. Laurens Smith, Jr.
Interim Dean of Graduate Studies

UTAH STATE UNIVERSITY
Logan, Utah

2006

ABSTRACT

Hydrologic Analysis of a Steep Forested Watershed Using
Spatially Distributed Measurements of Soil Moisture
and Soil Infiltration Properties

by

Gregory Charles Loscher, Master of Science

Utah State University, 2006

Major Professor: Dr. David Tarboton
Department: Civil and Environmental Engineering

A primary determining factor in watershed runoff response to rainfall is the storage of water in the soil. In engineering practice the storage of water is generally estimated empirically, due to the high degree of spatial and temporal variability associated with watershed soil moisture. The purpose of this work was to explore practical methods for soil moisture measurement and to contribute generally to an improved understanding of steep, forested, hillslope hydrologic processes.

Soil volumetric water content (VWC), both across the watershed and along the depth of the soil profile, was measured at 66 sites on six sampling occasions over a 4-month period in a 17-ha watershed. The temporal variation of VWC was measured at hourly intervals at three locations in the watershed. Soil saturated hydraulic conductivity, soil depth, and soil porosity were measured at 51 sites across the watershed. Results showed that the shallow soil moisture profile (top 30 - 40 cm) remained at or near

saturation at the base (~ 40 cm), with soil moisture above this level pivoting about this value retaining an approximately linear profile during wetting and drying cycles.

Watershed topography was not found to be a significant factor in the distribution of soil moisture. The stormflow portion of the stream hydrograph appeared to result from flow along the soil-bedrock interface with response times on the scale of hours to days, while the baseflow portion of the stream hydrograph appeared to result from soil matrix drainage with response times on the scale of weeks to months.

Soil VWC and soil depth measurements were combined to form synoptic estimates of the spatial distribution of soil water storage that were used to convert hourly changes in soil water storage, to an hourly record of estimated watershed soil water storage that could be compared to a water balance based on precipitation, streamflow, and evapotranspiration.

Finally, the VWC measurement sites were analyzed for temporal stability to evaluate potential single site surrogacy for average watershed soil moisture conditions. A linear relationship between measurements of VWC at one of the continuously monitored sites and the six synoptic estimates of watershed average soil water storage obtained from sampling 66 sites was used to estimate hourly changes in watershed soil water storage. For wet periods, the result compared well with hourly changes in watershed soil water storage estimated from the water balance, noting that the calculated evapotranspiration used in the water balance was likely overestimated during dry periods.

ACKNOWLEDGMENTS

I would like to thank Dr. David Tarboton for his support and guidance throughout the research and writing process associated with the completion of this work. I am particularly grateful for his patient encouragement during prolonged periods of slow writing progress.

I am also grateful to Dr. Helga Van Miegroet for providing a prospective engineer with a unique opportunity to work in and to gain a greater appreciation for the beautiful Great Smoky Mountains. I have never regretted the time I spent in the Southern Appalachians, nor the increased awareness of the merits of environmental preservation that it provided me.

I would also like to thank Dr. Irena Creed, Dr. Dani Or, Dr. David Chandler, Dr. Upmanu Lall, and Dr. Rodger Grayson for their insights and contributions to the direction and content of this work.

Further thanks to the USDA and USGS for the grants that funded this work; to Dr. Niki Nicholas, for her support of research efforts in the Noland Divide Watershed; to John Schubzda and Dr. James Smoot for providing access to streamflow data; and to the National Park Service for providing access to and use of facilities and data.

I am especially grateful to my parents for their continued support and for instilling in me a desire for education and a love for learning.

Finally, I would like to thank my wife, Nicole, for her faith in me and continued support and encouragement during the completion of this work, the pace and duration of which would have taxed the mettle of Job.

Gregory C. Loscher

CONTENTS

v

	Page
ABSTRACT.....	ii
ACKNOWLEDGMENTS	iv
LIST OF TABLES.....	viii
LIST OF FIGURES	ix
CHAPTER	
1. INTRODUCTION	1
2. LITERATURE REVIEW	6
Hillslope Hydrology.....	6
Conceptual hydrologic response mechanisms	7
Mathematical hillslope hydrologic models.....	8
Soil Hydrologic Data Collection Methods.....	10
Soil matrix hydrologic properties	10
Soil moisture data collection.....	14
Watershed Water Balance.....	16
Optimization of Field Data Collection Efforts.....	19
Watershed Nutrient Cycling	20
3. FIELD SITE AND DATA COLLECTION.....	23
Topographical and Meteorological Data	24
Topographical data.....	24
Streamflow data	26
Meteorological data: Clingman’s Dome.....	27
Meteorological data: Noland Divide Watershed.....	30
Soil Hydrologic Data Collected During the 1999 Summer Field Study Period.....	33
Soil saturated hydraulic conductivity.....	36

	vi
Soil depth	42
Soil porosity	43
Soil moisture monitoring	46
Continuous soil moisture monitoring.....	47
Biweekly soil moisture mapping	55
4. DATA ANALYSIS AND RESULTS.....	70
Noland Divide Watershed Delineation	71
Watershed delineation based on topographic data.....	71
Drainage culverts crossing the highway	74
Discussion of northeast and southwest subbasin delineation results	78
Spatial Distribution of Hydrologic Parameters.....	80
Soil saturated hydraulic conductivity.....	81
Soil porosity	83
Soil depth	85
Potential soil water storage	85
Spatial Distribution of Soil Moisture.....	87
Spatial distribution of degree of soil saturation	93
Watershed soil water storage	94
Potential relationships between soil hydrologic parameters and soil moisture.....	98
Variation of Soil Moisture with Depth	102
Water Balance for Noland Divide Watershed	106
Precipitation	106
Streamflow	107
Evapotranspiration	107
Soil water storage changes.....	108
Soil water residence time	111
Temporal Variation in Soil Moisture.....	114
Relationship Between Soil Moisture and Streamflow	127
5. SUMMARY AND CONCLUSIONS	130
Conceptual Understanding of NDW Hydrology.....	130
Quantitative Description of NDW Hydrology.....	131

	vii
Methods of Measurement and Analysis.....	133
Potential for using Point Measurement to Represent Average Watershed Soil Moisture Conditions.....	134
REFERENCES	137
APPENDICES	143
Appendix A : Available Digital Streamflow Data for the NDW – 1991 to 1999	144
Appendix B : Method for Conversion of Analog Streamflow Data to Digital Streamflow Data for NDW Stream Gages.....	146
Appendix C : Guelph Permeameter C-Factor Based on Soil Type.....	150
Appendix D : Rainfall and Total Streamflow Records for NDW for May through October 1999	152
Appendix E : Description of Portable Soil Moisture Probe Laboratory Calibration Using NDW Soils	154
Appendix F : Statistical Comparison of Portable Probe, Static Probe and Gravimetric Measurements of Volumetric Water Content.....	157
Appendix G : Scatter Plots of Biweekly Soil Moisture Measurements versus Various Soil Hydrologic Parameters	161
Appendix H : Representative Biweekly Measurement Site Soil Moisture Profiles	164
Appendix I : Comparison of Estimated Evapotranspiration and Evapotranspiration Derived from NDW Water Balance	167
Appendix J : Cumulative Rainfall, Streamflow, Evapotranspiration and Soil Water Storage Changes for the NDW for May to October 1999	169
Appendix K : Streamflow Hydrographs for Selected NDW Storm Events During the May through October 1999 Study Period.....	171

LIST OF TABLES

Table		Page
2.1	Soil matrix properties pertinent to hillslope hydrology	11
3.1	List of topographical and meteorological data sources.....	25
3.2	Noland Divide Watershed climate station data.....	28
3.3	Clingman's Dome climate station data	30
3.4	Field rain gage calibration	32
3.5	Field data collected during summer 1999.....	34
3.6	Soil hydrological parameter data collected during the 1999 field season	40
3.7	Soil depth measurements at plot F5600	42
3.8	Bulk density estimation for plot F5600 soil samples.....	45
3.9	Continuous soil moisture monitoring sites	49
3.10	Weather conditions during biweekly soil moisture measurements.....	62
3.11	Biweekly soil volumetric water content averages by site.....	66
4.1	Summary of results for NDW drainage basin delineation	79
4.2	Sample line volumetric water content averages on six sampling occasions.....	92
4.3	Watershed average soil water storage.....	98
4.4	Potential relationships between soil hydrologic parameters..... and soil volumetric water content investigated for the NDW	99
4.5	Standard deviation of volumetric water content measurements by depth	104
4.6	Water balance results for the NDW	109
4.7	Approximate soil water residence times for the NDW	113
4.8	Results of CASMM analysis for NDW	117
4.9	Soil effective depth estimates used to approximate continuous soil water..... storage records for Pits #1, #2, and #3	123

LIST OF FIGURES

Figure	Page
1.1 NDW location map	2
3.1 Southwest and northeast weir stream gages.....	27
3.2 NDW 1999 field rain gage.....	31
3.3 NDW field rain gage versus CD weather station hourly precipitation	33
3.4 Soil hydrologic parameter sampling sites	35
3.5 Photographs of NDW field permeameter test.....	39
3.6 Soil moisture monitoring locations.....	48
3.7 Continuous soil moisture monitoring pit installation (Pit #2)	49
3.8 Continuous soil moisture monitoring Pits #1, #2 , and #3 , one month after installation	51
3.9 Time series plot of soil moisture at Pit #1	52
3.10 Time series plot of soil moisture at Pit #2	53
3.11 Time series plot of soil moisture at Pit #3	53
3.12 Determination of a_0 and a_1 using field and lab calibrations.....	59
3.13 Calibration of portable impedance probe for NDW	60
3.14 Portable Theta probe access tube schematic.....	61
3.15 Typical biweekly soil moisture sampling site.....	64
4.1 D8 watershed delineation for the NDW.....	74
4.2 D_{∞} watershed delineation for the NDW.....	75
4.3 Dependence function watershed delineation for the NDW	75
4.4 D8 watershed delineation for the NDW (revised for highway drainage culverts)	76

4.5	D ∞ watershed delineation for the NDW (revised for highway drainage culverts)	76
4.6	Dependence function watershed delineation for the NDW (revised for highway drainage culverts)	77
4.7	Manual watershed delineation for the NDW using contours generated from topographic survey	77
4.8	Manual watershed delineation for the NDW using USGS quadrangle map.....	78
4.9	Estimated spatial distribution of soil saturated hydraulic conductivity	82
4.10	Estimated spatial distribution of natural log of soil saturated hydraulic conductivity.....	83
4.11	Estimated spatial distribution of soil porosity	84
4.12	Estimated spatial distribution of soil porosity (adjusted for soil organic content)	84
4.13	Estimated spatial distribution of soil depth.....	86
4.14	Estimated spatial distribution of potential soil water storage	86
4.15	Estimated spatial distribution of volumetric water content for June 3, 1999	89
4.16	Estimated spatial distribution of volumetric water content for June 16, 1999	89
4.17	Estimated spatial distribution of volumetric water content for June 30, 1999	90
4.18	Estimated spatial distribution of volumetric water content for July 14, 1999	90
4.19	Estimated spatial distribution of volumetric water content for July 28, 1999	91
4.20	Estimated spatial distribution of volumetric water content for Oct 2, 1999.....	91
4.21	Estimated watershed degree of saturation pattern for June 3, 1999	95
4.22	Estimated watershed degree of saturation pattern for June 16, 1999	95
4.23	Estimated watershed degree of saturation pattern for June 30, 1999	96
4.24	Estimated watershed degree of saturation pattern for July 14, 1999	96

		xi
4.25	Estimated watershed degree of saturation pattern for July 28, 1999	97
4.26	Estimated watershed degree of saturation pattern for October 2, 1999	97
4.27	NDW elevation versus volumetric water content	102
4.28	Average soil moisture profiles for the NDW	103
4.29	Results of CASMM analysis for the NDW.....	116
4.30	Potential CASMM sites for the NDW	120
4.31	Pit volumetric water content versus estimated watershed soil water storage	121
4.32	Estimated hourly soil water storage record for the NDW.....	124
4.33	Cumulative plot of soil water storage predicted using volumetric water content measured as Pit #2	126
4.34	Plot of Pit #2 volumetric water content versus total streamflow for the NDW	128

CHAPTER 1

BACKGROUND AND INTRODUCTION

The Noland Divide Watershed (NDW) is a 17 hectare experimental watershed located in the Great Smoky Mountains National Park on the Tennessee-North Carolina border (see Figure 1.1). The climate in the area is temperate, with average annual rainfall of approximately 210 cm, and temperatures ranging from -8 °C to 18 °C. For the past decade, this research site has served as the basis for studies involving spruce-fir forest ecosystem processing of nutrient inputs. Industry and automobiles in the region are believed to be factors in high atmospheric deposition rates of nitrogen and sulfur, both sources of acid rain. In general, such nutrient inputs may be partially buffered by forest ecosystem processes, particularly nitrogen uptake by plants. High acid rain deposition common to the Tennessee Valley region, however, has precipitated questions as to the ability of such watersheds to buffer large nutrient quantities, as well as the effects of nutrient saturation on sensitive high-elevation forest ecosystems. Since the primary transport mechanism for these nutrients is water, an understanding of the hydrologic processes which govern the flux of water through an ecosystem is central to any attempt at analyzing nutrient cycling in and export from forested watersheds.

A hydrologic analysis of the NDW presents an interesting challenge, since the conceptual and mathematical constructs which govern the translation of rainfall into soil water storage and stream runoff are for steep, forested watersheds are still evolving and are not universally agreed upon. Technological advances in measurement techniques in recent years provide encouraging opportunities for more detailed and comprehensive collection of hydrologic data, which should contribute to improved conceptual and

eventually mathematical understanding of watershed hydrology.

The overall purpose of the work described here was to understand the hydrologic processes at work in the NDW through analysis of field data, and from this understanding contribute to knowledge of soil hydrologic processes in Southern Appalachian high-elevation spruce-fir forest ecosystems.

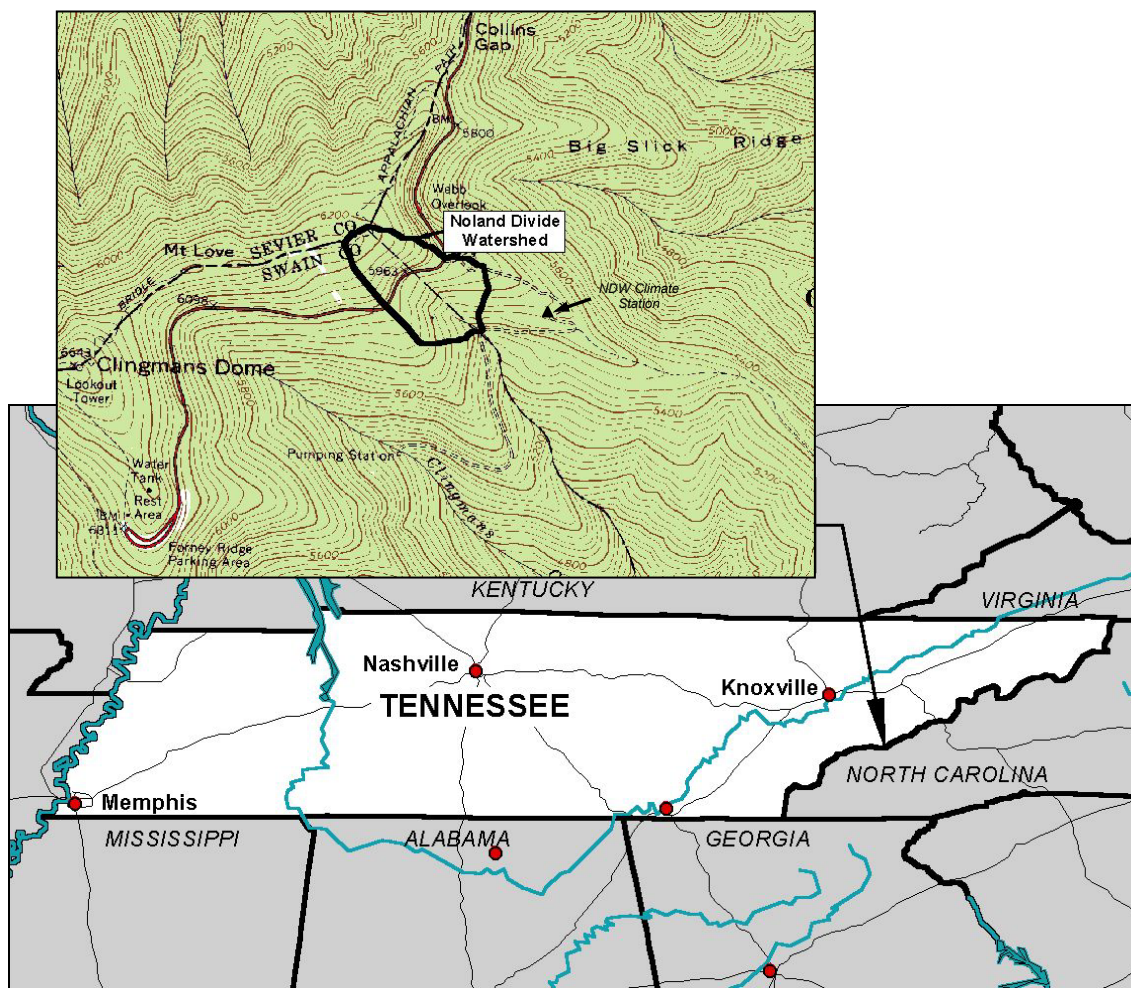


Figure 1.1. NDW location map.

Hydrologic data collection and analysis were undertaken for the NDW with the following objectives:

1. Collect, measure, and assemble a comprehensive hydrologic data set for a three-month field season in the NDW, including all major hydrologic elements and soil properties pertinent to hydrology
2. Complete a water (mass) balance for the field season
3. Identify general spatial patterns and apparent response mechanisms evident in the translation of rainfall to streamflow in the NDW
4. Examine opportunities for optimizing future hydrologic data collection efforts
5. Provide a hydrologic basis for present and future nutrient cycling research conducted by others.

The choice of the first four of these objectives is rooted in the often-discussed gap between scientific hydrology and applied hydrology. Reasons for this gap have been postulated to result, among other factors, from the tendency toward development of increasingly sophisticated computer models that are “inaccessible to the practitioner” (Delleur, 1971). While computer technology and layman savvy have come a long way since this observation was made, the gap between the state of the art in hydrology and the state of the practice has persisted, as evidenced by ongoing attempts at introducing the practicing engineer to computer model alternatives for widely-used empirical methods of hydrologic analysis (Garbrecht et al., 2001). The divide between science and practice has historically been exacerbated by difficulties associated with collecting detailed hydrologic data. To avoid confronting these hurdles, civil engineers often rely on the century-old rational method, or lumped parameter methods requiring minimal data such

as the SCS (Soil Conservation Service) curve number method. Referring to hydrological modeling research and practice in general, one hydrologist has described hydrology as plagued by “a glut of hope and a shortage of skepticism,” relying too much on faith when technological advances in measurement techniques have made “real evidence observable and measurable” (Philip, 1992). Simply stated, advances in modeling have “outstripped equivalent progress in field measurement and observation” (O’Loughlin, 1990).

It would seem that a concerted effort is warranted to assemble a foundation of detailed hydrologic data for testing existing models and for developing future models (Anderson and Burt, 1990a). Recent advances in this vein include the establishment in 2001 of the Consortium of Universities for the Advancement of Hydrologic Science, a national organization intended to foster broad-scale collection and dissemination of hydrologic data for use in both scientific research and engineering practice. In light of the need for detailed hydrologic data, the NDW presents an excellent opportunity for a rigorous hydrologic data collection effort, due to the existence of local rainfall and runoff monitoring equipment, as well as the relatively small scale and easy accessibility of the watershed.

As a civil engineer I have observed, as have others, that applied hydrology is often viewed as subjective tinkering, aimed at achieving an economically-driven, sometimes predetermined result (i.e. maximization of developable areas and minimization of flood control improvement costs). The work presented here is an effort to contribute, in the form of extensive field data collection, to a better understanding of the physical processes which govern hydrologic responses in a steep, forested watershed. It is my hope that this effort can contribute to further bridging the gap between state of

the art physical hydrology and standard engineering practice.

The following is a list of tasks that were completed to achieve the previously-listed objectives. A summary of work completed, data collected, and analyses performed for each of these tasks is presented in Chapters 2, 3, 4, and 5 of this thesis:

1. Review of pertinent literature (Chapter 2)
2. Collection and initial processing of hydrologic data for the NDW (Chapter 3)
3. Processing and analysis of data (Chapter 4)
4. Conclusions and recommendations based on results of analysis (Chapter 5).

CHAPTER 2

LITERATURE REVIEW

One of the primary tasks completed in the course of this work was a review of past and present theoretical development, technical advancement, and general research efforts in the areas of hillslope hydrology and hydrologic data measurement. This chapter presents a summary of literature reviewed, relied upon, and referenced in completing the work objectives.

Hillslope Hydrology

Comprehensive historical summaries of the evolution of hillslope hydrology are well-documented and will not be presented here (e.g. Kirkby, 1978; Anderson and Burt, 1990a, 1990b). Some of the earliest and most well-known work in formulating a conceptual watershed hydrologic model was completed by Horton (1933). In general, his conceptual model of infiltration proposed that precipitation falling on a watershed was divided by soil infiltration into two components. The first, overland flow, produced the peak flow observable in a typical watershed runoff hydrograph. The second much slower component, subsurface flow, produced the observable baseflow portion of the typical watershed runoff hydrograph. While Horton's conceptual model of rainfall infiltration and runoff at the watershed scale has formed the basis of much subsequent work in the field, it has long been noted that Hortonian overland flow is seldom observable in the real world (with the notable exception of some semi-arid watersheds). Furthermore, it has also been widely noted that subsurface flow in various forms can account for a significant portion of the hydrograph peak (Kirkby, 1978). These observations have resulted in

various revised conceptual models of watershed hydrological response mechanisms, as well as the more recent development of corresponding computer models.

Conceptual hydrologic response mechanisms

Various studies of watershed response to rainfall as measured along the soil profile have confirmed that infiltration excess overland flow is rare, and observable overland flow is generally restricted to saturation excess overland flow produced from a dynamic area of watershed saturation (Dunne and Black, 1970a). Relative contributions to runoff from dynamic areas of saturation have been studied by McGlynn and McDonnell (2003).

Potential forms of subsurface flow contributing to the storm runoff hydrograph can be divided into four categories:

1. Litter zone flow in forested watersheds (Lamson, 1967).
2. Subsurface flow in the upper soil horizons (Hursh and Brater, 1941).
3. Preferential flow via the soil-bedrock interface in shallow soils (Peters et al., 1995).
4. Preferential flow via macropores (Germann and Beven, 1981)

One of the common aspects in all of these forms of subsurface stormflow has been the observation, confirmed by chemical tracing studies, that a majority of flow contributing to a storm runoff hydrograph is old water displaced from the soil profile by new water entering as rainfall (Sklash, Stewart, and Pearce, 1986). The mechanism governing this displacement has been explored by McDonnell (1990) and is a topic of ongoing research.

Mathematical hillslope hydrologic models

A variety of hydrologic models have been developed over the years, reflecting evolving concepts of hillslope hydrology and driven by technological advances in model processing capabilities. A reasonably comprehensive list of mathematical watershed models developed to date is provided by Singh and Woolhiser (2002). Mathematical approaches to watershed hydrology range from empirical “black box” models to physically-based distributed models. Various comparisons of modeling approaches have been completed (Chiew, Stewardson, and McMahon, 1993) and while it is generally conceded that a physically-based model representing all of the complex hydrologic processes occurring in a watershed would be preferable, the data required to initiate such a model would be difficult if not impossible to compile.

Physically-based mathematical models which support the concept of saturation excess overland flow and utilize readily available spatially distributed data provide an encouraging direction of advance in hydrologic modeling, in that these types of models could eventually become accessible to the practicing engineer. Examples of these types of models include SHE (Bathurst, 1986) and TOPMODEL (Beven and Kirkby, 1979). In general, these models rely on topographic data to predict watershed zones of soil saturation and subsequent runoff production. Increasing availability of geographic information system (GIS) data and digital elevation models (DEMs) in particular, as well as advances in remote-sensing capabilities, have led to increasing efforts to incorporate these types of models into practice (Sun, Cornish, and Daniell, 2002; Fortin et al., 2001; Wang and Hjelmfelt, 1998). A summary of currently-available distributed hydrologic models and available supporting data has been compiled by Garbrecht et al. (2001) with

the intention of introducing the practicing engineer to advances in hydrologic modeling.

As with other mathematical hydrological models, a number of difficulties associated with physically-based distributed models remain. First, physically based hydrologic models are limited by extensive field data requirements for model parameterization. Direct measurements are seldom available and available field data are often too sparse to be meaningful at a watershed scale. This typically necessitates an *a priori* estimation of an extensive set of parameters, under the “misperception that model complexity is positively correlated with confidence in the results” despite the lack of sufficient supporting field data (Grayson, Moore, and McMahon, 1992b).

Second, detailed measurement of watershed rainfall, soil moisture storage, and runoff for the purpose of model testing is difficult to achieve. As stated by Klemes (1986), development of measurement techniques to yield spatial distributions of “hydrologic variables such as precipitation, evapotranspiration, and soil moisture would be a much better investment for hydrology than the continuous pursuit of a perfect message that would squeeze the nonexistent information out of the few poor anaemic point measurements.” Technological advances in methods of soil moisture measurement and remote-sensing of spatial distributions of rainfall are enabling progress in this regard.

The final general difficulty associated with physically-based distributed hydrologic modeling is the problem of assessing the validity of the physical concepts, assumptions, and algorithms used to develop the model. As demonstrated by Grayson, Moore and McMahon (1992a), models known to be conceptually incorrect can be assigned parameters which will simulate watershed response just as well as conceptually-sound models. These difficulties illustrate the need for intensive fieldwork yielding data

for use in verification and validation of model results. Field data collection in support of model development is critical to preserving “the link with reality” (Grayson, Moore, and McMahon, 1992b).

Soil Hydrologic Data Collection Methods

One of the advantages to the concept of Hortonian overland flow is that while runoff generation is dependent on soil infiltration, the process that governs runoff or stormflow (storm hydrograph volume in excess of baseflow) overland transport is independent of properties of the soil matrix. Application of more recent concepts recognizing significant subsurface flow contributions to stormflow, however, requires an understanding of properties of the soil matrix governing subsurface flow.

Soil matrix hydrologic properties

A list of some of the soil properties pertinent to subsurface flow and watershed response is given in Table 2.1. In addition to the soil properties listed in Table 2.1, soil moisture profile characteristic wetting and drying curves are important properties of the soil matrix. In general soils may exhibit some degree of hysteresis, meaning that suction and hydraulic conductivity for a given water content are not unique and depend on the wetting and drying history. The effect of hysteresis is often neglected.

There are a variety of methods available for measuring saturated hydraulic conductivity in the field. Hydraulic conductivity can be indirectly estimated using field measurements of soil texture and a pedo-transfer function. Methods for direct measurement of saturated hydraulic conductivity are generally variations of two basic

Table 2.1. Soil matrix properties pertinent to hillslope hydrology

Soil Property	Definition and Typical Units	Hydrologic Significance
Saturated Hydraulic Conductivity	Rate of water flow through a porous medium under the influence of a unit potential energy gradient (cm/s)	Upper bound for Darcian flow through the saturated soil matrix
Bulk Density	Dry density or mineral mass per total volume (g/cm ³)	Indirect measurement of soil water-holding capacity
Porosity	Ratio of pore space volume to total volume	Reflects soil texture, structure, and the soil maximum potential volumetric water content
Depth	Length measurement downward from ground surface to layer or object of interest (m or cm)	Combined with porosity to determine the total soil water storage potential at a point

laboratory tests: the falling head test and the constant head test. Both tests rely on Darcy's Law to measure soil permeability. The falling head test measures the change in head over time as water infiltrates through a soil sample of known thickness. Variations of the falling head test used to estimate saturated hydraulic conductivity above the water table in the field include the double-tube method, the permeameter method, and the air entry permeameter method. The constant head test measures the volume of water passing through a soil sample of known thickness over time. Variations of the constant head test appropriate for field testing above the water table include the shallow well pump-in method as well as the Guelph permeameter method (Hendrickx, 1990). With the exception of the Guelph permeameter, which uses a manometer apparatus to maintain a constant head in a small field borehole, the drawback to all of these methods is that they require a significant amount of time (one to six hours), and water (anywhere from 10 to

1000 liters per test). The steep relief and dense vegetation in the NDW make the Guelph permeameter essentially the only practical option for measurement of saturated hydraulic conductivity for a large number of points in the watershed.

Measurement of soil bulk density is simple and straightforward using the gravimetric method. Various types of core samplers exist for the purpose of extracting soil samples of known volume. The soft, shallow soils in the NDW lend themselves to a small handheld variety that is pushed into the soil to extract a sample. Sharp mitered edges at the mouth of the sampler are intended to minimize any compaction associated with insertion. Soil porosity is derived directly from estimates of soil bulk density and soil solids density, the latter of which can generally be assumed with an acceptable degree of accuracy.

The shallow (generally less than one meter) and loosely compacted NDW soils require little consideration of highly disruptive soil depth measurement methods, such as excavation, or of methods requiring complex equipment. A small-diameter graduated rod, with a handle to facilitate vertical insertion, will suffice for collecting spatially distributed measurements of soil depth to probe refusal. Lack of significant soil and vegetation disruption and the ease of obtaining measurements facilitate the collection of multiple depth readings at a given location. Averaging of multiple measurements at a site should help to compensate for local variability associated with subsurface rocks or other heterogeneities.

The collection of detailed, spatially distributed measurements of the soil hydrologic properties listed in Table 2.1 is a daunting prospect for watersheds in general. Heterogeneity of these soil properties within a given watershed requires that a large

number of measurements be taken at spacing small enough to allow for reasonable interpolation between point measurements. The size of a representative elementary area for measurement of a given soil property (i.e. the area large enough to represent instantaneous average site conditions) is the subject of ongoing research and discussion, and will not be explored here (Wood et al., 1988; Bear, 1972). In addition to heterogeneity, field data collection in mountain watersheds poses added difficulties, most notably lack of accessibility and relatively high degree of climate variability associated with significant topographic relief (Klemes, 1988). The NDW, established as an experimental watershed for forest ecosystem and biogeochemistry research, presents an excellent opportunity for an aggressive, spatially distributed soil hydrologic data collection effort in a steep, forested, mountain watershed, due to the following:

1. Established streamflow monitoring weirs and climate stations, providing rainfall and runoff records
2. Watershed accessibility via highway and forest service road
3. Relatively small watershed size, allowing for relatively detailed spatial measurements across the watershed
4. Previously established, marked, and surveyed vegetation plots, allowing for navigation and spatial orientation within the watershed.

Soil moisture data collection

An additional important watershed hydrologic variable that, in the past, has been infrequently measured in spatial detail is soil moisture. As stated by O'Loughlin (1990), "it is difficult to nominate any hydrologic output variable that is not *primarily* dependent on soil moisture." There are a variety of methods for measuring soil moisture content, the most obvious being gravimetric methods. This method, although simple and reliable, is poorly-suited to large number of field measurements, since it requires removal of soil samples from the field, transport to a laboratory, overnight drying, and subsequent weighing. Technological advances in this field in recent decades have produced less disruptive techniques, more suitable for field measurements. These include soil moisture measurement using neutron probes, a widely-accepted technique (Bell, 1973).

Research conducted by Topp, Davis, and Annan (1980) contributed to the determination that the dielectric constant of a soil sample is dependent on the volumetric water content of the soil. Time-domain reflectometry (TDR) probes developed based on this research have become a well-established means of measurement for soil volumetric water content. In general, these probes measure the velocity of an electromagnetic signal traveling along two or three transmission rods of specific length, as affected by the dielectric constant of the material surrounding the rods (i.e. soil). This propagation velocity is inversely proportional to the square root of the dielectric constant, which is related empirically to soil volumetric moisture content.

For many mineral soils, a single standard TDR calibration is acceptable, independent of soil composition and texture (Topp, Davis, and Annan, 1980). For soils with high organic contents, a specific calibration is generally necessary (Jones, Wraith,

and Or, 2002). Complex instrumentation and limitations on sensor-to-instrument distance associated with TDR probes can, however, be economically and physically impractical in many applications. Variations of the TDR principle have been used to develop more compact and economical electronic probes for measuring soil volumetric water content. These probes can generally be divided into the categories of frequency- and amplitude-domain reflectometry (FDR and ADR, respectively). ADR is also commonly referred to as impedance. The drawback to these technologies relative to TDR is that they operate at a lower range of frequencies and are therefore more sensitive to variations in soil composition and texture. Consequently, these types of probes generally require calibration for specific applications.

Development and testing of specific probe designs, incorporating multiple rods of various lengths has been successfully completed by Gaskin and Miller (1996) among others. A comparison of dual rod designs versus multiple rod designs concluded that, in general, dual rod designs have the advantage of larger sampling volumes, while multiple rod designs produce a clearer signal in situations where shorter rods are required, such as in portable applications (Whalley, 1993). The final rod length settled on by Gaskin and Miller for their ADR probe prototype was 60 mm. Soil volumetric water content, measured using the prototype, was found to compare well with results from a standard neutron probe under laboratory and field conditions (Gaskin and Miller, 1996; Miller, Gaskin, and Anderson, 1997)

A soil moisture impedance probe known as the ThetaProbe has been developed by Delta-T Devices, based on the prototype designed by Gaskin and Miller. Two variations of this four-rod probe are available, one designed for burial and continuous measurement

recorded by a datalogger, the other designed for periodic portable insertion and measurement, with a digital readout (Delta-T Devices, 1998). This portable version has been successfully used to validate soil moisture measurements using remote-sensing techniques (Famiglietti et al., 1999).

Static and portable versions of a dual-rod FDR probe have also been developed. The Campbell Scientific CS615 Water Content Reflectometer uses significantly longer rods (30 cm) than the ThetaProbe (Campbell Scientific, 1996). This probe was compared with two other probe designs and found to yield satisfactory results, although it was noted that the CS615 periodically produced soil saturation measurements in excess of estimated soil porosity (Walker et al., 2004). The fact that maintaining the distance between the two rods is critical to accurate measurement makes the CS615 static probe suitable for buried, continuously-monitored applications, where careful insertion and installation of the probe can be controlled. For spatially-distributed periodic measurement applications, the portable ThetaProbe is intuitively better-suited to repeated insertion at multiple locations. This is particularly the case in the NDW, where shallow soils would make portable use of a long, dual-rod type probe difficult.

Watershed Water Balance

Once hydrologic data for a watershed have been collected, the task of processing, combining, and analyzing these data to form a coherent picture of watershed response presents itself. The most fundamental and conceptually simple form of watershed hydrologic analysis is completion of a water balance. Mathematically, this relationship can be written as:

$$P - ET - \Delta S = Q$$

Where P represents rainfall, ET represents combined evaporation and plant transpiration, ΔS represents changes in soil water storage (i.e. infiltration minus exfiltration), and Q represents runoff in the form of streamflow. Despite its mathematical simplicity, collection of the data required for a watershed water balance is seldom trivial. Rainfall and runoff are the variables most commonly monitored, leaving either evapotranspiration, changes in soil water storage, or both to be estimated.

Since one of the primary practical applications of the water balance has been to create regional accounting for purposes of water resources planning, various methods and models have been developed to circumvent the need for detailed data. As noted by Alley (1984), these models generally do not perform well for periods shorter than one year. One method for surmounting this difficulty is to choose a time period for the water balance that is sufficiently long (i.e. annual or greater) to allow changes in soil water storage to be neglected (Tuzinsky and Gavenciak, 1988). Completion of a water balance for shorter periods has been successfully accomplished in the past (Rawitz, Engman, and Cline, 1970) using field measurements of soil moisture and pan evaporation. As noted in the study cited, a water balance relies on the assumptions that:

1. conservation of mass is valid
2. topographic watershed boundaries coincide with groundwater boundaries
3. the watershed does not leak (i.e. all runoff is accounted for at monitoring stations).

With regards to a conceptual understanding of hydrologic response mechanisms, it is interesting to note that research conducted by Rawitz, Engman, and Cline (1970) for

a small catchment in a humid area (east-central Pennsylvania) supports a partial contributing area concept of hillslope hydrology, with relatively quick streamflow response to rainfall but little or no observable overland flow during rainfall events. The concept of partial contributing area (or variable source area) is described by Hewlett and Hibbert (1967) using a conceptual reservoir model, where soils adjacent to the stream channel are near saturation, and have little or no excess capacity to buffer the translation of rainfall to runoff. In contrast, upslope areas exhibit lower degrees of soil matrix saturation and therefore have greater capacity to attenuate the effect of infiltrating rainfall on streamflow. Thus a wet watershed has a greater stormflow-generating source area than the same watershed in dry conditions.

Hewlett and Hibbert also observed that although no overland flow was apparent in their watershed study, the timing of streamflow response to rainfall was similar to basins where overland flow was common. Based on the results of their studies, they concluded that the majority of the stormflow component of the hydrograph was pre-rainfall event water stored in the soil matrix and displaced by infiltrating rainfall. They termed this displacement “translatory flow”.

Research conducted by Dunne and Black (1970b) in a small Vermont watershed further supports the concept of partial contributing area. The primary distinction in their conclusions is that based on their results they maintained that stormflow was primarily due to overland flow generated by rainfall falling on the saturated portion of the watershed adjacent to the stream.

The cited research by Rawitz, Engman, and Cline (1970, p. 1120) appears to favor the Hewlett and Hibbert approach to partial contributing area. Rawitz postulated that the

soil matrix “acts as a capacitor type regulator of moisture flux” and concluded that “improved understanding of soil moisture dynamics on a watershed scale is a prerequisite for the improvement of methods designed to predict watershed behavior.”

Optimization of Field Data Collection Efforts

Even with advances in portable field soil moisture measurement techniques, the extensive effort required to collect spatially distributed soil moisture measurements dictates that opportunities for economy be explored. The spatial heterogeneity of soil moisture across a watershed essentially prohibits continuous measurement of this variable for the entire watershed; however, for many applications where the desired measurement is a continuous record of soil water storage (corresponding to continuous records of rainfall and runoff), watershed average soil moisture is adequate. Ideally, one could judiciously choose one point or a small group of points in the watershed that accurately reflect average watershed soil moisture (average soil depth for the watershed would need to be determined independently). Development and testing of this concept, particularly as it applies to soil moisture accounting for lumped-parameter watershed modeling purposes, has been pursued by Kalma, Bates, and Woods (1995). Grayson has further developed the idea, and termed such representative sites “catchment average soil moisture monitoring (CASMM) sites” (Grayson and Western, 1998, p. 68). Central to the idea of catchment average soil moisture is the concept of time stability introduced by Vachaud et al. (1985) and tested for watersheds of minimal relief. This concept can be defined as the temporal persistence of a spatial pattern, founded on the notion that soil volumetric water content is deterministically related to time-stable properties of the soil

matrix (i.e. porosity and saturated hydraulic conductivity) and location in the watershed (i.e. topography).

Research indicates that while temporal persistence of a pattern is often the case under wet soil conditions, soil moisture is distributed much more randomly during the drying phase of the soil matrix (Grayson, Western, and Chiew, 1997). Relying on a statistical procedure for evaluating the variation of point measurements from the mean (Vachaud et al., 1985), Grayson and Western (1998, p. 70) revised the concept of temporal pattern persistence to investigate “whether certain locations, irrespective of the overall pattern, exhibit definable mean or extreme behavior.” CASMM research also extended the work of Vachaud to watersheds of significant relief. Mapping of soil moisture patterns in the NDW provides an opportunity to further test the CASMM hypothesis using data from a steep, forested mountain watershed.

Watershed Nutrient Cycling

While watershed average soil moisture conditions are adequate to explore watershed-scale response, patterns of soil moisture distribution within the watershed retain importance for development of a better conceptual understanding of hillslope hydrology, as well as for studies in forest ecosystem nutrient cycling. Since one of the objectives of this study is to provide a hydrologic basis for others to evaluate nutrient cycling implications, a brief summary of related research reviewed as a background for hydrologic work in the NDW is presented here.

Interest in the effects of manmade sources of pollution on the environment has increased steadily over the past decades, keeping pace with technological advances in air

and water quality monitoring. In the Tennessee Valley region, anthropogenic effects on the acidity of rainfall have received particular attention. Pure rainfall is slightly acidic, with a pH of approximately 5.7. In the last half-century, however, typical rainfall in the Tennessee Valley has had an average pH of approximately 4.3, with measurements as low as 3.1 (Parkhurst and Barnard, 1990). The largest manmade sources of acid rain are sulfur and nitrogen dioxides, produced by fossil fuel combustion and vehicle exhaust. These become nitrate and sulfate ions in rainwater. Average atmospheric nitrogen deposition rates in the Southern Appalachians are estimated to be $30 \text{ kg ha}^{-1} \text{ year}^{-1}$ (Van Miegroet et al., 2001). While atmospheric nitrogen and sulfur dioxide levels in the Tennessee Valley region have been significantly reduced in recent years in response to improved air quality standards (TVA, 2003), concerns remain about the effects of acidic deposition on sensitive high-elevation forest ecosystems. Nitrogen is required by plants, meaning that vegetation uptake in forest ecosystems may partially buffer atmospheric nitrogen deposition. The process by which nitrogen enters the soil from the atmosphere and is taken up by vegetation or leaches to surface streamflow is known as the nitrogen cycle (Hessen et al., 1997). One of the purposes of research at the NDW is to explore how hydrology affects the nitrogen dynamics within and the nitrogen export from a watershed subjected to large atmospheric inputs.

Soil porosity and the hydrologic pathway taken by rainfall as it translates to stream runoff are important factors in solute transport and transformation (Bache, 1990). Nitrogen cycle processes are dependent on the depth to which water transports nutrient concentrations as well as residence time of water in the soil (Mulder et al., 1995). Recent research and modeling efforts in watershed nitrogen cycling have focused on concepts of

nitrogen “flushing” whereby nitrogen accumulates in a watershed during dry periods and is “flushed” out during wet periods (Creed et al., 1996). Export of nitrogen during dry periods is postulated to be “flush-limited” by the transport mechanism (water), while export of nitrogen during wet periods would be “source-limited” by nitrate availability (Creed and Band, 1998a). Common to all of these recent studies has been the conceptualization of hydrological controls on nitrogen processing, particularly the spatial distribution of soil saturation. Possible nutrient cycling implications of a partial watershed contributing area concept have been explored by Creed and Band (1998b).

In light of the significant role played by watershed hydrology in nutrient cycling, it is hoped that the field data collected for this work, particularly the spatially distributed hydrologic properties of the soil matrix, as well as detailed spatially distributed measurements of soil volumetric water content, will provide a hydrologic foundation for others to evaluate nitrogen cycling processes and buffering capabilities for forest ecosystems like the NDW.

CHAPTER 3

FIELD SITE AND DATA COLLECTION

The Noland Divide Watershed (NDW) is located on the Tennessee-North Carolina border in the southeastern United States. Elevations in the 17-ha Southern Appalachian mountain watershed range from 1675 to 1930 meters. Forest vegetation in the watershed consists primarily of red spruce, fraser fir, and yellow birch. The distribution of these vegetation types differs significantly from the lower watershed (below the highway, which was constructed in 1935) to the upper watershed. The forest canopy is more dense in the lower watershed as a result of two factors. First, an insect infestation killed many of the large fir trees, which were more abundant at higher elevations. Second, two hurricanes in the early 1990's downed a large number of trees in the more topographically exposed upper watershed.

Average annual precipitation in the NDW is approximately 210 cm. Average rainfall amounts during the months of May, June, July, August, and September are 15, 18, 21, 17, and 13 cm, respectively. July is typically the wettest month of the year, and September is typically the driest, although average rainfall amounts for each of the 12 months of the year generally does not vary drastically from an overall monthly average of 17 cm. The summer season of 1999 was chosen for logistical reasons as the field season for this work. Relative to typical local monthly rainfall amounts, the months of June through September 1999 were approximately 30 percent wetter than average.

A variety of resources were utilized to gather data necessary for a characterization of the hydrologic response of the Noland Divide Watershed. Initial efforts focused on obtaining readily available data from public sources as well as past research efforts.

These data were used to identify specific areas where further field collection and monitoring efforts would be most effective and most useful in terms of watershed hydrologic analysis. Types of data collected as part of this work can be separated into two general categories:

1. Topographical and meteorological data
2. Soil hydrologic data collected during the 1999 summer field study period.

Topographical and Meteorological Data

Topographical and meteorological data were collected to establish the general characteristics of topography and climate for the NDW, both assumed to be strong determining factors in the hydrologic behavior of the basin. These data are summarized in Table 3.1.

Topographical data

Digital elevation model (DEM) data is available from the U.S. Geological Survey (USGS). The 30-meter DEM for the Clingman's Dome (CD) quadrangle was obtained in SDTS (Spatial Data Transfer Standard) format. The CD DEM was converted to an ArcView[®] GIS binary grid format using an SDTS conversion extension for ArcView available via the ESRI[™] website (www.esri.com). The grid data obtained was in a Universal Transverse Mercator (UTM) projection, Zone 17N, North American Datum (NAD) of 1927, with units of meters. A digital image of the USGS 7.5 minute quadrangle map registered in the same coordinate system was also obtained from GIS Data Depot on the web (www.gisdatadepot.com), along with state and county boundaries and general geographic features.

Table 3.1. List of topographical and meteorological data sources

Name	Source	Date	Precision/ Frequency
CD ¹ digital elevation model	U.S. Geological Survey	1992	30 meter
CD quadrangle map	U.S. Geological Survey	1964	7.5 minute
NDW area topographic survey	Aerial photograph	1992	5 – 30 meter
NDW climate data	NDW climate station (maintained by the University of Tennessee)	1998-1999	Hourly
NDW streamflow	Two gaged weirs at NDW stream outlets (maintained by the University of Tennessee)	1991-1999	Hourly
CD climate data	CD climate station (maintained by the National Park Service)	1992-1999	Hourly

(1) - Clingman's Dome

Topographical and planimetric data for the NDW including streams and roads were previously generated from survey data and aerial photography. These data consist of a set of three CAD drawings in the North Carolina State Plane coordinate system, NAD 1983, with units of U.S. Survey feet. One of these drawings includes original topographic survey points on a semi-regular grid at intervals ranging from approximately 15 to 90 feet. These points were imported into ArcView and projected from State Plane coordinates to UTM coordinates for consistency with the other GIS data for the project. A five-meter grid surface was interpolated from the original topographic survey data

using the ArcView Spatial Analyst tension spline interpolation algorithm with default parameters. The five-meter grid was chosen to take advantage of the areas with higher resolution topographic data, recognizing that a significant portion of the data is at a lower resolution. Vector data include the highway passing through the watershed, the Noland Divide Trail, and locations of monitoring stations, culverts, and discharge flumes. In addition, the locations of fifty vegetation plots, previously established in the watershed, were obtained. These data were also projected from State Plane coordinates to UTM coordinates.

Streamflow data

Streamflow from the NDW is measured using two V-notched weirs. These weirs were installed in 1991 and are located at the intersection of a U.S. Forest Service jeep trail and the two streamlets which drain the watershed. Each weir has a float attached to a Steven's Water Level Recorder which keeps a continuous analog record of stream stage. These recorders were also monitored by dataloggers programmed to convert stage data to a digital daily discharge record. Equipment monitoring and data collection were performed by the University of Tennessee, under the direction of Dr. James Smoot from the Department of Civil and Environmental Engineering. Digital streamflow records for the two stations were available from 1991 to 1999; however, only the 1993-1995 datasets were substantially complete, with digital data existing for greater than 85 percent of the annual record. A detailed record of available data for the entire period of operation was compiled and is included in Appendix A. Photographs of the streamflow monitoring weirs are shown in Figure 3.1.



Figure 3.1. Southwest and northeast weir stream gages, respectively.

The majority of the missing digital streamflow record exists in analog form as stage charts from the water level recorders. The period of primary interest for this work was the 1999 field season (May through September). Digital data for approximately three of these months were not available, necessitating the digitization of hourly stage data from charts for these months. In particular, chart stage records for both the southwest and northeast gages were digitized for the following time periods:

1. June 1, 1999 through June 22, 1999
2. July 14, 1999 through August 20, 1999
3. September 24, 1999 through October 15, 1999.

Digitization of analog data from these charts was completed according to the method specified by the gage manufacturer. A detailed description of this method is included in Appendix B.

Meteorological data: Clingman's Dome

A climate station was installed on a tower just outside the NDW in the spring of 1998. The tower is located approximately 300 meters east of the discharge weirs, adjacent to the Forest Service jeep trail (see Figure 1). The station is maintained by the

Department of Civil and Environmental Engineering at the University of Tennessee.

Data from the station were available beginning in August of 1998. The data listed in Table 3.2 were recorded at 15-minute intervals, as well as averaged hourly and daily.

Data from this weather station were obtained from the University of Tennessee for the period from August 26, 1998 to November 6, 1999. Two primary problems with this set of data were noted. First, a large portion of the data, coincidental with the 1999 field study season, was missing from the record. Second, the accuracy of the precipitation data recorded by the datalogger was questionable. Rainfall is recorded at the station using a typical tipping bucket gage. A plot of the entire hourly data set appears to indicate either a malfunction of the gage or a mistake in the datalogger program. Precipitation was only recorded in increments of approximately 0.17 inches (four mm), with a maximum recorded magnitude of 0.51 inches (12 mm).

Table 3.2. Noland Divide Watershed climate station data

Data	Units	Type
Wind speed	Miles per hour	Instantaneous and average
Wind direction	Degrees	Instantaneous and average
Solar radiation	Watts per square meter	Average
Relative humidity	Percent	Instantaneous
Soil water content	Fraction	Instantaneous
Air temperature	Degrees Celsius	Average
Precipitation	Inches	Total
Vapor pressure deficit	Kilopascals	Average

In addition, many of the storms recorded during this period at the Clingman's Dome weather station (approximately one-half mile southwest of the NDW) were not recorded at the NDW weather station. The University of Tennessee was apprised of these problems and has since taken measures to remedy the situation. A solution which would facilitate the recovery of some portion of the existing precipitation data, however, was not found. Consequently, none of the data from the NDW climate station was used for the work presented here.

The Clingman's Dome (CD) weather station was the next nearest reliable source of meteorological data for the 1999 field season. The location of CD relative to the NDW is shown in Figure 1.1. Hourly data for the Great Smoky Mountains National Park CD station were obtained from the National Park Service (NPS) Air Resources Division for the period from January 1, 1992 to September 30, 1999. The CD weather station is located at latitude 35 degrees 41' 48" and longitude 83 degrees 56' 31" and elevation 2033 meters above mean sea level (the elevation of the Clingman's Dome peak is the highest in the Great Smoky Mountains National Park). The station is identified as NPS site number 53 and Aerometric Information Retrieval System (AIRS) site number 47-155-0102. Table 3.3 is a list of data measured at this site.

In general, the CD weather station is operational during the period from May 1 to October 31, although some years include data as early as mid-April or as late as mid-November. For the years of 1993 to 1999 the CD dataset is substantially complete (no data were recorded at the climate station in 1992).

Table 3.3. Clingman's Dome climate station data

Data	Units	Type
Scalar wind speed	Meters per second	Average
Vector wind speed	Meters per second	Average
Vector wind direction	Degrees	Average
Air temperature	Degrees Celsius	Average
Relative humidity	Percent	Average
Precipitation	Millimeters per hour	Total
Solar radiation	Watts per square meter	Average

It is necessary to note that the CD data set is based on Standard Time (rather than Daylight Savings) and hourly data are referenced by the beginning of the hour (i.e. data collected between 3:00 p.m. and 4:00 p.m. is referenced as 3:00 p.m.). Prior to analysis of data for the 1999 field season, the CD dataset was shifted forward by two hours to achieve consistency with other data (i.e. streamflow and soil moisture data) from the period that are based on Daylight Savings Time, with hourly measurements referenced by the end of the hour.

Meteorological data: Noland Divide Watershed

For a portion of the 1999 field season, a tipping-bucket rain gage was installed in the NDW. The purpose of this gage was to check the applicability of the CD precipitation record for the NDW, since the CD weather station is located outside the NDW and at a higher elevation (approximately 230 meters higher than the average

elevation in the NDW). This gage was installed on June 25, 1999 and maintained through October 3, 1999. The gage was located at an elevation of approximately 1800 meters, near vegetation plot E5910 in a relatively clear area of the understory, on a stand approximately one meter above ground level (see Figure 3.2). Precipitation data were recorded at hourly intervals on a Campbell Scientific CR10X datalogger. The rain gage was calibrated prior to installation using a 500 cm³ volumetric flask. The results of a calibration of the rain gage performed prior to installation are summarized in Table 3.4. The cross-sectional area of the rain gage was 343.1 cm² (derived from a gage diameter of 20.9 cm).



Figure 3.2. NDW 1999 field rain gage.

Table 3.4. Field rain gage calibration

Test number	Tips per 500 cubic centimeters	Equivalent millimeters rainfall per tip (mm)
1	73	0.200
2	72	0.202
3	80	0.182
4	69	0.211
5	76	0.192
Average	74	0.197

The average equivalent depth of rainfall per tip was calculated by dividing the total volume for all tests by the gage cross-sectional area and then by the total number of tips from all tests. This result was used as the conversion factor for all precipitation data recorded by this gage.

Hourly precipitation totals recorded at the NDW field gage and the CD weather station gage between June 25, 1999 and September 30, 1999 were compared in order to determine whether or not a consistent relationship was evident. A scatter plot of the data is included as Figure 3.3.

It is evident from Figure 3.3 that a positive correlation exists between precipitation at the CD site and precipitation in the NDW, and that hourly rainfall at the NDW may be estimated as 1.23 times precipitation measured at the CD station. This correction factor was used to estimate NDW precipitation using the CD precipitation record for the 1999 field season.

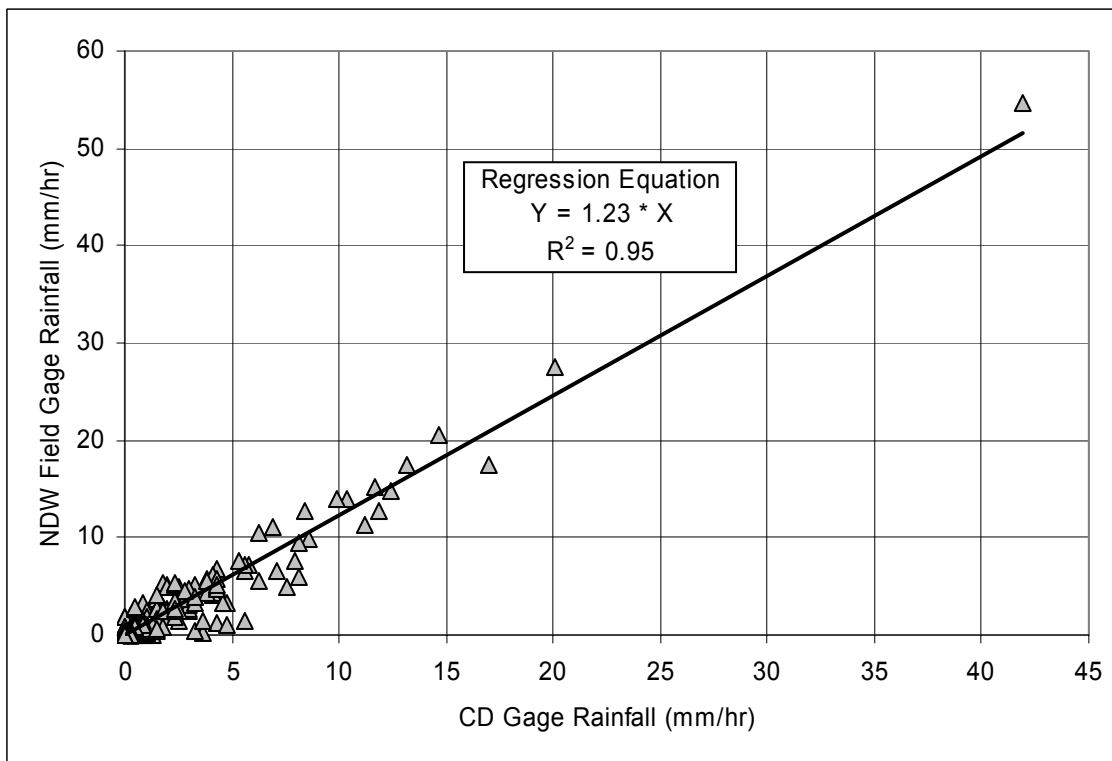


Figure 3.3. NDW field rain gage versus CD weather station hourly precipitation.

The physical basis for consistently greater precipitation totals in the NDW as compared with CD is difficult to surmise, although it may be related to wind at the CD tower reducing the precipitation recorded there, whereas the NDW field gage was located in a more sheltered location near the ground.

Soil Hydrologic Data Collected During the 1999 Summer Field Study Period

Following collection and examination of available GIS, streamflow, and climate data resources for the NDW, a field plan was established to organize further hydrologic monitoring and data collection efforts. This field plan was carried out during the 1999 field season, in the months of May through August. Table 3.5 is a summary of data collected during this period.

Table 3.5. Field data collected during summer 1999

Name	Method of Measurement	Location	Precision/ Frequency
Soil saturated hydraulic conductivity	Guelph Permeameter	50 established vegetation plot sites within NDW	~ 50 meter intervals, one measurement per plot
Soil porosity	Soil core sampler	50 established vegetation plot sites within NDW	~ 50 meter intervals two samples per plot
Soil depth	Rod	50 established vegetation plot sites within NDW	~ 50 meter intervals, depths recorded in 5-cm increments, 16 measurements per plot
Soil volumetric water content profile	Campbell Scientific CS615 30-cm probes with accompanying dataloggers	Three soil pits within the NDW	Hourly, three to four probes per site
Spatially distributed soil volumetric water content profile	Portable Theta Probe (6-cm rods)	66 sites within the NDW	Biweekly, five to 10 measurements per site

Soil saturated hydraulic conductivity, soil depth, and soil porosity were measured at 50 pre-established vegetation plot locations in the watershed, as well as at the stream outlet. These 20-meter by 20-meter vegetation plots were established in 1993 for the purpose of estimating the composition and spatial distribution of overstory tree species as well as the spatial distribution of nitrogen pools (Pauley et al., 1996). Between one and eight plots were established at approximately 30-meter intervals along nine contour lines (at approximately 30-meter elevation intervals) spanning the watershed. Each of these

plots is staked at the center and at each of the four corners. Actual measurements and samples associated with the work described here were taken just outside the plots, generally near one of the plot corners to minimize disturbance to plot vegetation and ecological processes. Measurements were typically taken near the northeast plot corner, although in several cases topography, surface characteristics, and vegetation made this infeasible, in which cases one of the other three corners was selected. Figure 3.4 shows the locations of these sampling sites. Following is a description of the methods that were used to estimate the spatial distribution of the first three parameters listed in Table 3.5 for the NDW.

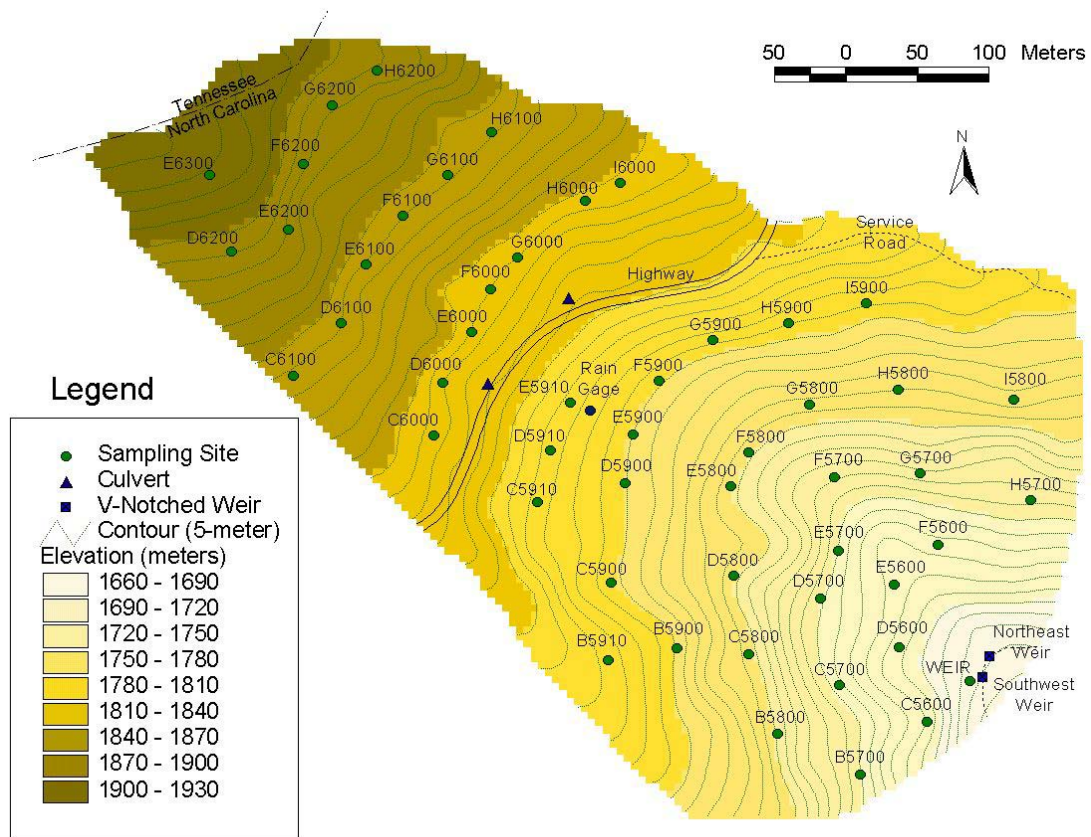


Figure 3.4. Soil hydrologic parameter sampling sites.

Soil saturated hydraulic conductivity

Saturated hydraulic conductivity (K_{sat}) was measured using a Guelph Permeameter. Specific instructions for use are found in the manufacturer's manual (Soilmoisture Equipment Corp., 1986). The apparatus is designed to facilitate a permeability test in a borehole with a constant well height. The constant well height is maintained by a manometer-type device and the volume of water per unit time required to maintain the well height is recorded until a constant value is achieved, assumed to correspond to a saturated hydraulic condition in the soil surrounding the borehole. Two tests at two different well heights (H_1 and H_2) are required for each borehole. The two resulting flux measurements are converted to saturated hydraulic conductivity using the following equation:

$$K_{sat} = G_2 * Q_2 - G_1 * Q_1$$

Q_1 and Q_2 (corresponding to well heights H_1 and H_2 respectively) are obtained by multiplying the final flux reading (cm/s) by the cross-sectional area of the permeameter reservoir. The reservoir includes both an inner and an outer chamber, allowing for two possible modes of operation. The first mode of operation allows both chambers to supply the volume needed to maintain the well height. The cross-sectional area of the combined chambers, identified as X in the manufacturer's manual, is 35.59 cm². When percolation rates are very slow (i.e. in low permeability soils) the inner chamber can be isolated to decrease the amount of time required to observe a change in the reservoir volume. The cross-sectional area of the inner chamber, identified as Y in the manufacturer's manual, is 2.17 cm². G_1 and G_2 are constants based on the two chosen well heights (H_1 and H_2) and two C-factors (C_1 and C_2) based on both the soil type and a normalized well height (H_1/a

or H_2/a where a is the radius of the well or borehole).

The soil types for all tests were assumed to be loam, based on field observations and previous soil analyses conducted by the University of Tennessee (Branson, Dunn, and Ammons, 1996). This previous soil work included excavations to bedrock at five sites in the NDW, soil descriptions, and chemical analyses of soil samples. Soils at each of the five sites were classified as: loamy, sandy, coarse-loamy, and loamy-skeletal at two of the sites. There is no C-factor given by the Guelph Permeameter manufacturer for loamy-skeletal soils (i.e. rocky loams); however, this does not pose a problem since it is not possible to bore a hole and perform a test in a location where large amounts of rock are present. Note that basing the estimation of the permeameter C-factor on the assumption the NDW soils consist primarily of sand results in only a slight increase (approximately two percent) in the average estimated saturated hydraulic conductivity for the basin (see Appendix C plot for determining C-factor).

The equations for calculating G_1 and G_2 are as follows:

$$G_2 = \frac{H_1 C_2}{\pi(2H_1 H_2 (H_2 - H_1) + a^2 (H_1 C_2 - H_2 C_1))}$$

$$G_1 = \frac{G_2 H_2 C_1}{H_1 C_2}$$

Saturated hydraulic conductivity tests using the permeameter were conducted at 51 sites in the NDW (adjacent to each of the 50 established vegetation plots as well as near the watershed outlet). The permeameter apparatus used in the field is shown in Figure 3.5. The majority of tests were done at well heights (H_1 and H_2) of 5 and 10 cm. The approximate borehole radius (a) for all tests (as dictated by the size of auger) was 3.0 cm. For the NDW, borehole depths ranged from approximately 20 to 30 cm. Shallow soils

throughout most of the watershed prohibited measurements at depths significantly greater than 30 cm. The minimum feasible borehole depth to run the test is approximately 20 cm, since the standard well heights used are 5 and 10 cm. Corresponding typical H/a values for the NDW were 1.67 and 3.33. Tests required anywhere from 45 minutes to 1.5 hours to complete.

The complete results of the permeameter test conducted at plot F5600 are provided here as a sample calculation. The permeameter well was bored to a depth of 20 cm near the northeast corner of the plot. The initial well height was established at 5 cm, and readings were taken using the both reservoirs at ten minute intervals. A total of five readings were taken. The last three differential reservoir readings were equal at 0.9 cm, reflecting a steady state (saturated hydraulic conductivity) in the immediate vicinity of the borehole. The well depth was then increased to 10 cm, and readings were taken at four minute intervals (five readings total) until a steady state was once again achieved at a differential reservoir measurement of 1.2 cm. K_{sat} was estimated as follows:

$$H_1 = 5 \text{ cm} \quad H_2 = 10 \text{ cm} \quad a = 3.0 \text{ cm}$$

$$R_1 = 0.9 \text{ cm} / 10(60) \text{ sec} = 1.50 \times 10^{-3} \text{ cm/s}$$

$$R_2 = 1.2 \text{ cm} / 4(60) \text{ sec} = 5.00 \times 10^{-3} \text{ cm/s};$$

The cross-sectional area of the reservoir in this case was 35.59 cm^2 . This area is multiplied by the rate R to estimate flow:

$$Q_1 = 0.0534 \text{ cm}^3/\text{s} \quad Q_2 = 0.1780 \text{ cm}^3/\text{s}$$

Normalizing the well depths using the well radius:

$$H_1/a = 1.667 \quad H_2/a = 3.333$$



Figure 3.5. Photographs of NDW field permeameter test.

Using the figure included in Appendix C, for a loam soil type, the corresponding C-factors were:

$$C_1 = 0.85 \quad C_2 = 1.31;$$

Using the equations cited earlier, the constants G_1 and G_2 are were estimated to be $5.60 \times 10^{-3} \text{ cm}^{-2}$ and $4.33 \times 10^{-3} \text{ cm}^{-2}$, respectively.

Saturated hydraulic conductivity was estimated to be $4.72 \times 10^{-4} \text{ cm/s}$ by subtracting the product of G_1 and Q_1 from the product of G_2 and Q_2 (Soilmoisture Equipment Corp., 1986). The results of the calculation of saturated hydraulic conductivity for the 51 measurement sites are included in Table 3.6.

All of the soil hydrologic parameter estimates shown in Table 3.6 represent measurements taken from the A horizon (ranging in depth from 5 to 15 cm) and the layer of soil below (ranging in depth from 15 to 25 cm). The sole exception is soil depth, which includes the O horizon, estimated to have a depth of 5 cm.

Table 3.6. Soil hydrological parameter data collected during the 1999 field season

Plot ID	K_{sat} (cm/s)	Depth (cm)	Bulk Density (g/cm ³)	Porosity	Organic Content (%)	Adjusted Porosity
B5700	1.43E-03	60.6 ± 16.2	0.70	0.74	17.2	0.66
B5800	1.04E-02	24.1 ± 10.0	0.90	0.66	12.5	0.59
B5900	1.84E-02	36.6 ± 11.4	0.48	0.82	12.7	0.78
B5910	3.94E-03	48.1 ± 21.4	0.61	0.77	15.7	0.71
C5600	2.50E-03	35.6 ± 16.5	0.80	0.70	11.6	0.64
C5700	1.15E-03	35.9 ± 12.0	0.84	0.68	17.2	0.59
C5800	3.59E-02	51.9 ± 21.1	0.58	0.78	17.9	0.71
C5900	1.71E-01	12.3 ± 8.3	0.49	0.81	15.6	0.77
C5910	1.66E-03	23.1 ± 6.8	0.62	0.77	16.6	0.70
C6000	1.29E-03	47.8 ± 17.0	0.62	0.76	15.7	0.70
C6100	5.14E-04	25.9 ± 11.3	0.76	0.71	16.2	0.64
D5600	1.45E-02	7.5 ± 3.7	0.59	0.78	14.5	0.72
D5700	1.02E-02	17.5 ± 15.2	0.74	0.72	10.2	0.67
D5800	7.40E-03	12.8 ± 6.3	0.81	0.69	24.1	0.57
D5900	8.90E-04	20.3 ± 10.6	0.87	0.67	13.3	0.60
D5910	5.16E-05	17.5 ± 9.1	0.41	0.84	10.9	0.81
D6000	1.88E-02	26.9 ± 8.3	0.57	0.78	16.9	0.72
D6100	2.61E-03	25.6 ± 12.0	0.41	0.85	14.6	0.81
D6200	6.81E-04	35.9 ± 10.8	0.49	0.81	24.8	0.73
E5600	6.37E-03	42.2 ± 9.3	0.26	0.90	12.0	0.88
E5700	4.10E-02	17.2 ± 6.8	0.57	0.78	12.2	0.74
E5800	1.28E-02	28.4 ± 11.4	0.78	0.71	20.6	0.60
E5900	6.07E-03	23.1 ± 11.1	0.72	0.73	11.4	0.67
E5910	8.98E-05	20.9 ± 9.2	0.92	0.65	14.6	0.57
E6000	7.80E-04	27.2 ± 9.3	0.69	0.74	18.7	0.66
E6100	6.59E-03	15.3 ± 5.6	0.54	0.79	14.6	0.74
E6200	1.35E-02	28.8 ± 12.0	0.35	0.87	16.7	0.83

Table 3.6. Continued

Plot ID	K_{sat} (cm/s)	Depth (cm)	Bulk Density (g/cm ³)	Porosity	Organic Content (%)	Adjusted Porosity
E6300	9.79E-03	40.9 ± 11.0	0.57	0.78	13.2	0.73
F5600	4.72E-04	40.0 ± 14.5	0.82	0.69	14.0	0.62
F5700	8.41E-04	18.8 ± 9.4	0.49	0.81	19.7	0.75
F5800	1.32E-03	19.7 ± 10.1	0.81	0.69	14.5	0.62
F5900	3.24E-02	33.8 ± 7.4	0.65	0.75	13.8	0.70
F6000	4.39E-04	23.4 ± 11.1	0.39	0.85	16.4	0.81
F6100	1.01E-02	17.2 ± 11.3	0.60	0.77	16.6	0.71
F6200	1.08E-03	19.7 ± 9.9	0.66	0.75	14.7	0.69
G5700	5.57E-03	32.8 ± 9.5	0.85	0.68	14.1	0.60
G5800	2.40E-02	29.7 ± 6.4	0.50	0.81	14.7	0.76
G5900	1.50E-03	35.6 ± 11.4	0.84	0.68	13.4	0.61
G6000	1.66E-03	25.0 ± 14.1	0.71	0.73	15.1	0.66
G6100	1.33E-02	29.1 ± 12.4	0.72	0.73	11.4	0.68
G6200	1.78E-03	28.8 ± 8.9	0.55	0.79	14.6	0.74
H5700	1.47E-03	28.8 ± 14.5	0.51	0.81	16.1	0.75
H5800	3.17E-05	20.9 ± 8.4	0.67	0.75	11.4	0.70
H5900	2.29E-02	35.6 ± 11.4	0.74	0.72	11.2	0.67
H6000	9.79E-04	17.8 ± 6.8	0.81	0.70	11.8	0.63
H6100	3.37E-03	21.3 ± 10.2	0.69	0.74	10.6	0.69
H6200	1.15E-03	31.3 ± 10.6	0.83	0.69	12.6	0.62
I5800	7.65E-03	27.8 ± 7.5	0.76	0.71	10.1	0.66
I5900	1.02E-03	31.3 ± 15.7	0.85	0.68	14.4	0.60
I6000	3.06E-04	45.3 ± 11.6	0.60	0.77	8.0	0.74
WEIR	1.66E-03	10.9 ± 4.9	0.67	0.75	11.4	0.69
Mean	1.05E-02	28.1	0.66	0.75	14.6	0.69
Min	3.17E-05	7.5	0.26	0.65	8.0	0.57
Max	1.71E-01	60.6	0.92	0.90	24.8	0.88

Soil depth

A graduated metal rod was used to measure depth of soil above the impenetrable or bedrock layer in the NDW. The rod was approximately 0.5 cm diameter and 1 meter long with a handle attached to the top for easier insertion. Soils in the NDW consist generally of non-compacted sandy and rocky loams underlain by sandstone at an average depth of less than 50 cm (Branson, Dunn, and Ammons, 1996). Although measurements in a few locations exceeded 80 cm, no depths were encountered that were greater than the length of the 1-meter measuring rod. These conditions were conducive to the use of such a rod for soil depth measurements, whereas a more robust (and longer) device might be required in circumstances where the soil is deeper and more dense. Due to the high spatial variability in soil depth observed in the watershed, multiple depth readings were taken at each of the 51 sites where saturated hydraulic conductivity was measured. Sixteen measurements were taken randomly at each site in the immediate vicinity of the permeameter test location, and the site measurements were averaged to produce a site depth estimate. Depth measurements were recorded to a precision of 5.0 cm; a higher degree of precision would not have been defensible in this application due to the high compressibility and variability in the organic layer which overlays the soil. Sample results of soil depth measurements for plot F5600 are included in Table 3.7. The sixteen recorded soil depths for this site were as follows:

Table 3.7. Soil depth measurements (cm) at plot F5600

40	50	50	60
45	40	50	55
35	15	60	20
30	40	35	15

The mean and the median of these measurements for plot F5600 are both 40 cm, with a standard deviation of 14.5 cm. Estimated average depths for each of the 51 soil sites are shown in Table 3.6. It should be noted that measured depths include an organic layer, which is estimated to have a thickness of approximately five cm. Standard deviations for the sixteen measurements at each site are also included in Table 3.6, demonstrating the significant variability of local measurements.

Soil porosity

Porosity was estimated using a bulk density soil sampler. This device, involving a set of removable rings, allows for the extraction of a relatively undisturbed soil sample of known volume that can be weighed and oven-dried to determine bulk density (ρ_d). Samples in the NDW were taken at depths ranging from approximately 10 to 20 cm. Porosity (n) was estimated using the following relationship:

$$n = \left(1 - \frac{\rho_d}{\rho_s} \right)$$

Solids density (ρ_s) can, in most cases, be estimated with reasonable accuracy as 2.65 or 2.70 g/cm³, depending on the amount of clay present. For the NDW, solids density was assumed to be 2.65 g/cm³. Two bulk density samples were taken from each of the 51 sites in the NDW, in the immediate vicinity of the permeameter test location. The average of the two resultant porosity estimations was used as the representative porosity for a given site. A representative calculation for site F5600 is provided here.

Two samples were taken from plot F5600. For each measurement, the sampling device was inserted into the soil and then removed. The rings were removed from the sampler and trimmed flat on the top and bottom using a small putty knife. In this

particular case, the ring contents were emptied into a previously weighed and labeled tin and sealed in a Ziploc® bag. Samples were transported to a local U.S. Forest Service field laboratory, weighed, and oven-dried at a temperature of 105 °C overnight. The soil dry weight was divided by the ring volume, determined to be 69.015 cm³, to estimate dry or bulk density. Total density, mass-based, and volumetric-based water contents were estimated using standard relationships, although these are not necessary for estimation of porosity. Table 3.8 summarizes this process for the soil samples taken at plot F5600.

Porosity results for all 51 sites estimated using the equation given previously and an assumed solids density of 2.65 g/cm³ are presented in Table 3.6. The resulting average porosity for the NDW was 0.75, with individual results ranging from 0.65 to 0.90. These results are higher than typical values for a sandy-loam or loam soil. It was therefore considered necessary to make an adjustment to these estimates that would take into consideration the high organic content of the NDW soils.

Van Miegroet (2000) reported carbon content estimates for the O and A soil horizons, as well as the underlying soil layers, in increments of 10 cm. Bulk density samples in the NDW were taken from depths of 10 to 20 cm, i.e. from the A horizon (ranging in depth from 5 to 15 cm) and the layer just below (ranging in depth from approximately 15 to 25 cm). The average of the mass-percent soil carbon content for these two layers was considered representative of the carbon content for each bulk density sample. It is recognized that actual organic analysis of each bulk density sample would yield a more accurate estimate; however, in the absence of such, the available carbon content data were considered a more reliable estimate than a blanket adjustment for the entire watershed. The carbon content averages for each plot were multiplied by

Table 3.8. Bulk density estimation for plot F5600 soil samples

Sample	1	2
Tin mass (g)	46.09	46.58
Ziploc® bag mass (g)	6.44	6.44
Soil and Ziploc® mass (g)	131.34	150.98
Wet soil mass (g)	78.81	97.96
Soil and tin dry mass (g)	95.88	109.9
Dry soil mass (g)	49.79	63.32
Total density (g/cm ³)	1.14	1.42
Bulk density (g/cm ³)	0.72	0.92
Water content (mass-based)	0.58	0.55
Water content (volumetric)	0.42	0.50

the Van Bemmelen factor of 1.72 to arrive at approximate percent organics (Nelson and Sommers, 1996). The average organic content of mineral soil for the NDW estimated using this method was 14.6 percent.

In addition to the above soil organic content information, two five-gallon buckets of soil were removed from the NDW just south of the Forest Service road, near the highway. Following the 1999 field season, these were transported from the field to Utah State University (USU) for calibration of the portable Theta soil moisture probe. Three samples were taken from this soil and analyzed for organic content in the USU Soil Analytical Lab. The resulting estimates of organic content were 7.1, 7.9, and 8.0 percent, with an average of 7.7 percent. The most probable reason for the discrepancy between

this result and the average organic content estimation for the watershed is that the contents of the bucket were taken indiscriminately from depths ranging from 10 to 40 cm; the presence of soils from deeper horizons would likely result in a lower soil organic content for a given sample.

The following relationship was used to obtain a revised solids density estimate (ρ_s') for each of the bulk density sampling sites:

$$\rho_s' = \frac{1}{\frac{a}{\rho_o} + \frac{1-a}{\rho_s}}$$

Mass percent organic matter is represented by the “a” term in the expression, while mass percent mineral matter is shown as $1 - a$. The density of organic solids (ρ_o) was assumed to be 1.0 g/cm^3 , while the density of mineral solids (ρ_s) was assumed to be 2.65 g/cm^3 . Revised solids density estimates ranged from 1.88 to 2.34 g/cm^3 , with an average of 2.14 g/cm^3 . These revised solids density estimates were used in conjunction with bulk density estimates to arrive at porosity estimates adjusted to account for soil organic content. The net effect of this adjustment was an 8 percent reduction in the estimated average porosity for the watershed, the result being 0.69 . The adjustment was most notable for lower porosities, with a reduction of 12 percent in the minimum (0.57) compared with only a 2 percent reduction in the maximum (0.88). Adjusted porosity estimates are shown in Table 3.6.

Soil moisture monitoring

In an effort to quantify the amount of water stored in the soil in the NDW as well as the spatial and vertical distribution of soil water, a soil moisture monitoring system

was implemented during the 1999 field season. This system consisted of two types of monitoring: first, continuous recording of soil moisture measurements at three pits within the watershed; and second, biweekly soil moisture mapping at 66 sites distributed across the watershed. The locations of both the continuous monitoring and the biweekly mapping sites are shown in Figure 3.6.

The three continuous monitoring locations were selected with the concept of catchment average soil moisture measurement (CASMM) in mind (Grayson and Western, 1998). Locations were selected based on ostensibly average watershed characteristics of slope, aspect, and elevation. The highway and associated rock fill prevented installation of multiple pits near the watershed mean elevation. Site selection adjustments were also required in the field in order to find sites suitable for excavation and sensor installation.

The 66 synoptic soil moisture measurement sites were laid out approximately along contour lines with the intent of systematically spanning the watershed while also avoiding disturbances to the 50 vegetation plots.

Continuous soil moisture monitoring. The continuous soil moisture monitoring effort required pit excavations at three sites. The first monitoring pit was installed on May 24, 1999 at a location approximately 14.0 meters at 104 degrees from the southeast corner of vegetation plot E5910. The pit was excavated using a shovel to a depth of approximately 45 cm. Rock was encountered beginning at an estimated depth of 25 to 30 cm. Approximate pit plan dimensions were 60 cm by 80 cm. Excavation continued until a point was reached where rocks were too large to be removed without enlarging the hole (assumed to be the approximate depth of the bedrock layer). Three 30-cm Campbell Scientific CS615-L water content reflectometer probes were installed at different depths

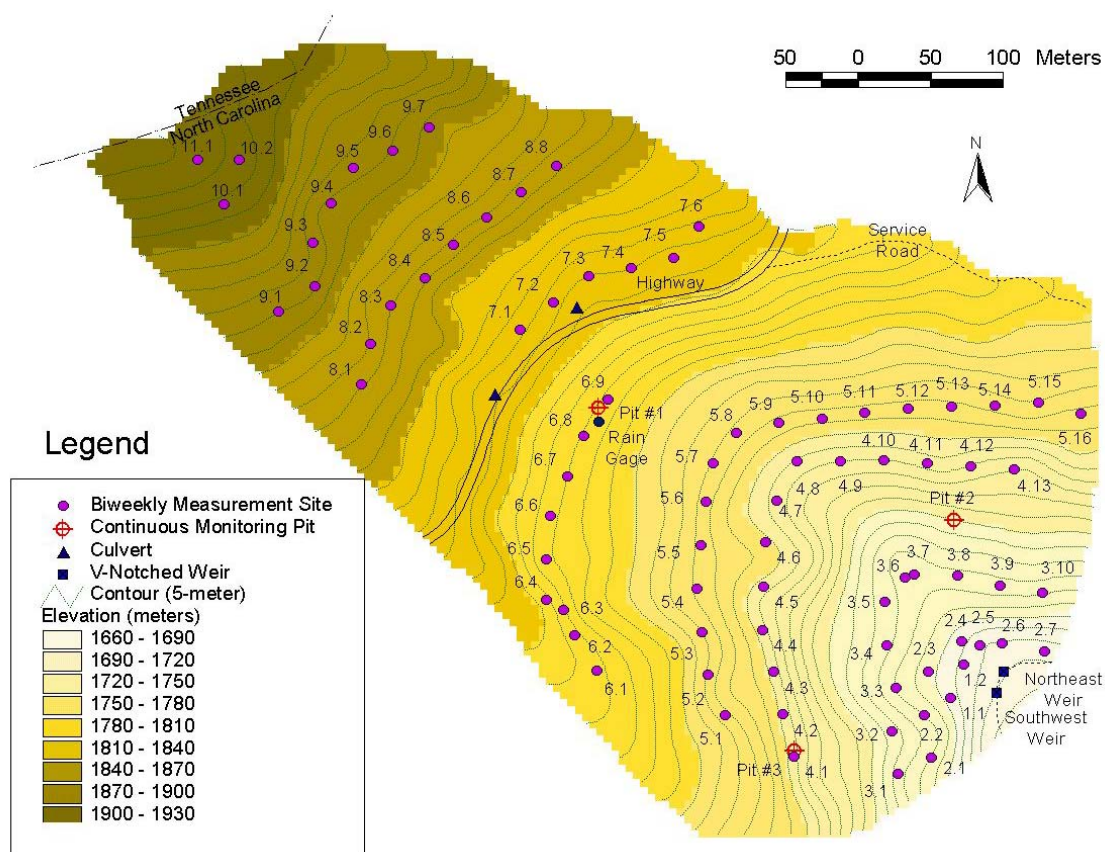


Figure 3.6. Soil moisture monitoring locations.

in the sides of the pit, each at a downward angle of about 30 degrees from horizontal. By installing each probe at a 30 degree angle, each probe vertically spanned an approximately 15-cm layer of the soil profile.

The first probe was inserted as near as possible to the bottom of the pit (for Pit #1, approximately 45 cm below the surface). A pilot tool provided by the manufacturer was used for the initial insertion and to assure, to the extent possible, correct spacing between the probe dual rods. The second probe was installed at a depth of approximately 30 cm, and the third at a depth of 15 cm. By installing the probes in approximately 15-cm increments, nearly all of the vertical soil profile at each pit location was monitored. The locations, pit sizes, and probe depths for all three sites are shown in Table 3.9.

Table 3.9. Continuous soil moisture monitoring sites

Site Number	Pit Location	Pit Plan Area	Pit Depth	Probe Depths	Date of Installation
Pit #1	14.0 meters @ 104 degrees from NE corner of plot E5910	60 cm x 80 cm	45 cm	15 cm 30 cm 45 cm	May 24, 1999
Pit #2	18.3 meters @ 100 degrees from SE corner of plot G5700	60 cm x 80 cm	57 cm	15 cm 35 cm 57 cm	May 24, 1999
Pit #3	13.0 meters @ 18 degrees from SE corner of plot B5800	50 cm x 70 cm	50 cm	Surface 15 cm 30 cm 50 cm	June 23, 1999

The later installation of equipment at Pit #3 was due to late acquisition of a datalogger for this site. Photographs of the pit excavation and probe installation for Pit #2 are shown in Figure 3.7.



Figure 3.7. Continuous soil moisture monitoring pit installation (Pit #2).

As shown in Figure 3.8, vegetation at each pit recovered quickly from the disturbance associated with installation. It should be noted that any effects on soil moisture associated with vegetation recovery were not accounted for in subsequent analyses.

A Campbell Scientific CR10X datalogger was installed in a weatherproof container adjacent to each pit. Power for each datalogger was provided via a 12-volt battery pack. The dataloggers at Pit #1 and Pit #2 were initially programmed to record soil moisture readings at 15-minute intervals. Initial readings indicated that this sampling frequency was unwarranted due to much slower rates of change in soil moisture. As of July 16, 1999 all three dataloggers were programmed to record at one-hour intervals, as well as tallying four-hour and daily averages. Data were downloaded from the dataloggers using a laptop computer approximately once every two weeks during the months of May, June, and July.

No field personnel were in Tennessee during the months of August and September. Data were downloaded from the dataloggers for the final time in early October during a return trip one of the purposes of which was performing an additional synoptic soil moisture measurement for the watershed. At that time, all three dataloggers were in working order and had sufficient battery capacity to allow for approximately three to five additional months of data collection. Soil moisture data compiled for the work presented here from Pits #1 and #2 begin at 3:00 p.m. on May 24, 1999 and continue through 11:00 a.m. on September 30, 1999. Soil moisture data from Pit #3 were collected for a short period between June 24 and July 2, 1999 using a Campbell Model 21X datalogger, and then beginning on July 8, 1999 at 5:00 p.m. (when the datalogger



Figure 3.8. Continuous soil moisture monitoring Pits #1 (top), #2 (right), and #3 (bottom), one month after installation.

was replaced with a late-arriving CR10X) and continuing through 11:00 a.m. on September 30, 1999. Time series plots of continuous soil moisture measurements for the three pits are shown in Figures 3.9, 3.10, and 3.11. Local precipitation data for the same period are included as Appendix D.

All three pit installations remained in the field through the winter months. The dataloggers and probes at Pits #1 and #3 were removed by employees of the Tennessee Valley Authority (TVA) on March 1, 2000. The datalogger at Pit #1 had been disinterred and thoroughly examined by a bear on October 3, 1999. The unit did not sustain any significant damage; however, it was disconnected from the battery and ceased to record data on this date. The datalogger at Pit #3 continued to function up until the removal

date. The two dataloggers and seven soil moisture probes, as well as the rain gage from Pit #1, were shipped to USU, where data was retrieved from the dataloggers. Additional soil moisture records from this site are available for the period from October 27, 1999 through March 1, 2000 (the majority of data from the month of October were overwritten due to insufficient memory capacity for the winter months). Only data from the 1999 field season (May through September) was used in the work presented here.

Due to an accident in the field en route to removal of equipment from the Pit #2 site, the datalogger and three soil moisture probes at this site were left in the field, assumed to be intact and functional as of March 2000. Collaborators from the University of Western Ontario have taken responsibility for the maintenance of this equipment, with the intention of collecting further observations at this site.

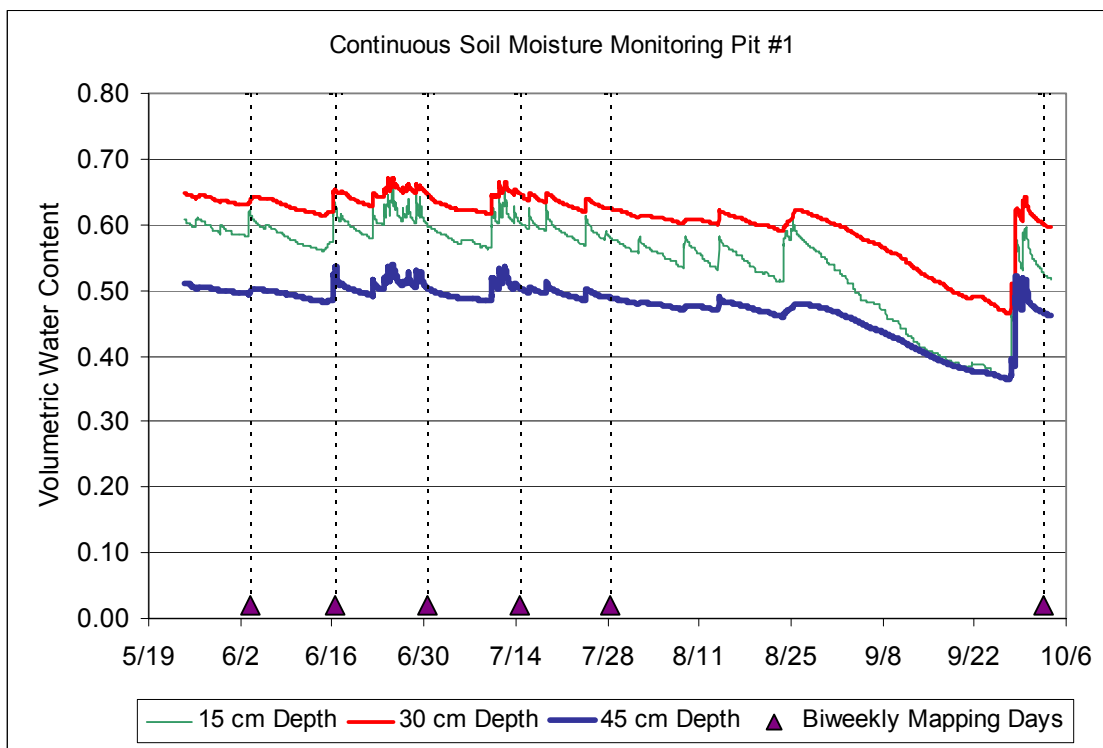


Figure 3.9. Time series plot of soil moisture at Pit #1.

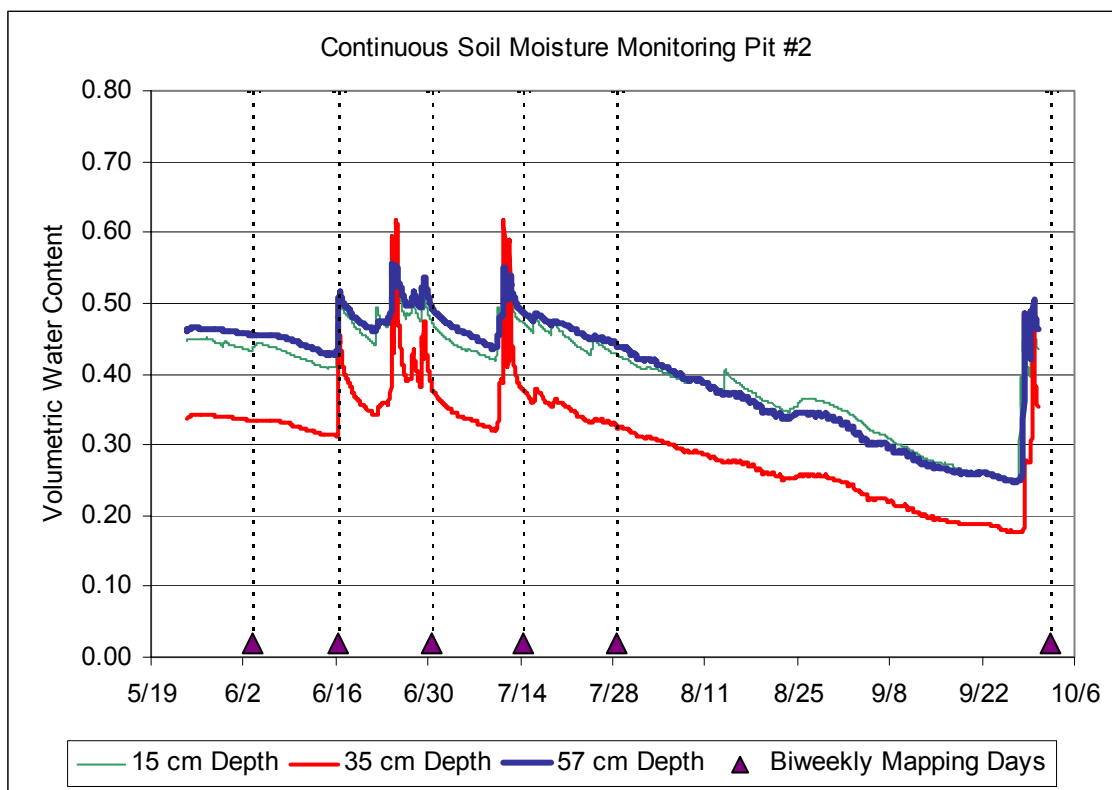


Figure 3.10. Time series plot of soil moisture at Pit #2.

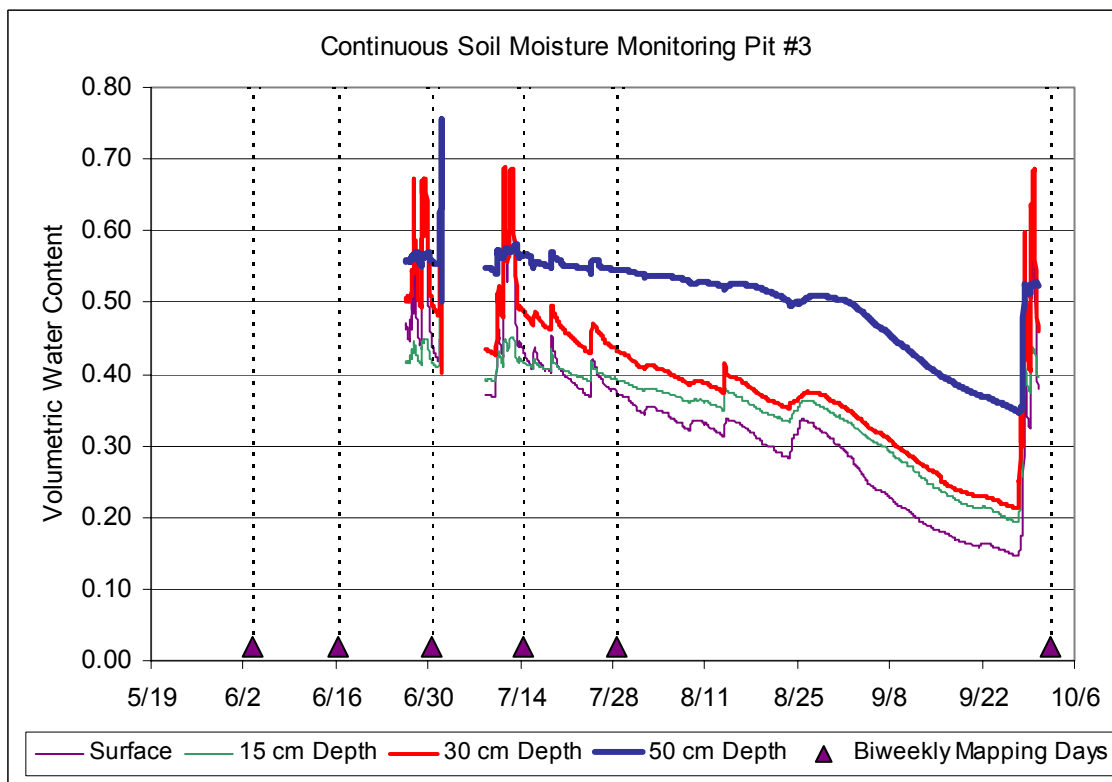


Figure 3.11. Time series plot of soil moisture at Pit #3.

In general, Pit #1 was the wettest of the three sites, with an average volumetric moisture content (average of all three probes for the period from May 24 to September 30, 1999) of 0.56 and a range in measurements of 0.36 to 0.67. The standard deviation for these measurements was 0.07. Pits #2 and #3 were similar to one another in average response, Pit #3 having an average soil moisture content of 0.41 and individual measurements ranging from 0.15 to 0.76 (standard deviation of 0.12). Pit #2 had an average recorded volumetric water content of 0.40, with measurements ranging from 0.18 to 0.62 and a standard deviation of 0.08.

In general, the variation of soil moisture with depth is inconsistent across the three pit profiles. The probe readings taken at Pit #3 displayed the greatest range in single event response, while event hydrographs for Pit #1 are more subtle. Almost without exception, the 30 cm probe at Pit #1 was wettest, while the deepest probe (45 cm) was driest. At Pit #2, the deepest probe (57 cm) recorded the wettest observations on average, although the 35 cm probe (generally the driest in this case) displayed two large event responses significantly wetter than the other two probes. In addition, the 15 cm probe which on average recorded moisture contents only slightly lower than the deepest probe, surpassed the 57 cm probe in wetness during an extended period of drought. Finally, of the four probes at Pit #3, the deep probe (50 cm) was significantly wetter on average than the other three, while both the surface (driest on average) and 30 cm probes displayed large event responses wetter than this. The general pattern for this site was increasingly wet from the surface to the deepest probe, with the noted exception of large event responses.

The manufacturer's calibration for the Campbell Scientific probes was considered

adequate for the purposes of this monitoring effort. Use of these probes in similar applications has contributed to a well-established and validated relationship between the travel time of a wave moving along the probe rods and volumetric water content of the surrounding soil (Campbell Scientific Inc., 1996). Raw data recorded by the dataloggers are available in both the signal period and derived volumetric water content forms. Research by Seyfried and Murdock (2001) confirms that the manufacturer's standard calibration is valid for sandy soils with relatively low clay content. Soils data for the NDW reported by Branson, Dunn, and Ammons (1996) indicate that while clay contents of 20 percent or more are common in the uppermost soil horizon (0 to 10 cm), clay contents are generally much lower at depths greater than 10 cm (i.e. less than 10 percent).

Although there is some concern that the manufacturer's calibration is not valid for use in sandy-loam soils with high organic contents, the range and distribution of volumetric water content using the Campbell Scientific probes was consistent with the range and distribution of gravimetric measurements taken from the NDW, as will be shown later.

Biweekly soil moisture mapping. The impetus of the second phase of the soil moisture monitoring effort was to characterize the spatial distribution of soil moisture across the watershed. This was accomplished by means of biweekly mappings of volumetric water content readings at 66 sites established approximately along 11 contour lines. Water content was measured using a portable Theta probe soil moisture sensor (Delta-T Devices, 1998). The portable version is a relatively new instrument, and operates on the principle of amplitude domain reflectometry (or impedance). The Theta probe uses four 6-cm rods, which make the probe more suitable for portable

measurements than the longer Campbell probes, especially in shallow soils such as are present in the NDW.

All portable probe readings were recorded as voltage to allow for a calibration tailored to the specific soil conditions in the NDW. Two separate calibration efforts were undertaken to establish the relationship between probe voltage and local soil volumetric water content: first, a field calibration, and second, a laboratory calibration.

The field calibration was conducted along with the soil dry density sampling effort. Following the extraction of each soil specimen using the soil density sampler, the Theta probe was inserted into the remaining hole and a voltage reading was taken. Soil samples were processed as described previously, and volumetric water content was estimated based on the results.

Specific instructions for calibration of the portable probe are provided in the Theta probe User Manual (Delta-T Devices, 1998). The manufacturer provides two general calibrations (organic and mineral) and asserts that the repeatability of volumetric water content measurements using the appropriate general calibration is $\pm 0.05 \text{ m}^3/\text{m}^3$. A soil-specific calibration effort was undertaken in this case, due to both the high organic content of NDW soils and the large variability in soil moisture readings at any given site.

The user manual provides two equations which are necessary for soil moisture sensor calibration. The first describes the relationship, well-defined and specific to this instrument, between the probe voltage reading (V) and the square root of the dielectric constant (ϵ) of the material surrounding the probe rods:

$$\sqrt{\epsilon} = 1.1 + 1.44V$$

In most cases this linear relationship is adequate; however, a third-order polynomial

relationship is also provided in the user manual if a more precise result is desired:

$$\sqrt{\varepsilon} = 1.07 + 6.4V - 6.4V^2 + 4.7V^3$$

This second relationship was used for all NDW calibrations, since it provides a better result at higher voltages (corresponding to high soil volumetric water content as was often the case in the NDW).

The other necessary relationship, where θ represents volumetric water content and a_0 and a_1 are constants, is given here:

$$\theta = \frac{\sqrt{\varepsilon} - a_0}{a_1}$$

Calibration is accomplished by measuring probe voltage and using the third-order polynomial to arrive at a corresponding estimate of the square root of the dielectric constant. These results are plotted against volumetric water content as determined by gravimetric methods. A total of 80 soil samples were taken for which probe voltage was measured at depths ranging from approximately 10 to 26 cm (probe voltage was not measured for every one of the 102 soil density samples). A linear regression applied to these points yields a slope and intercept, which are then used to arrive at a_0 and a_1 . The established calibration is summarized as:

$$\theta = \frac{[1.07 + 6.4V - 6.4V^2 + 4.7V^3] - a_0}{a_1}$$

The results of the field-sampled volumetric water content did not display a clear relationship when plotted against the square root of the dielectric constant (see Figure 3.12a). This poor result could, at least in part, be due to high local variability in soil moisture. A single Theta probe was used for all measurements, so variability is not

attributable to differences among sensors. The probe voltage reading was taken from the layer of soil approximately 0 to 6 cm below the actual soil samples, since it was not possible to insert the probe into the actual field samples while maintaining the soil density core samples intact.

These results necessitated a laboratory calibration. To this end, two 5-gallon buckets of soil were transported to USU on the return trip from Tennessee at the end of the field season. The lab calibration was performed in January 2000. A total of 15 lab samples were prepared and processed. A detailed description of the steps that were carried out to complete this laboratory calibration effort is included in Appendix E. Note that the buckets of soil were taken indiscriminately from depths ranging from 10 to 40 cm, without regard for mixing of soil layers. Consequently, these samples were fully disturbed, as compared with the *in situ* field measurements.

Probe voltage measurements were plotted against volumetric water content (as determined gravimetrically) and a linear regression was performed to estimate slope and intercept. Slope and intercept were converted to the constants a_0 and a_1 as follows:

$$a_0 = - \text{intercept/slope} \quad a_1 = 1/\text{slope}$$

These constants were used to establish the final calibration relationship.

The values of a_0 and a_1 obtained were 1.14 and 8.32, respectively. Figure 3.12b includes graphical results of the linear regression used to arrive at these values. It is clear from this plot that the lab calibration was much more fruitful than the field calibration effort, especially considering the values of -1.17 and 12.41 for a_0 and a_1 , respectively, that resulted from the field calibration.

Figure 3.13 summarizes the curve-fitting results from both calibrations. Also

shown on this plot are the manufacturer's generalized organic and mineral calibrations for comparison.

The final calibrated laboratory curve compares well with the manufacturer's general organic calibration. The difference between the two becomes increasingly apparent at voltages greater than 0.80 (corresponding to volumetric water content greater than 0.40). Despite the fact that the field data-based curve-fitting procedure yielded poor results, especially in the lower ranges of voltage and water content, the approximate center of mass of the scattered field data corresponds well with the lab calibration curve. The laboratory calibration was considered appropriate for portable impedance probe measurements recorded in the NDW, and was used to convert all probe voltage outputs to volumetric water content.

Porosity was also calculated for the 15 lab samples. The results, which were adjusted using an approximate mass-percent organics of 7.7 percent (the average value obtained from the three samples analyzed for organic content at USU), ranged from 0.59

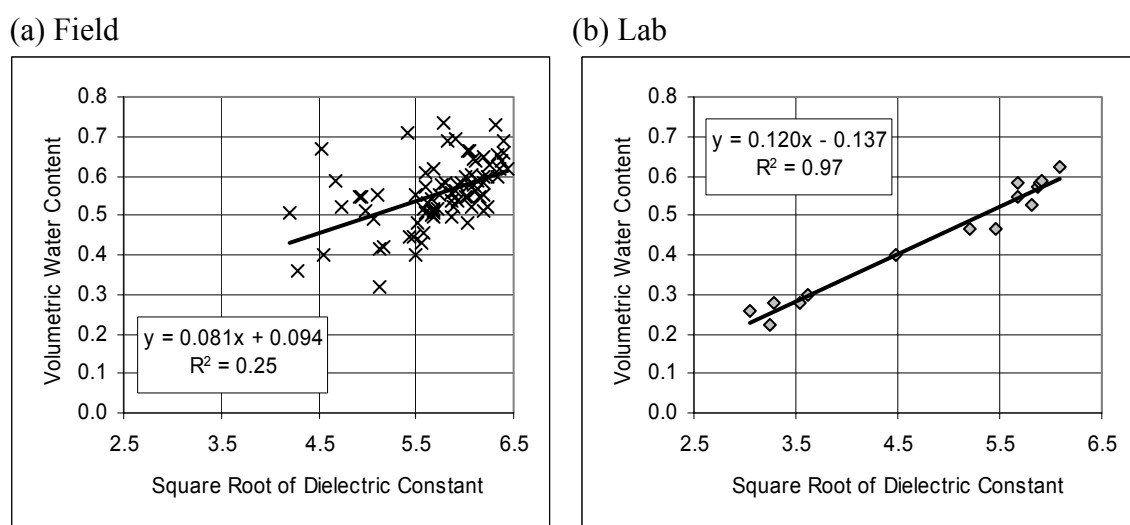


Figure 3.12. Determination of a_0 and a_1 using (a) field and (b) lab calibrations, respectively.

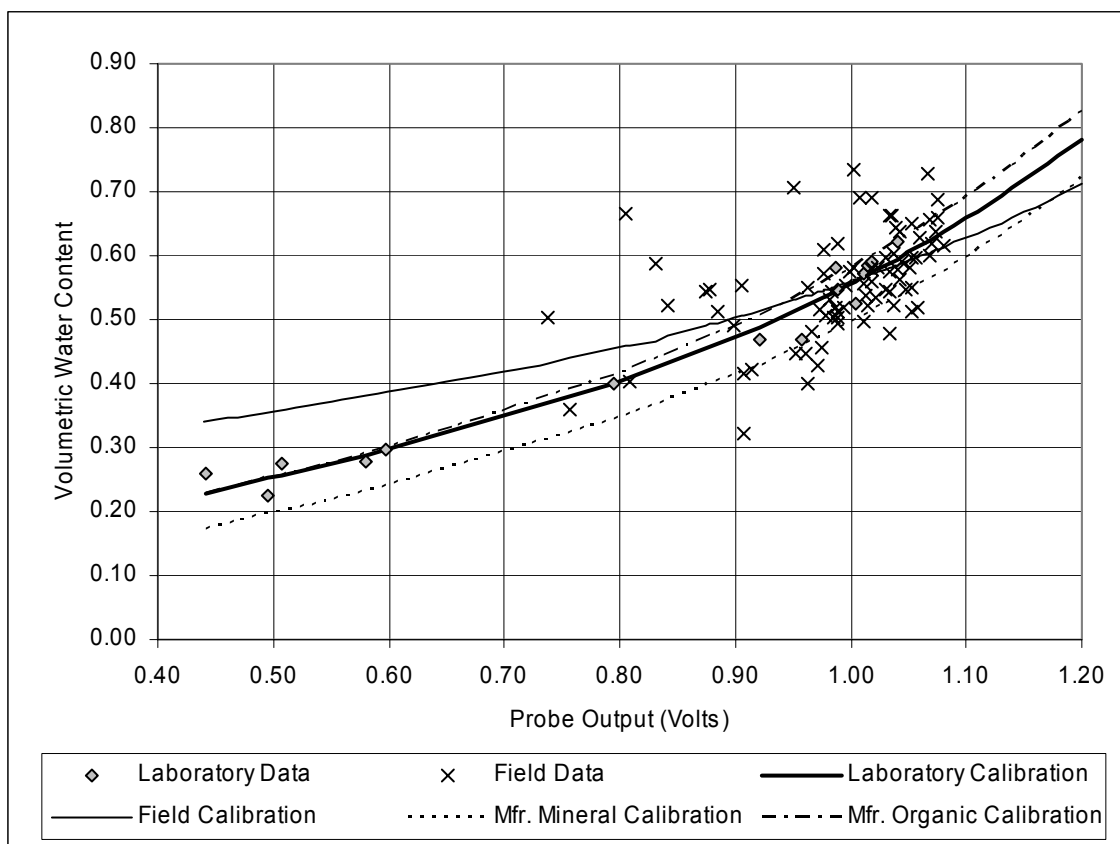


Figure 3.13. Calibration of portable impedance probe for NDW.

to 0.67 with an average of 0.62. These values are roughly consistent with the adjusted field porosity estimates previously discussed, which averaged 0.69 and ranged from 0.57 to 0.88. It is likely that the lower maximum result observed in the laboratory samples is due to sample compaction procedures.

In order to facilitate measurements at multiple depths for each site in the field, while also assuring that observations were made at precisely the same locations during each mapping, a number of access tubes were installed at each site. The access tubes were made by boring a hole in the soil sufficient to admit a two-inch Schedule 40 PVC pipe. A screen across the bottom of the tube prevented material from entering from the

bottom, and a 1.5-inch section of PVC, slightly shorter than the outer tube, was filled with excavated soil and inserted into the larger tube to maintain a relatively natural condition.

When measurements were made, the inner tube was removed and the probe inserted, penetrating the 6-cm soil layer beneath the access tube. Five shallow access tubes, 5-cm in depth, were installed at each site. Further tubes were added, one per depth, in 5-cm increments to a maximum depth of 30 cm, as shown in Figure 3.14. Auger refusal depth at the majority of sites prevented installation of access tubes deeper than 25 cm. From 5 to 10 lysimeter tubes were thus maintained at each site, at from 1 to 6 different depths. A total of 452 probe access tubes were installed in the watershed.

Measurements were made approximately once every two weeks, on the dates shown in Table 3.10. The large interval between the final two measurements was due to

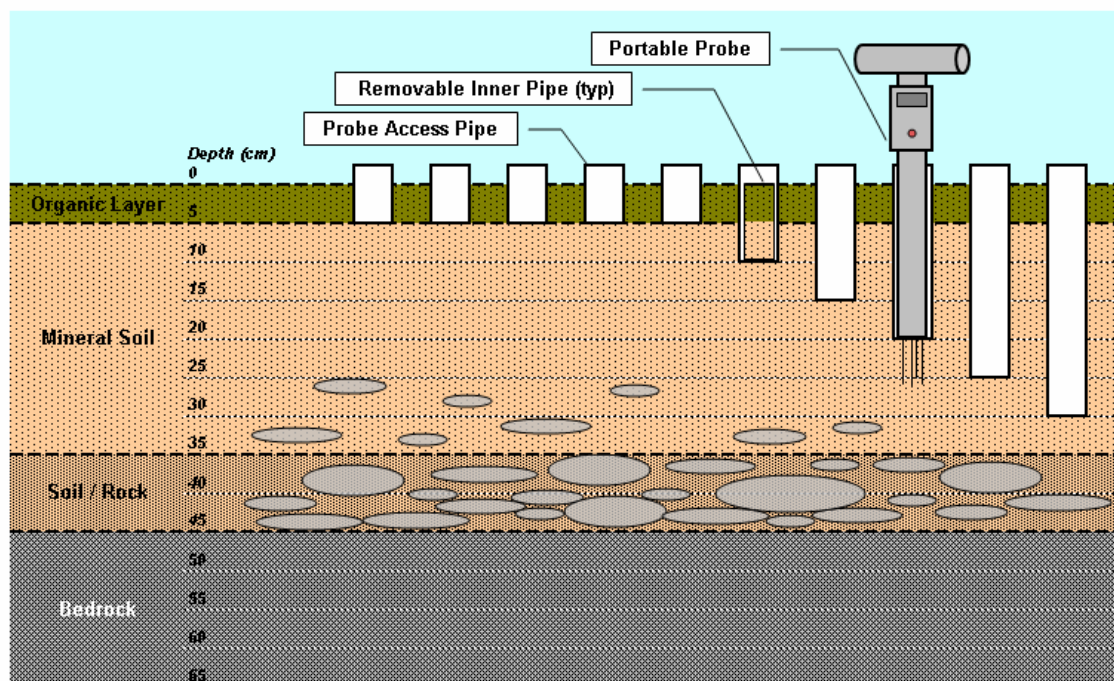


Figure 3.14. Portable Theta probe access tube schematic.

lack of field personnel in Tennessee during that period. On measurement days, manual readings were taken at each site beginning at approximately 7:00 a.m. in the upper half of the watershed (above the road) and finishing at the stream weirs at approximately 4:00 p.m. in the afternoon. The local weather conditions on each sampling day are also summarized in Table 3.10.

The objective of measuring volumetric water content at 66 sites in the watershed on a single field day was to obtain, to the extent possible, a snapshot of soil moisture storage in the watershed. It is recognized that the measurements made do not actually represent an instantaneous map of moisture conditions across the watershed. These results are considered a reasonable representation, however, for two reasons.

Table 3.10. Weather conditions during biweekly soil moisture measurements

Sampling Date	Weather Conditions
June 3, 1999	Rain began very early in the morning, continued off and on throughout the day
June 16, 1999	Rained most of the previous night; rained intensely all morning, lessening in intensity but enduring steadily for the remainder of the day
June 30, 1999	Rained on the previous day, sunny and clear during field measurements
July 14, 1999	Rained on the previous evening; no precipitation during measurements, cloudy and wet all day
July 28, 1999	Short cloudburst on previous afternoon, last significant storm four days prior; sunny and clear all day
October 2, 1999	Sunny and clear day; storms on September 27, 28, and 29 ended an extended dry that began in mid-July

First, it is assumed that the measurement strategy (beginning at the top of the watershed and working downward toward the weirs) helped to alleviate the problem of being unable to gather all measurements simultaneously, assuming that soil water movement proceeded in a downhill direction after local infiltration. Second, continuous measurement of soil moisture at the pits confirms that soil moisture response times are relatively slow (on the order of hours to days) even during periods of heavy precipitation. For example, average volumetric water content at Pit #2 during the June 3 field day hours of 7:00 a.m. to 5:00 p.m. ranged from 0.407 to 0.410, a change of less than one percent (0.7 percent). Average response at the same pit during the June 16 field day (very heavy precipitation) ranged from 0.410 to 0.494, a difference of approximately 20 percent. This is the most severe case, with the peak in soil moisture response at Pit #2 occurring at approximately 2:00 p.m. following a peak in precipitation around 9:00 a.m. that morning. Percentage change in soil moisture at this pit for the remaining sample days was much smaller; 2.9, 0.9, and 1.3 percent on June 30, July 14, and July 28, respectively. Data from Pit #2 were not available for October 2, but Pit #1 recorded variations in volumetric water content of 0.9 percent during this field day. These observations reinforce the validity of each field day's observations as a map of soil moisture across the watershed at a given time.

Photographs of a typical biweekly soil moisture measurement site are included as Figure 3.15. Each sampling site was marked with a flag, and the locations of all sites (bearing and distance from established locations) were recorded during installation.

Table 3.11 shows the average volumetric water content at each site for each of the six sampling days. Mean values were obtained by averaging the readings at the 5

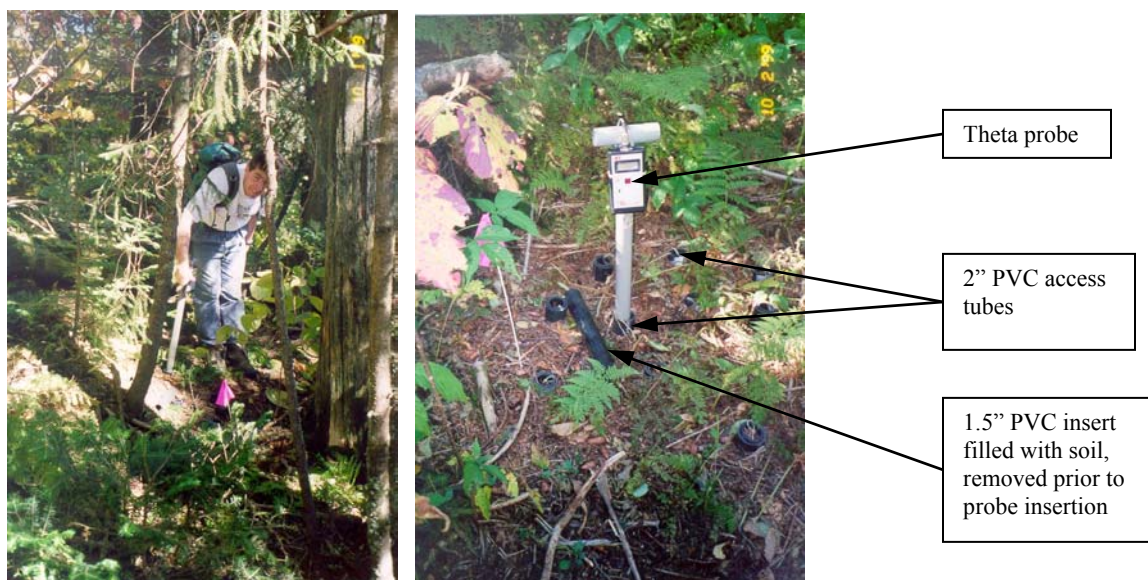


Figure 3.15. Typical biweekly soil moisture sampling site.

surface probes (5-cm access tubes) and then averaging this result with readings at other depths. In this manner, each depth was given equal weight. The number of readings taken at each site compensates for single-site variability by averaging a number of measurements to achieve what is hoped to be a representative estimate of site average soil moisture conditions. Note that the sites with no data values were initially staked; however, no access tubes were installed at these locations due to conditions such as large roots or rocks and/or very shallow soil.

Standard deviations of Theta probe measurements on a given day at a particular site averaged 0.056 (roughly 10 percent of the average reading) and ranged as high as 0.138 (about 26 percent of the average reading). The high degree of variability in readings at an individual site is likely due at least in part to the relatively small area penetrated by the 6-cm probe rods (as compared with the 30-cm Campbell probe rods). The Theta probe manufacturer supplied 12-cm interchangeable rods for use with the

probe; however, at the time of this sampling effort, the manufacturer had yet to establish calibrations for the longer rods, and did not support their use with the probe.

The average reading for all sites (at soil depths ranging from five to 36 cm) on all days was 0.52, with a maximum individual reading of 0.68 and a minimum of 0.18.

These results compare well with measurements from the Campbell Scientific probes for these days, with average measurements (at soil depths ranging from zero to 72 cm) of 0.56, 0.40, and 0.41 for Pits #1, #2, and #3, respectively, minimum measurements of 0.36, 0.18, and 0.15, and maximum measurements of 0.67, 0.62, and 0.76, respectively.

Note also that the maximum measurement from the portable probes and the maximum measurements (for the sampling days) from the continuously monitored probes correspond well to the mean adjusted porosity estimate for the watershed of 0.69. Using the gravimetric analysis results for the 102 soil samples collected to determine bulk density and porosity, volumetric water content was calculated for each of the bulk density samples. The results for these samples collected between May and July 1999 (representing volumetric water content at depths ranging from 10 to 20 cm), ranged from a minimum of 0.32 to a maximum of 0.73, with an average of 0.55.

Table 3.11. Biweekly soil volumetric water content averages by site

Site	June 3	June 16	June 30	July 14	July 28	October 2
1.1	0.56	0.58	0.57	0.54	0.51	0.46
1.2	0.59	0.61	0.58	0.58	0.55	0.47
2.1	0.56	0.55	0.50	0.48	0.41	0.36
2.2	0.56	0.55	0.56	0.54	0.48	0.37
2.3	--	--	--	--	--	--
2.4	0.65	0.64	0.66	0.65	0.64	0.52
2.5	0.56	0.59	0.56	0.54	0.55	0.51
2.6	--	--	--	--	--	--
2.7	0.33	0.49	0.44	0.42	0.36	0.27
3.1	0.54	0.57	0.57	0.57	0.51	0.41
3.2	0.36	0.48	0.44	0.41	0.36	0.29
3.3	--	--	--	--	--	--
3.4	--	--	--	--	--	--
3.5	0.50	0.56	0.51	0.53	0.40	0.34
3.6	0.40	0.57	0.58	0.58	0.50	0.36
3.7	0.42	0.52	0.39	0.45	0.37	0.33
3.8	0.51	0.59	0.56	0.58	0.52	0.46
3.9	0.34	0.55	0.45	0.44	0.41	0.29
3.10	0.54	0.57	0.56	0.54	0.50	0.40
4.1	0.45	0.51	0.49	0.48	0.39	0.36
4.2	0.51	0.59	0.57	0.54	0.52	0.43
4.3	0.54	0.56	0.54	0.56	0.40	0.40
4.4	--	--	--	--	--	--
4.5	--	--	--	--	--	--
4.6	0.56	0.59	0.59	0.58	0.53	0.40
4.7	0.48	0.61	0.49	0.46	0.43	0.35
4.8	0.54	0.54	0.51	0.44	0.44	0.39

Table 3.11. Continued

Site	June 3	June 16	June 30	July 14	July 28	October 2
4.9	0.54	0.56	0.54	0.55	0.49	0.44
4.10	--	--	--	--	--	--
4.11	0.43	0.51	0.44	0.48	0.38	0.38
4.12	0.55	0.61	0.60	0.57	0.58	0.51
4.13	0.49	0.58	0.52	0.53	0.44	0.38
5.1	0.52	0.63	0.60	0.60	0.56	0.43
5.2	0.52	0.58	0.59	0.56	0.55	0.45
5.3	0.52	0.61	0.53	0.51	0.48	0.35
5.4	0.54	0.66	0.63	0.59	0.53	0.38
5.5	--	--	--	--	--	--
5.6	--	--	--	--	--	--
5.7	0.53	0.55	0.56	0.56	0.54	0.41
5.8	--	--	--	--	--	--
5.9	0.50	0.57	0.60	0.59	0.52	0.42
5.10	0.56	0.59	0.61	0.59	0.57	0.46
5.11	0.39	0.53	0.53	0.50	0.48	0.40
5.12	--	--	--	--	--	--
5.13	0.55	0.59	0.60	0.58	0.54	0.43
5.14	0.44	0.56	0.51	0.49	0.43	0.32
5.15	0.50	0.55	0.56	0.54	0.47	0.41
5.16	0.47	0.61	0.52	0.54	0.48	0.34
6.1	--	--	--	--	--	--
6.2	0.37	0.51	0.50	0.47	0.44	0.37
6.3	--	--	--	--	--	--
6.4	0.54	0.61	0.61	0.58	0.60	0.50
6.5	0.52	0.58	0.54	0.51	0.48	0.36
6.6	0.40	0.58	0.57	0.58	0.53	0.37

Table 3.11. Continued

Site	June 3	June 16	June 30	July 14	July 28	October 2
6.7	0.55	0.60	0.61	0.60	0.58	0.46
6.8	0.50	0.61	0.58	0.57	0.54	0.42
6.9	0.49	0.57	0.53	0.54	0.48	0.38
7.1	0.56	0.54	0.55	0.56	0.52	0.39
7.2	0.50	0.57	0.55	0.55	0.52	0.47
7.3	0.51	0.57	0.61	0.58	0.54	0.51
7.4	0.51	0.59	0.51	0.52	0.46	0.47
7.5	0.52	0.58	0.54	0.58	0.51	0.40
7.6	0.61	0.63	0.63	0.62	0.60	0.58
8.1	0.54	0.61	0.60	0.60	0.54	0.45
8.2	0.60	0.61	0.60	0.61	0.59	0.50
8.3	--	--	--	--	--	--
8.4	0.46	0.53	0.50	0.51	0.44	0.38
8.5	0.61	0.61	0.61	0.60	0.56	0.46
8.6	0.53	0.55	0.57	0.55	0.49	0.45
8.7	0.61	0.61	0.59	0.59	0.57	0.51
8.8	0.60	0.62	0.61	0.61	0.59	0.52
9.1	0.59	0.63	0.60	0.60	0.57	0.52
9.2	0.58	0.63	0.61	0.62	0.60	0.47
9.3	0.63	0.64	0.63	0.63	0.62	0.58
9.4	--	--	--	--	--	--
9.5	0.61	0.64	0.66	0.64	0.64	0.52
9.6	0.49	0.54	0.54	0.52	0.47	0.36
9.7	0.61	0.60	0.62	0.61	0.57	0.47
10.1	0.60	0.63	0.62	0.63	0.59	0.48
10.2	0.58	0.63	0.61	0.60	0.54	0.46
11.1	0.56	0.61	0.59	0.58	0.57	0.52

Histograms derived from portable probe and gravimetric volumetric water content data are included as Appendix F. Volumetric water content data collected using the Theta probe were separated into two groups: “shallow” data collected near the surface (i.e. using 5-cm access tubes) and “deep” data collected near the bottom of the soil profile (i.e. from the deepest access tube at each site). Note that data from sites with no tubes deeper than 5-cm were included in the deep histograms but not in the shallow histograms. Also included in Appendix F is a summary of basic statistics for all portable probe, static probe, and gravimetric volumetric water content measurements. The agreement between the distribution of these gravimetric results and the distributions of both the impedance probe and water content reflectometer results supports the validity of the probe measurements as representative of soil moisture conditions for the NDW.

CHAPTER 4

DATA ANALYSIS AND RESULTS

The intent of the hydrologic analyses for Noland Divide Watershed data was to combine the available watershed topographic and meteorological data with soil hydrologic data collected in the field to quantify the watershed hydrologic response to precipitation events, and to thereby advance the general understanding of forested hillslope runoff processes, particularly in the Southern Appalachians. Analyses of data consisted of the following tasks:

1. Delineation of the NDW using survey topography
2. Delineation of two drainage subbasins within the NDW corresponding to the northeast and southwest streamlets
3. Estimation of the spatial variation of soil hydrologic parameters, specifically porosity, saturated hydraulic conductivity, and soil depth
4. Estimation of the spatial distribution of soil moisture storage within the watershed based on biweekly soil moisture measurements
5. Analysis of the relationship between estimated biweekly soil moisture storage and continuous soil moisture records from three monitoring pits
6. Examination of general trends in the variation of soil moisture with depth
7. Analysis of precipitation, streamflow, and soil moisture observations to estimate a water balance for the NDW on a biweekly basis
8. Examination of potential predictors of watershed soil moisture and soil water storage.

Noland Divide Watershed Delineation

Given the topographic survey data for the study area, one of the foremost tasks was the delineation of the Noland Divide Watershed. The 5-meter digital elevation model, the creation of which is detailed in the previous chapter, was used for this purpose.

Watershed delineation based on topographic data

Delineation of the drainage area that contributes to the NDW basin outlet (at the V-notched weirs) was performed considering results from both a single flow direction (D8) and a multiple flow direction (D_{∞}) (Tarboton, 1997) model for DEM flow direction and contributing area accumulation.

The D8 algorithm, introduced by O'Callaghan and Mark (1984) and now a standard approach in digital elevation model analysis, assumes that water at a given DEM grid cell will flow to one of eight adjacent or diagonal neighboring grid cells, in the direction of steepest descent. Once flow directions are defined contributing area is calculated by accumulating the number of upstream grid cells flowing to a given grid cell. A stream is theoretically defined as a string of adjacent or diagonal grid cells with a contributing area greater than a specified threshold. A watershed is delineated by isolating all grid cells that drain to a specified outlet point along a stream. Following the analysis of contributing area for the NDW 5-meter DEM, two watershed outlet points were selected corresponding to the northeast and southwest stream gage weirs. The total of the two resulting watershed subbasin delineations was taken to be the Noland Divide watershed (see Figure 4.1).

The D_{∞} algorithm, developed by Tarboton (1997), is not constrained to eight flow directions, but rather assigns a floating point radian angle between 0 and 2π . This is accomplished for a given grid cell by forming eight triangular facets using the elevations of the eight adjacent and diagonal neighboring grid cells. The magnitude and direction of the vector of steepest descent on these triangular facets is taken to be the flow direction. If the resulting angle aligns with one of the four cardinal or four diagonal directions, the grid cell is said to contribute completely to the corresponding single downslope neighbor. Otherwise contributing area from a given cell is proportioned among two downslope grid cells. The proportion contributing to each is divided by comparing the estimated flow direction to the nearest two direct cardinal or diagonal angles (i.e. the cell that lies in a direction closest to the estimated flow direction is assigned the larger fraction of the contributing cell area). As with the D8 method, two watershed outlet points were selected corresponding to the northeast and southwest stream gage weirs, and the union of the two resulting watershed subbasin delineations was taken to be the Noland Divide watershed (see Figure 4.2).

It should be noted that for watershed delineation purposes, both the D8 and the D_{∞} flow direction determinations require a preliminary processing step to fill pits in the DEM (low elevation grid cells with no downstream neighbors).

One of the primary differences in the D_{∞} method as compared with the D8 method is that all grid cells that have the potential to contribute even a small fraction of runoff to a specified watershed outlet are included in the D_{∞} watershed delineation. This result tends to expand the watershed delineation beyond the physical watershed boundaries. In addition, the proportioning of contributing area used in the D_{∞} method

results in overlap between adjacent subbasins due to them sharing common or shared grid cells.

The D8 and D_{∞} methods define the lower and upper limits, respectively, for drainage area delineation. While the D8 method may not capture the total physical watershed area, the D_{∞} method often leads to the inclusion of boundary areas unlikely to physically contribute to watershed streamflow, and also does not allow for the delineation of separate subbasins within a watershed.

Consequently, a method based on the dependence function (Tarboton, 1997) calculated from the D_{∞} flow directions was used to delineate the overall NDW drainage basin and the northeast and southwest subbasins within the drainage basin. Given the D_{∞} flow directions, and a specified stream outlet, the dependence function algorithm calculates the proportion, as a number between zero and one, of each upslope grid cell contributing to the outlet. By selecting a dependence threshold (between zero and one), grid cells that contribute relatively little to a specified outlet point can be excluded from the watershed being delineated. In addition, where there is overlap between adjacent D_{∞} dependence areas, the boundaries of watershed subbasins can be delineated using the largest dependence value.

For the NDW, a dependence threshold value of 0.1 or greater was used to delineate the watershed. This value was arrived at by trial and error, seeking an overall watershed delineation result relatively consistent with a manual delineation using a USGS quadrangle map (a USGS quadrangle map was used for comparison since this is often the basis of watershed delineation in engineering practice when more detailed data is not available). The watershed delineations resulting from the three methods described

above are shown in Figures 4.1, 4.2, and 4.3. Also shown are delineation results for the northeast and southwest subbasins within the watershed. Contours generated from the 1992 topographic survey of the watershed are included in these figures for reference. Note how the delineation using the dependence function (Figure 4.3) results in watershed boundaries more consistent with what might be inferred from the 1992 survey contours, relative to the results in Figures 4.1 and 4.2 which show grid biases manifested by straight edges along grid directions.

Drainage culverts crossing the highway

The three watershed delineations shown in Figures 4.1, 4.2, and 4.3 were further refined by taking into account the highway dividing the upper area of the watershed from the lower. Water from the upper portion of the watershed reaches the lower through two culverts running underneath the road. A ditch along the uphill side of the highway diverts any runoff from the upper portion of the watershed through these culverts.

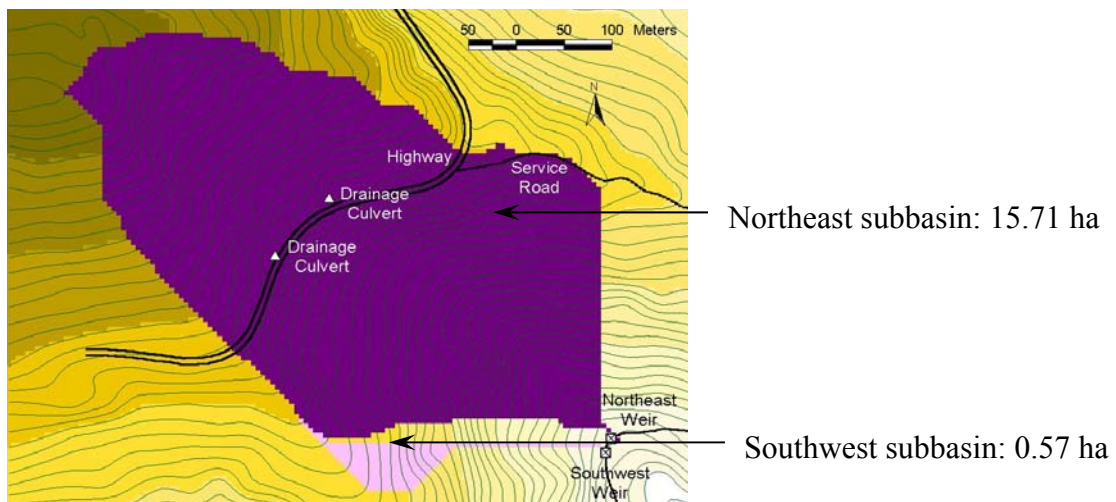


Figure 4.1. D8 watershed delineation for the NDW.

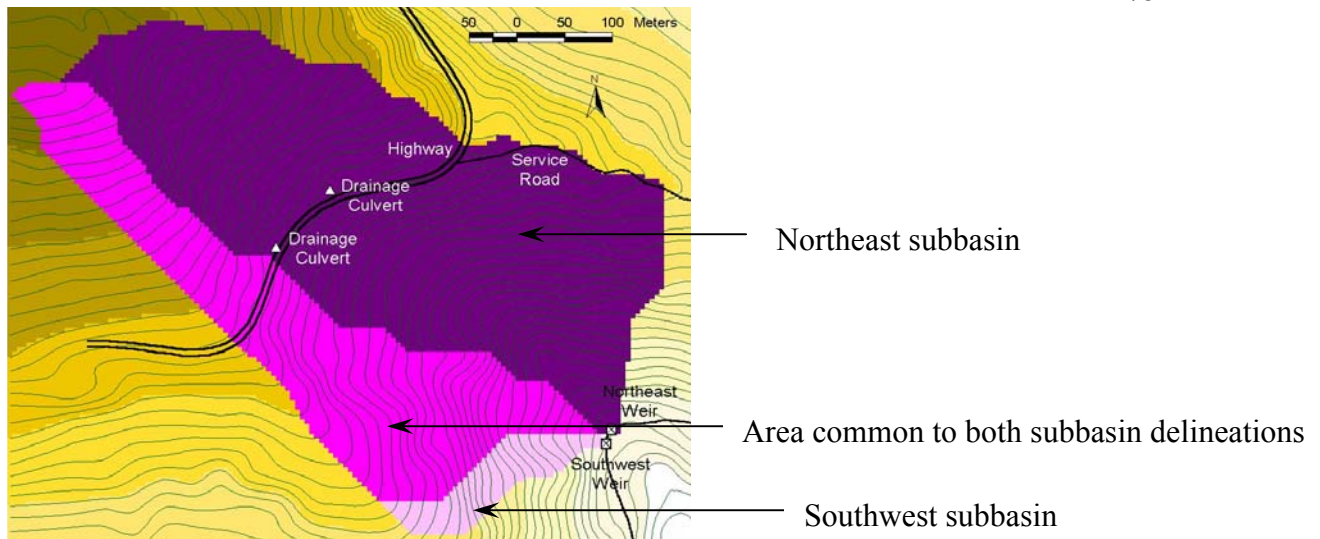


Figure 4.2. D_{∞} watershed delineation for the NDW.

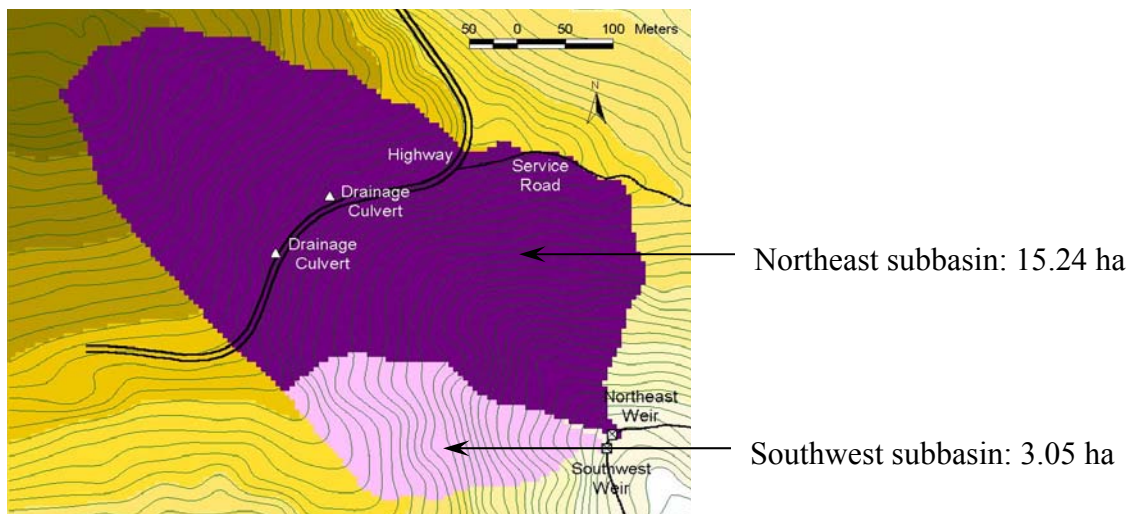


Figure 4.3. Dependence function watershed delineation for the NDW.

The culvert with the lowest elevation of the two crosses the road near the middle of the watershed. All upper watershed drainage arriving at the ditch downstream of the inlet to the lower culvert is conveyed along the highway and outside of the watershed. To account for this in the watershed delineation, an artificial barrier was created within the 5-meter DEM, and the three delineation methods described previously were applied at the inlet to the lowest elevation highway-crossing culvert to delineate the upper

watershed. The three methods were subsequently applied to the northeast and southwest streamlets to determine the lower subbasin areas. The results of these revised watershed delineations are shown in Figures 4.4, 4.5, and 4.6. A summary of the overall watershed delineated drainage area and subbasin results is given in Table 4.1. The revised dependence function watershed delineation resulted in an estimated drainage area of 17.24 hectares. This result was the final value used in subsequent calculations involving drainage area.

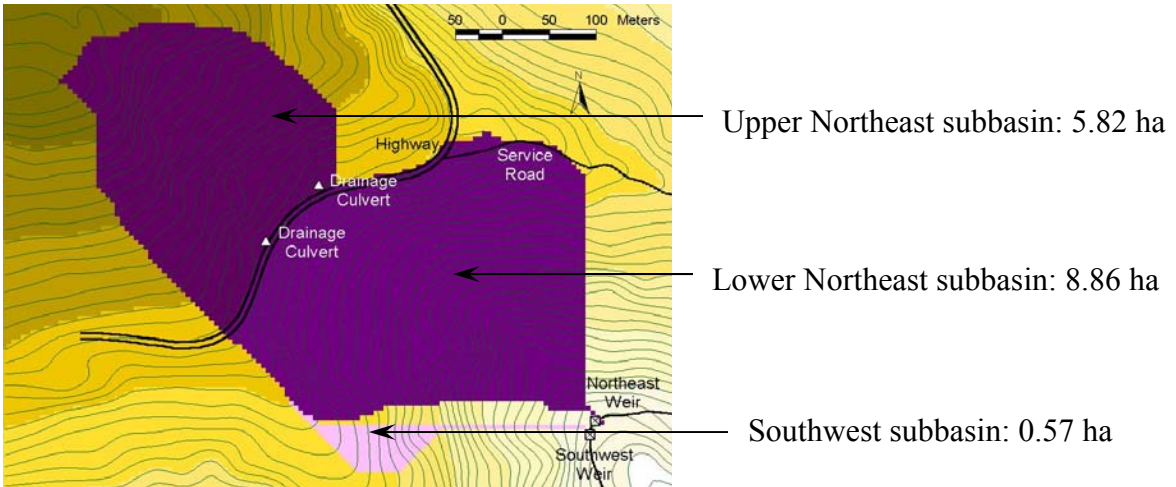


Figure 4.4. D8 watershed delineation for the NDW (revised for highway drainage culverts).

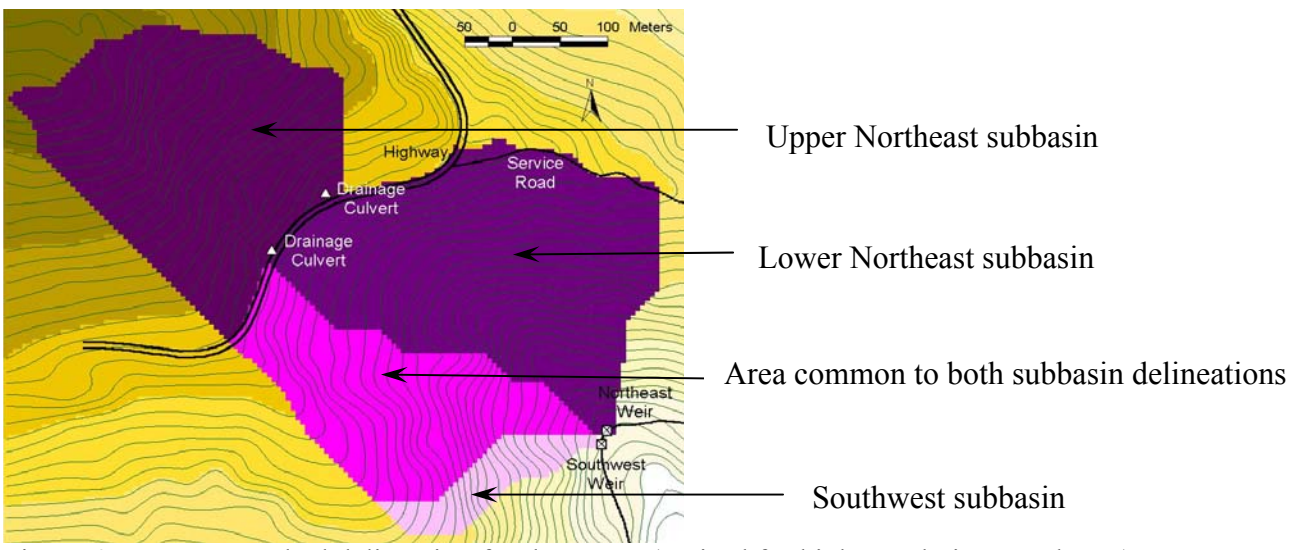


Figure 4.5. D ∞ watershed delineation for the NDW (revised for highway drainage culverts).

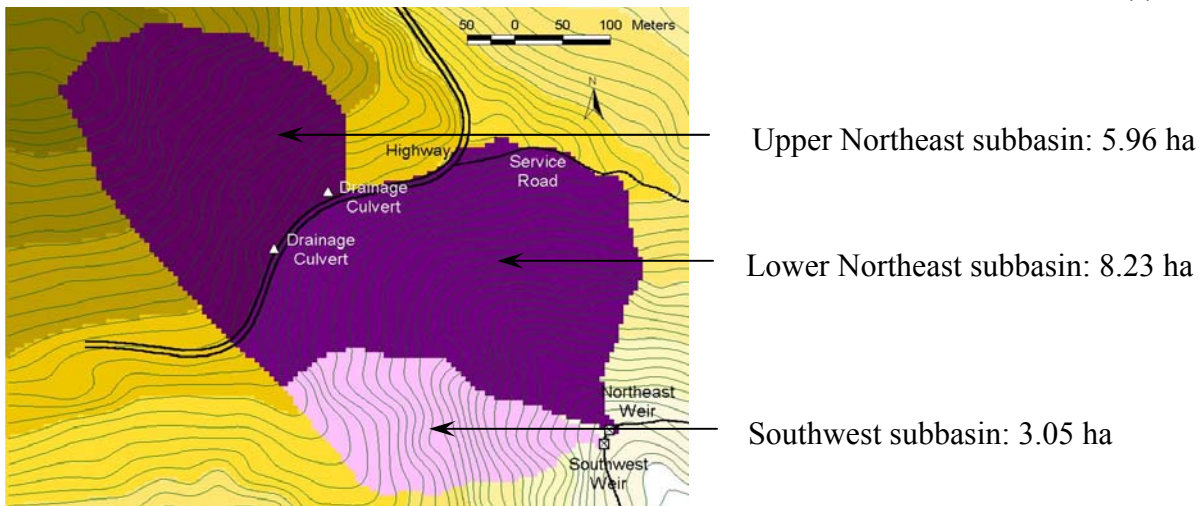


Figure 4.6. Dependence function watershed delineation for the NDW (revised for highway drainage culverts).

For comparison, manual delineations of the watershed were completed using contours generated from survey topography as well as USGS quadrangle map contours. The results of these delineations are included as Figures 4.7 and 4.8, respectively, and corresponding watershed and subbasin areas are shown in Table 4.1.

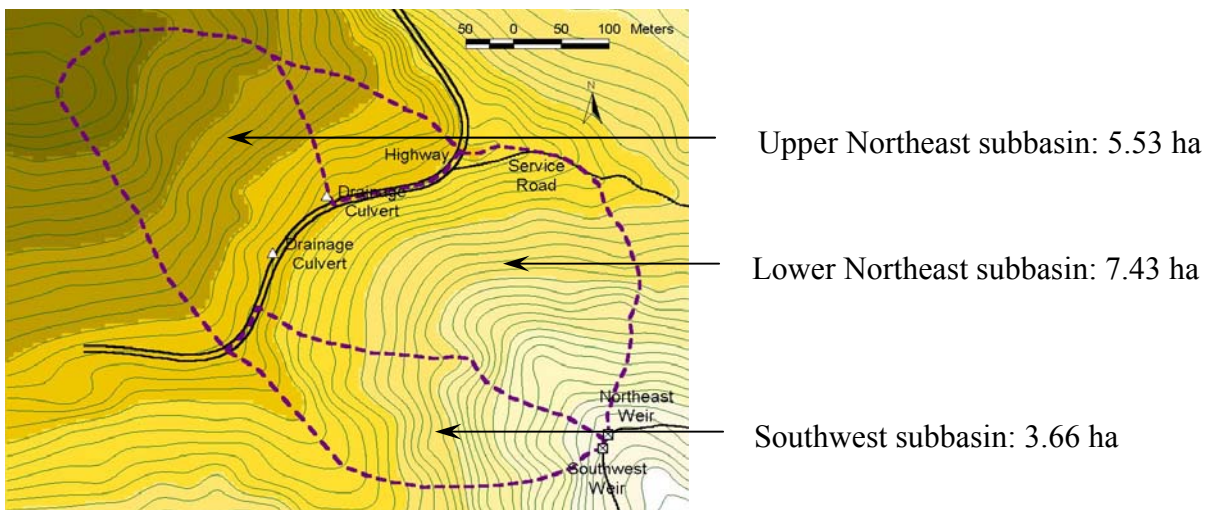


Figure 4.7. Manual watershed delineation for NDW using contours generated from topographic survey.

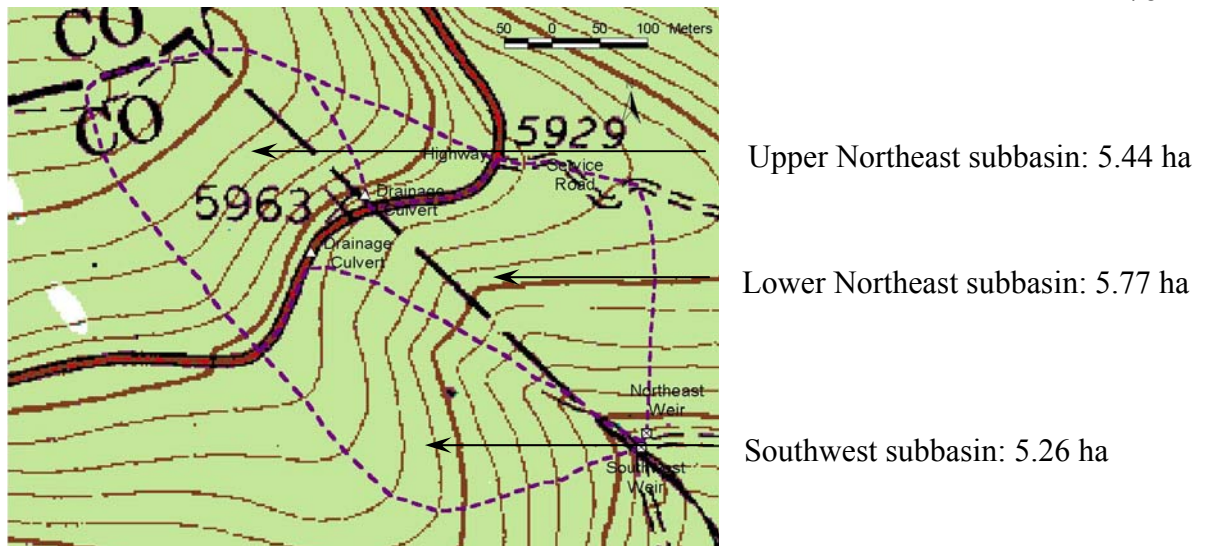


Figure 4.8. Manual watershed delineation for NDW using USGS quadrangle map.

Discussion of northeast and southwest subbasin delineation results

The final result of the dependence function delineation of the two subbasins within the NDW contributing to the northeast and southwest streamlets (see Figure 4.6) indicates that precipitation falling on the area of the watershed above the highway eventually drains entirely through the northeast outlet. If this subbasin delineation were correct, a similar proportionality would likely be apparent in observed flows. The estimated size of the subbasin areas implies that approximately 80 percent of the total flow discharging through the two weirs comes from the northeast outlet, while approximately 20 percent comes from the southwest. In other words, observed streamflow at the northeast weir should be, on average, about four times the observed streamflow at the southwest weir.

Table 4.1. Summary of results for NDW drainage basin delineation

Method	Northeast Subbasin Area (m ²)	Southwest Subbasin Area (m ²)	Total Drainage Area (m ²)	Total Drainage Area (ha)
D8	157,050	5,725	162,775	16.28
D ∞	193,100 ⁽¹⁾	71,075 ⁽¹⁾	202,250	20.23
Dependence Function	152,375	30,475	182,850 ⁽²⁾	18.29
5-Meter DEM Contours	144,338	36,640	180,978	18.10
Quadrangle Map Contours	124,017	52,569	176,586	17.66
<i>Modified Results Accounting for Highway Drainage Culverts</i>				
D8	146,700	5,725	152,425	15.24
D ∞	183,500 ⁽¹⁾	49,650 ⁽¹⁾	192,650	19.27
Dependence Function	141,925	30,475	172,400 ⁽²⁾	17.24
5-Meter DEM Contours	129,576	36,640	166,216	16.62
Quadrangle Map Contours	112,141	52,569	164,710	16.47

(1) The D ∞ method is not suited to subbasin delineation. The northeast and southwest subbasin area results using this method include overlapping areas and cannot be added together to estimate total drainage area.

(2) Total drainage area delineated by applying a dependence threshold of 0.1.

A comparison of measured flows from the existing streamflow record for the period from 1992 to 1999 indicates that the northeast flow is, in general, greater than the southwest; however, a comparison of daily streamflow volumes shows that generally the northeast flow is approximately 1.3 to 1.5 times greater than the southwest flow. The

probable reason behind the discrepancy is that the scale of the surveyed topography is not suited to reliable small-scale (i.e. subbasin) delineation efforts. This is also apparent when looking at a contour map of the basin. The ridges defining the overall basin are clearly distinguishable, while subbasin delineations are not as apparent and less reliably definable.

The overall watershed area delineation using the dependence function is considered acceptable given its consistency with a manual delineation using contours generated from the topographic survey data, with the concession that delineation of subbasins within the watershed is not achievable to a satisfactory level of accuracy under the constraints of the given data.

Spatial Distribution of Soil Hydrologic Parameters

As discussed in the previous chapter, field measurements of soil saturated hydraulic conductivity, soil porosity, and soil depth were taken during the summer of 1999 at 51 sites across the NDW. These measurements provided a basis for estimation of the spatial distribution of these soil hydrologic parameters. These estimates were combined with estimates of the spatial distribution of soil moisture (derived from biweekly measurements) to examine spatially distributed soil saturation and soil water storage. The estimated spatial distributions of soil parameters were also compared with spatially distributed soil moisture estimates to examine the predictive potential of one or more of the three soil hydrologic parameters listed above, as well as other common watershed wetness indicators.

The following five sets of measurements and results were compiled in a database

with 51 records (one for each sample site) along with sample site spatial coordinates:

1. Soil saturated hydraulic conductivity
2. Natural log of soil saturated hydraulic conductivity
3. Soil porosity
4. Soil porosity adjusted to account for soil organic content
5. Soil depth

This database was imported into ArcView and a 5-meter grid was interpolated for each result using the Spatial Analyst tension spline interpolation algorithm with default parameters. Spline interpolation was selected for this and all subsequent spatial interpolations based on the assumption that the soil hydrologic parameters in question vary relatively smoothly between sampling locations. The spatial distribution of each parameter was estimated for an area extending slightly beyond the delineated watershed extents in order to include all of the actual measured data.

Soil saturated hydraulic conductivity

Measurements of soil saturated hydraulic conductivity taken using the Guelph permeameter were used to estimate the spatial distribution of this parameter. The resulting map is shown in Figure 4.9. The estimated saturated hydraulic conductivity at point C5900 was not included in this interpolation, since the measurement taken at this location was considered unreliable. Multiple permeameter tests were conducted in the area surrounding this site, only one of which was successfully completed. The reason for these test failures was a very shallow soil layer (less than 15 cm) underlain by large rock with intermittent voids. These voids generally led to collapse of the permeameter borehole and draining of the entire apparatus in a matter of seconds. The single

successful permeability measurement at this site was significantly higher than any other permeameter test completed in the watershed and was therefore not considered representative of the same soil matrix infiltration mechanism observed at other sites.

To alleviate problems associated with interpolation of data over a wide range of magnitudes, the natural logarithm of saturated hydraulic conductivity was also taken for each data point. The estimated spatial distribution resulting from this interpolation is shown in Figure 4.10. Figure 4.10 reveals a general pattern of higher soil hydraulic conductivities along the lines of drainage concentration within the watershed. Ridges along the outside watershed boundaries as well as within the watershed generally appear to have lower soil saturated hydraulic conductivities.

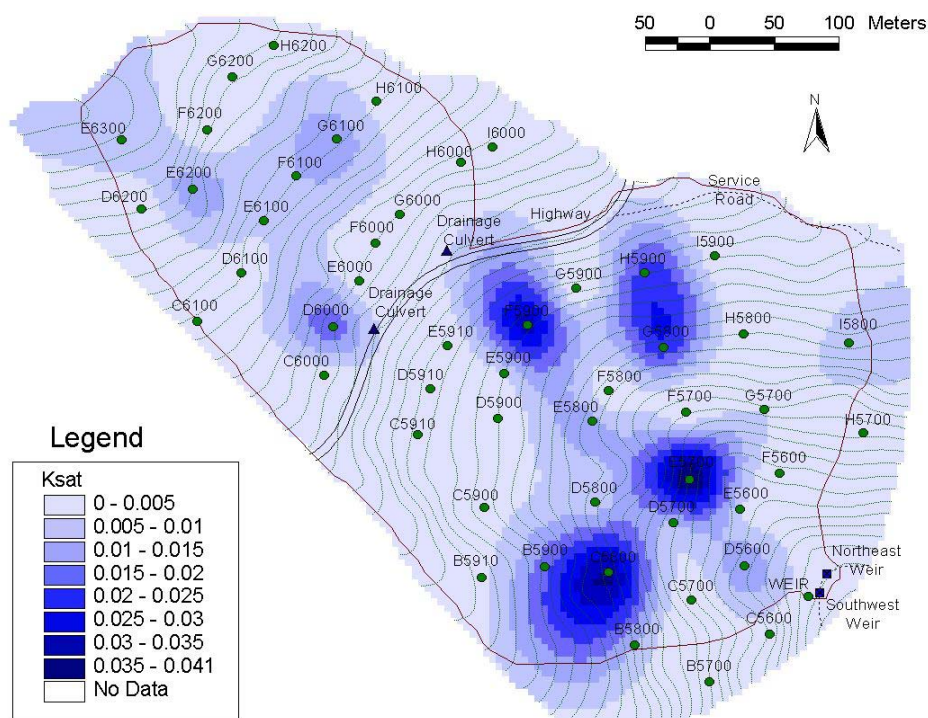
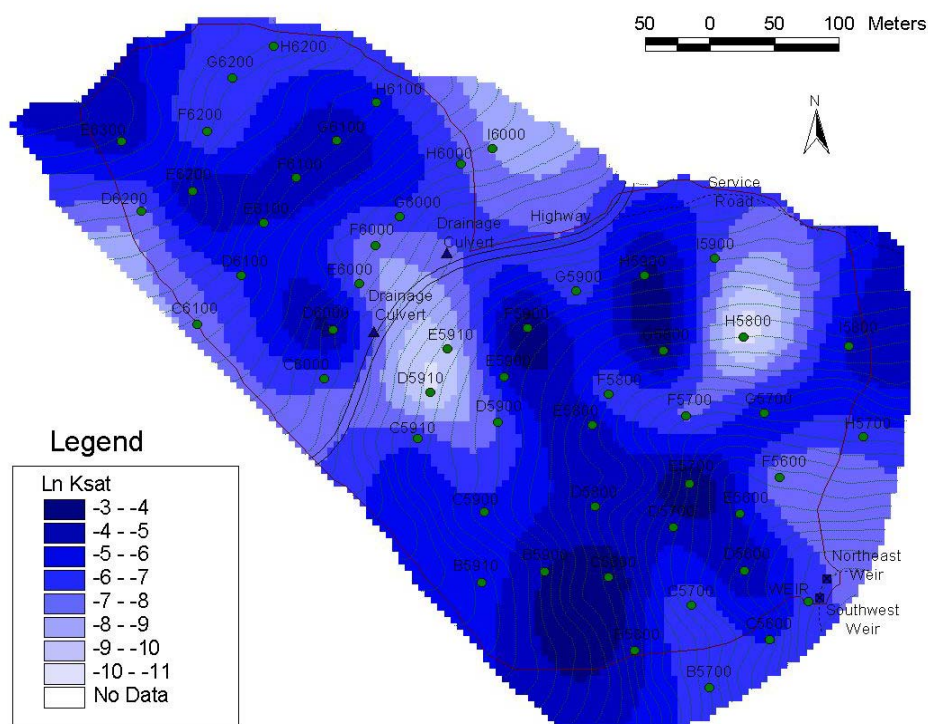


Figure 4.9. Estimated spatial distribution of soil saturated hydraulic conductivity (cm/s).



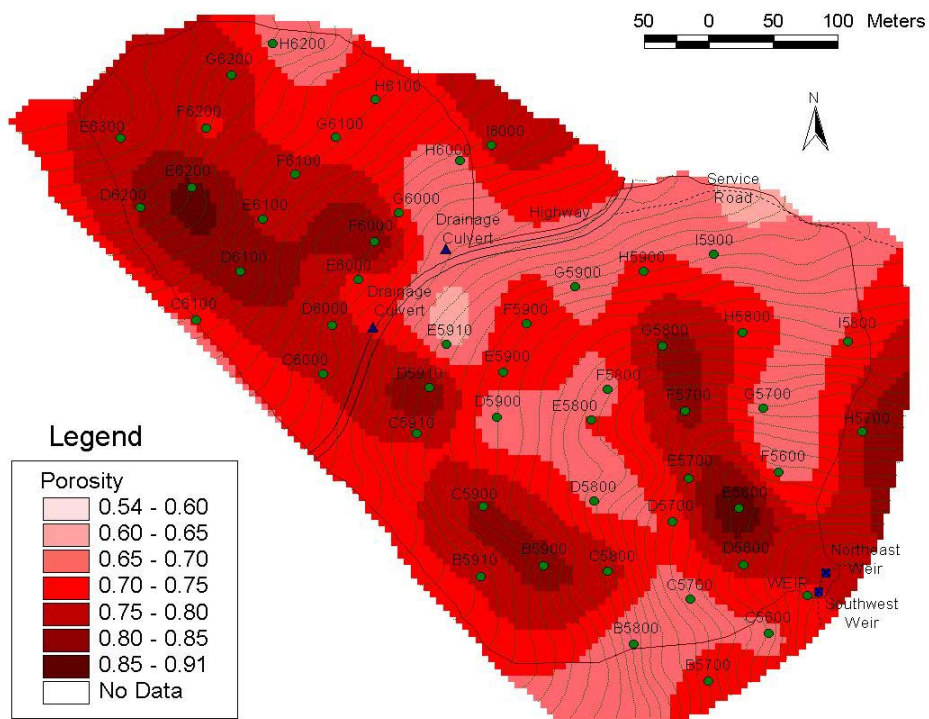


Figure 4.11. Estimated spatial distribution of soil porosity.

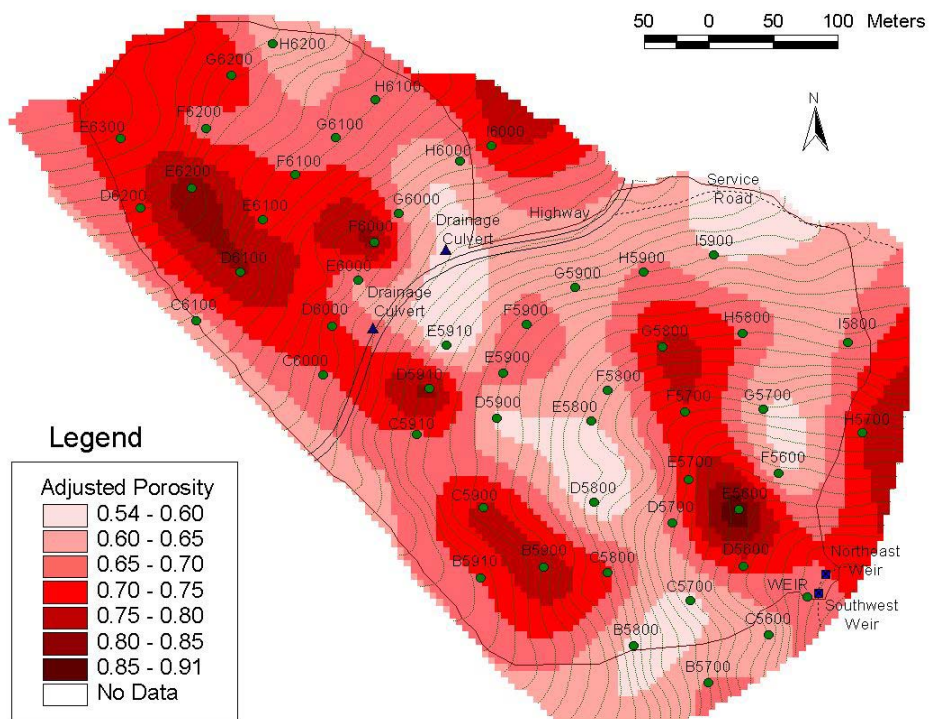


Figure 4.12. Estimated spatial distribution of soil porosity (adjusted for soil organic content).

Soil depth

The result of the interpolation of soil depths measured at the 51 sample sites across the watershed is shown in Figure 4.13. With the exception of sites E5600 and F5600, the depth of soil (measured as the distance from the ground surface to probe refusal) in the watershed is smallest along the central drainage and greatest near the southwest, northeast, and western watershed boundaries or ridges.

It is important to note that the purpose of soil depth measurement and interpolation as pertains to this work was to quantify the thickness of the soil profile that actively accepts, stores, and conveys rainfall to the streamlets. For this reason, effective soil depth as measured and quantified here represents the thickness of the soil matrix above the effective impermeable layer. It is recognized that the effective depth where water begins to move in a lateral rather than a vertical direction may be less than the absolute depth to competent bedrock, as evidenced by the pit excavations in excess of the depths shown in Figure 4.13.

Potential Soil Water Storage

The estimates of soil depth and soil porosity (adjusted for soil organic content) were combined to estimate the spatial distribution of soil water storage potential across the watershed, based on the following:

$$\text{Potential Soil Water Storage} = \text{Soil Porosity} * \text{Soil Depth}$$

The result is shown in Figure 4.14. As expected based on the estimates of the spatial distribution of soil porosity and depth, soil water storage potential is generally lowest along the drainage concentration lines in the watershed, and increases moving outward toward the ridges which define the watershed boundaries.

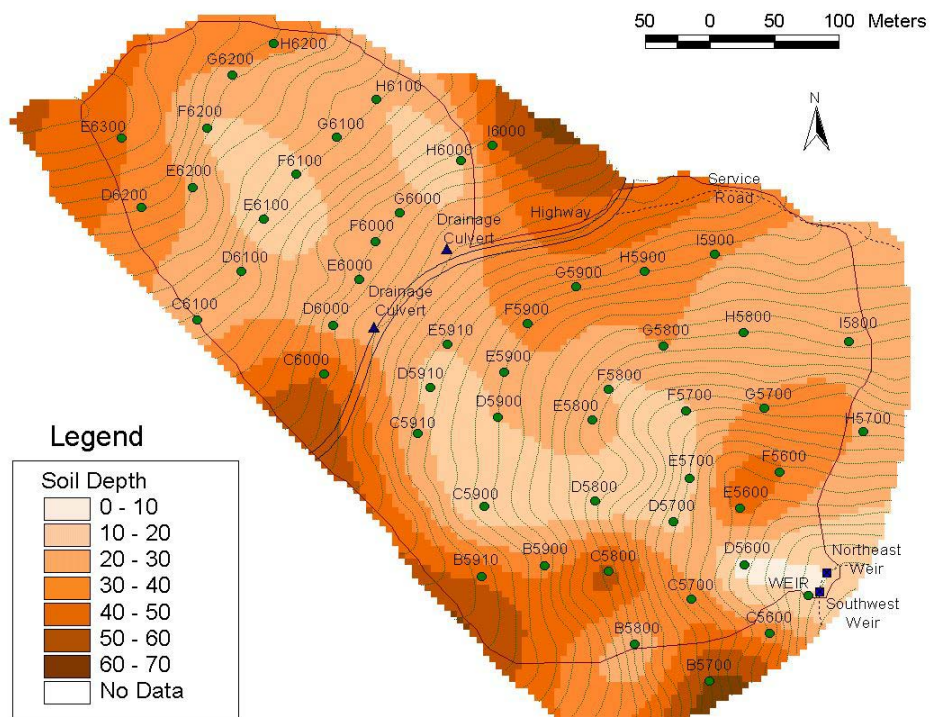


Figure 4.13. Estimated spatial distribution of soil depth (cm).

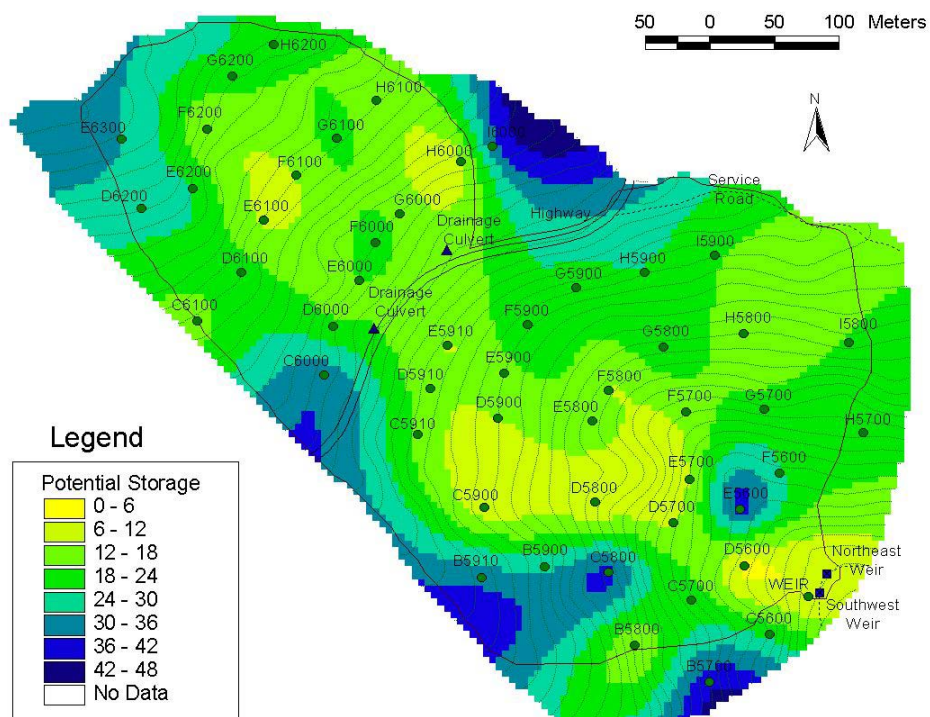


Figure 4.14. Estimated spatial distribution of potential soil water storage (cm).

Clipping the interpolated soil water storage map to the delineated watershed extents (see Figure 4.6), summing the estimated soil water storage in all grid cells, and multiplying this result by the area of a grid cell yields an estimate of the watershed total potential soil water storage volume. The result of this calculation for the NDW is 33,602 cubic meters of potential soil water storage, equivalent to an average potential water storage depth of approximately 19.5 cm.

Spatial Distribution of Soil Moisture

Biweekly measurements of soil volumetric water content for 66 soil moisture sampling sites in the NDW were used to estimate the spatial distribution of soil moisture for each of six observation days. As detailed in Chapter 3, soil volumetric water content measurements were taken at multiple depths for each sampling site. The single-site measurements were combined to estimate the average soil moisture condition at each site location. Spatial interpolation of soil volumetric water content was accomplished using the same method used to estimate the spatial distribution of soil saturated hydraulic conductivity, porosity, and depth. The resulting 5-meter grids for each sampling occasion are shown in Figures 4.15 through 4.20.

The following items should be noted for estimates of spatial distribution based on the biweekly measurements of soil volumetric water content:

1. Measurements were taken at 66 of the 81 sites shown in Figure 3.7. Only sites where measurements were taken are shown in Figures 4.15 to 4.20. (Shallow soils at the other 15 sites shown in Figure 3.7 precluded the installation of probe access tubes.)

2. There were no soil moisture sample sites established in the northeast area of the lower watershed (directly below the service road). Interpolation results in this and other areas of the watershed lacking sampling locations have a higher degree of uncertainty.

Furthermore, spatially distributed soil moisture results are presented here as snapshots of soil moisture patterns in the watershed. This is not actually the case, since each set of soil moisture measurements was taken over the course of approximately eight to ten hours. The general weather conditions on each of the sampling occasions are given in Table 3.10. As described in the previous chapter, sampling progressed from the top of the watershed to the bottom of the watershed. Therefore on days when it was raining and moisture content was increasing there may be an upward bias to those measurements collected last at the bottom of the watershed. Similarly, on drying days following rain the later measurements may show downward bias. Figures 3.10, 3.11, and 3.12, showing continuously monitored soil moisture at three locations, indicate small changes in soil moisture during the sampling days, so potential biases associated with the length of the sampling time were ignored.

Rainfall conditions on each of the sampling occasions are reflected in the volumetric water content results, i.e. the wettest day (June 16) resulted in the highest average volumetric water content, while the driest day (October 2) resulted in the lowest average volumetric water content. This is consistent with the approximate response times observed at the continuously monitored pits (on the order of hours to days), since precipitation occurred on the day or days just prior to wet measurement occasions. Table 4.2 shows volumetric water content averages on each of the six sampling occasions, for

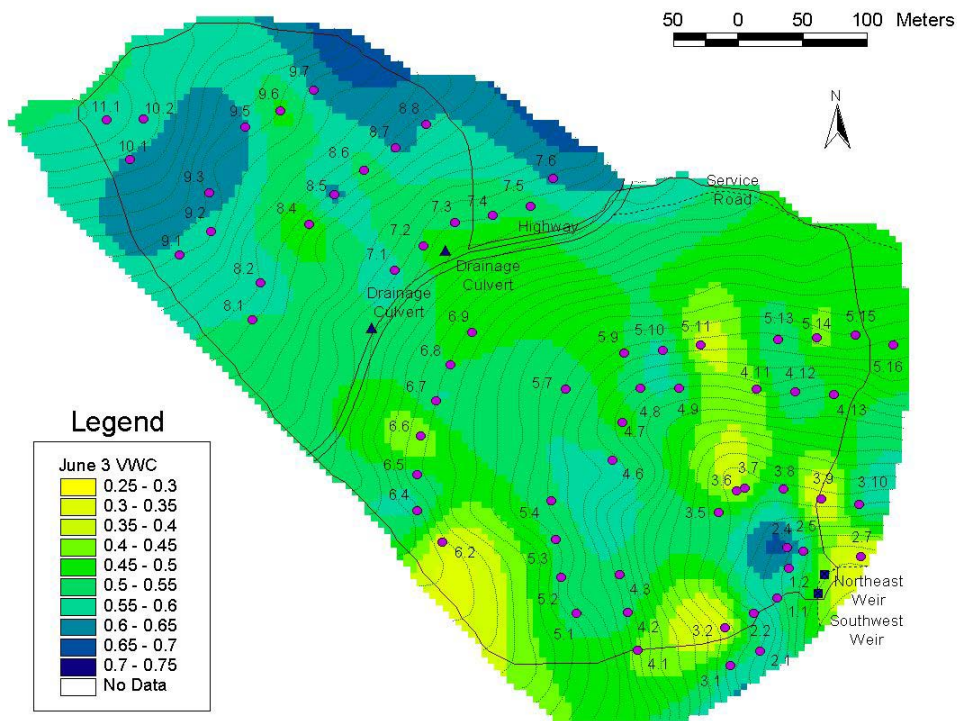


Figure 4.15. Estimated spatial distribution of volumetric water content for June 3, 1999.

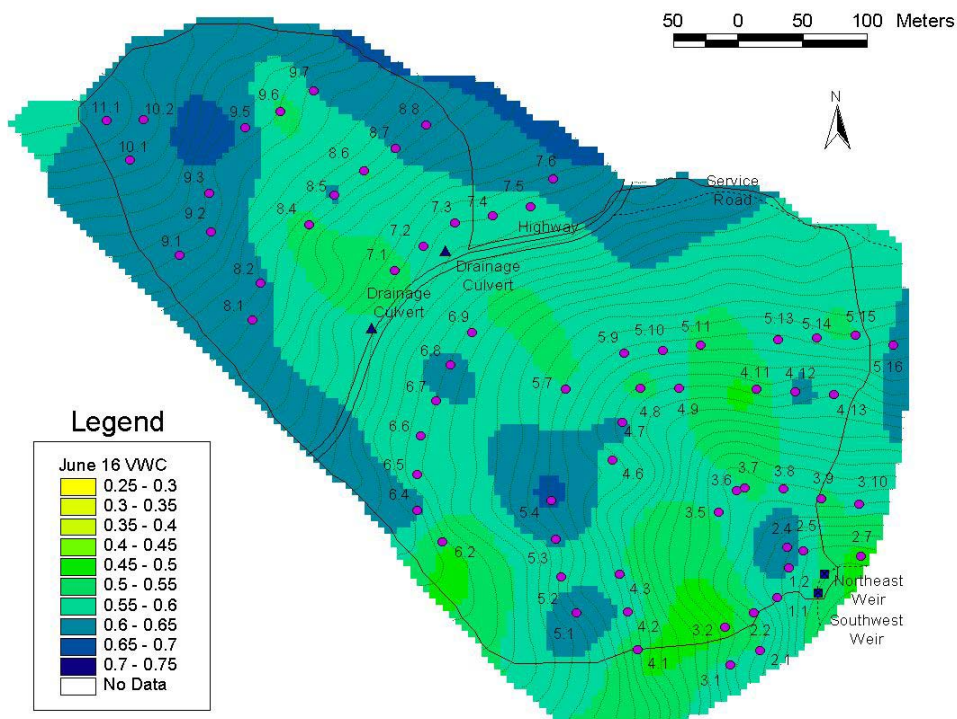


Figure 4.16. Estimated spatial distribution of volumetric water content for June 16, 1999.

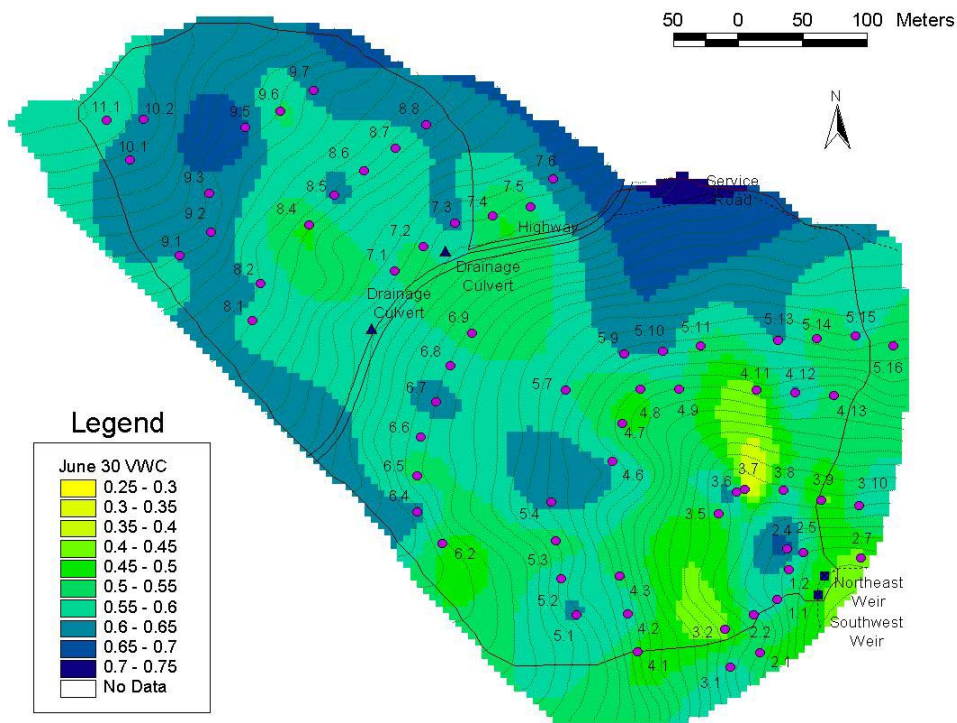


Figure 4.17. Estimated spatial distribution of volumetric water content for June 30, 1999.

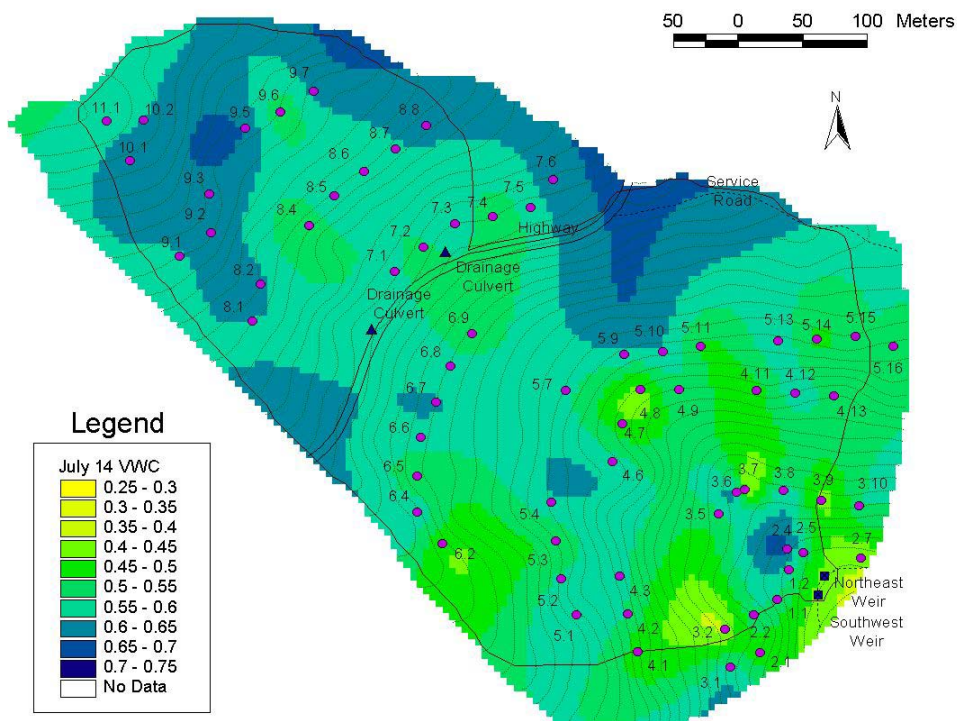


Figure 4.18. Estimated spatial distribution of volumetric water content for July 14, 1999.

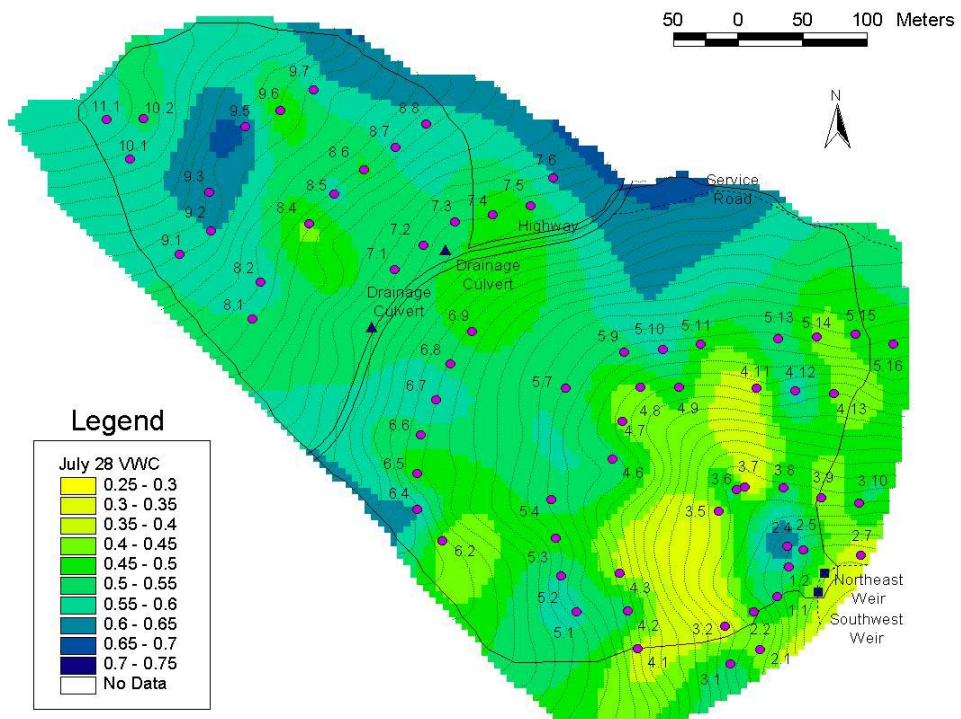


Figure 4.19. Estimated spatial distribution of volumetric water content for July 28, 1999.

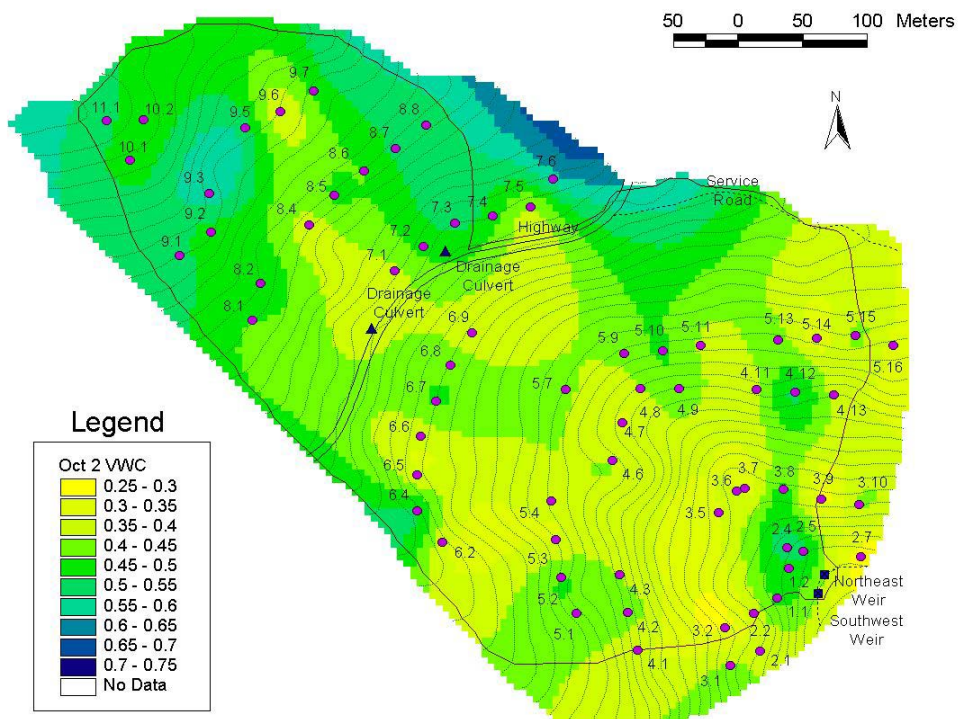


Figure 4.20. Estimated spatial distribution of volumetric water content for Oct 2, 1999.

all points as well as for the 11 sample line elevations (measurement points were established approximately along contour lines).

The estimated spatial distribution of soil moisture for June 3 shows the wettest areas high in the watershed, with the driest areas interspersed in the lower central region of the lower watershed. This general pattern is observable on all sampling occasions, including both the wettest day (June 16) and the driest (October 2). The estimated spatial distribution for June 16 displays the effects of rainfall during the previous night as well as throughout the day (refer to Appendix D for a complete record of rainfall and total streamflow for May through October 1999).

Table 4.2. Sample line volumetric water content averages on six sampling occasions

Sample Line	Average Elevation (meters)	Sampling Date					
		June 3	June 16	June 30	July 14	July 28	Oct 2
1	1686	0.586	0.605	0.578	0.564	0.539	0.477
2	1688	0.532	0.577	0.570	0.539	0.501	0.449
3	1705	0.470	0.554	0.528	0.531	0.471	0.386
4	1744	0.536	0.571	0.546	0.534	0.476	0.432
5	1762	0.526	0.594	0.592	0.575	0.542	0.426
6	1798	0.491	0.602	0.588	0.577	0.553	0.429
7	1821	0.528	0.593	0.574	0.578	0.530	0.503
8	1855	0.574	0.597	0.590	0.592	0.556	0.488
9	1880	0.591	0.608	0.613	0.602	0.571	0.491
10	1910	0.594	0.632	0.618	0.617	0.579	0.473
11	1918	0.563	0.611	0.586	0.577	0.574	0.516
All Sites	--	0.546	0.593	0.583	0.573	0.534	0.462

The estimated spatial distributions of soil moisture for June 30 and July 14 are similar to one another, reflecting rainfall on the previous day. The pattern is apparently not significantly altered by cloud conditions; the average watershed soil moisture condition on the sunny day (June 30) is similar in wetness and spatial pattern to the average watershed soil moisture condition on a cloudy day (July 14). Here again, it appears that the weather on the day prior to sampling had a greater effect on soil moisture conditions than weather on the sampling day.

The same holds true for the somewhat drier pattern shown on July 28, four days after a rainstorm. This pattern shows significant retention of soil moisture. In addition, although the watershed mean volumetric water content on this occasion is nearly equal to the watershed mean volumetric water content for June 3, the moisture is slightly more evenly distributed across the watershed. The estimated spatial distribution of soil moisture for October 2 reflects small storms in the previous week, preceded by a prolonged period of relative drought.

Spatial distribution of degree of soil saturation

The estimated spatial distributions of soil volumetric water content were combined with the estimated spatial distribution of soil porosity to create maps of the degree of soil saturation for the NDW and surrounding area. One map was created for each of the six sampling occasions. Note that estimated spatial distributions of volumetric water content on each sampling occasion are based on averages of measurements at multiple depths, for each of the 66 measurement sites.

The results of the spatial interpolation of porosity (using the values adjusted to account for soil organic content) are considered an estimate of spatially distributed

maximum volumetric water content for the watershed. Degree of saturation was estimated using the following relationship:

$$\text{Degree of Soil Saturation} = \text{Soil Volumetric Water Content} / \text{Soil Porosity}$$

The resulting degree of saturation maps included some areas of extrapolation (the northeast area of the lower watershed and in the portion of the upper watershed near the northeast watershed boundary) with estimated degree of soil saturation values slightly greater than one. Corrections were applied to all six maps in these regions, limiting the maximum degree of saturation to one. The estimated spatially distributed degree of soil saturation results are shown in Figures 4.21 through 4.26. The delineated watershed boundary is also included in these figures for reference. It appears that only relatively small portions of the watershed approached saturation (discounting areas south of the Forest Service road where extrapolated values are likely due to edge effects). This is consistent with the lack of overland flow observed in the field on days of significant rainfall. This result also seems to indicate that soil matrix infiltration and soil profile drainage along the soil-rock interface are rapid enough to prohibit full profile saturation during heavy precipitation.

Watershed soil water storage

The watershed potential soil water storage estimated previously (see Figure 4.14) and clipped to the delineated watershed extents was multiplied by each of the six soil saturation distributions to arrive at a spatially distributed average of soil water storage for the NDW on each of the six sampling occasions. This estimation is based on the following relationship, applied to each grid cell in the watershed:

$$\text{Soil Water Storage} = \text{Potential Soil Water Storage} * \text{Soil Saturation}$$

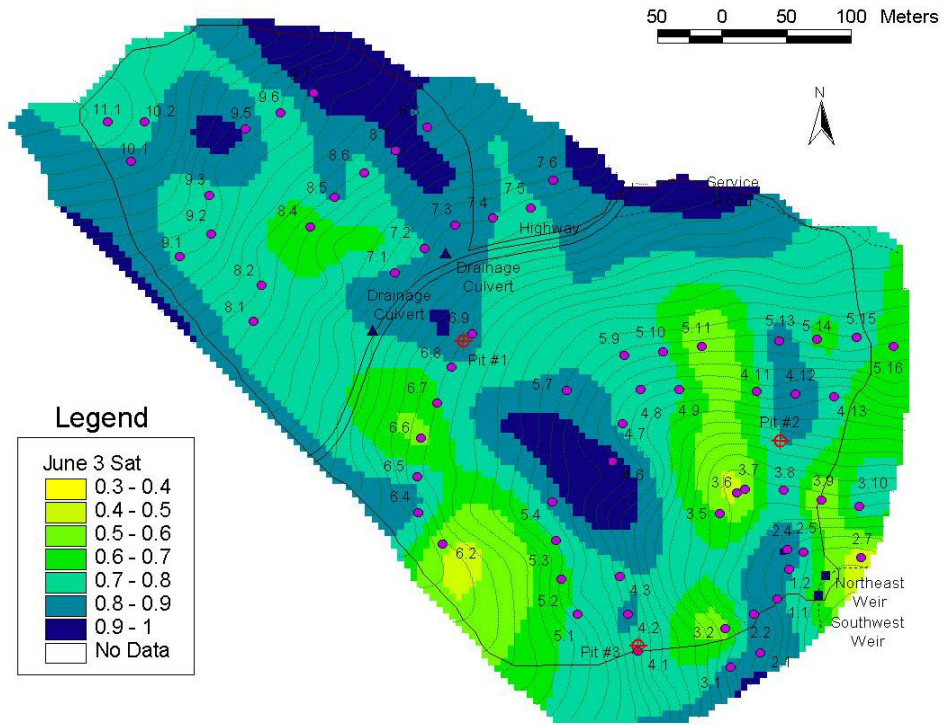


Figure 4.21. Estimated watershed degree of saturation pattern for June 3, 1999.

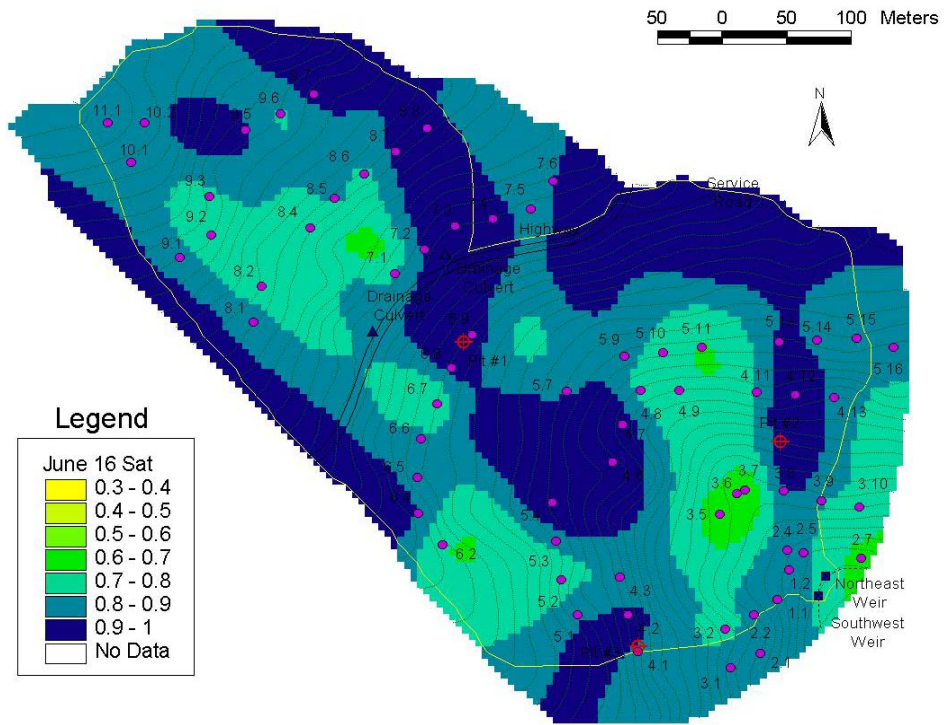


Figure 4.22. Estimated watershed degree of saturation pattern for June 16, 1999.

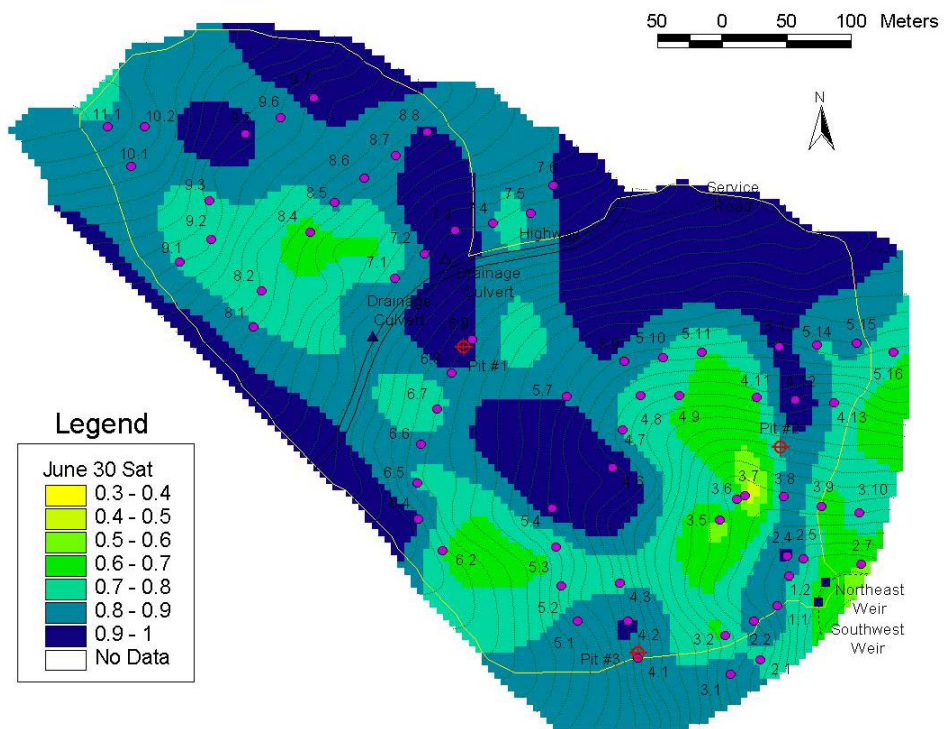


Figure 4.23. Estimated watershed degree of saturation pattern for June 30, 1999.

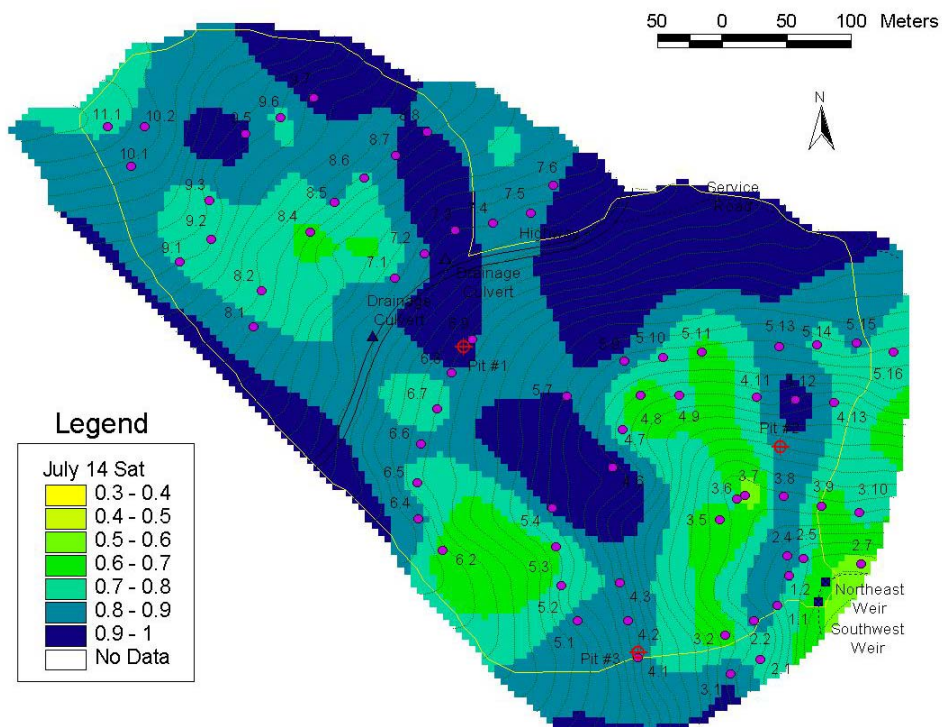


Figure 4.24. Estimated watershed degree of saturation pattern for July 14, 1999.

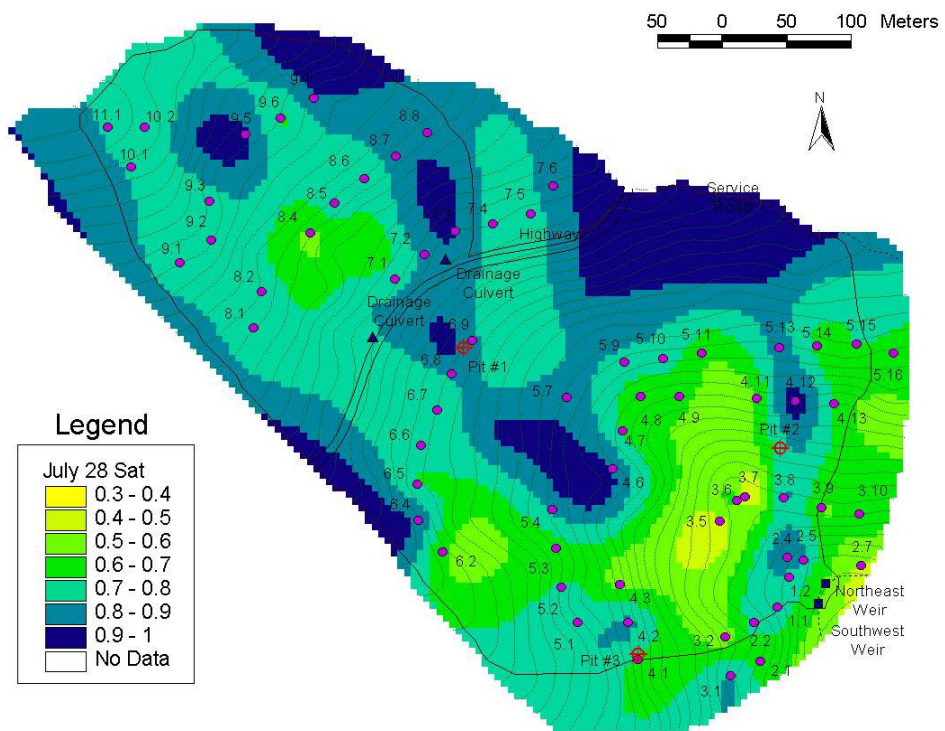


Figure 4.25. Estimated watershed degree of saturation pattern for July 28, 1999.

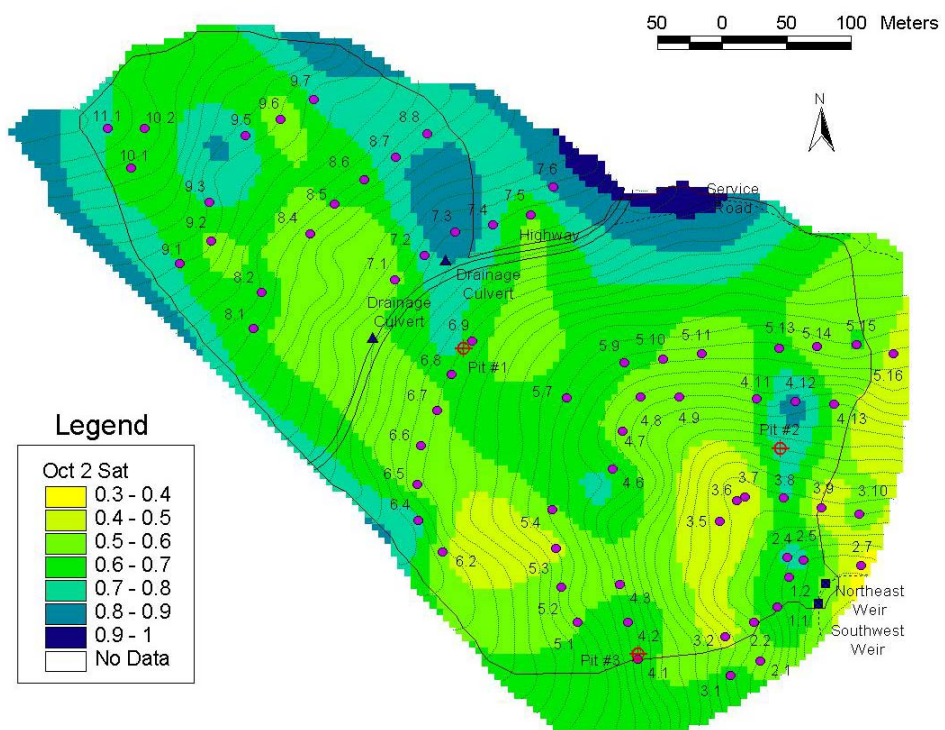


Figure 4.26. Estimated watershed degree of saturation pattern for October 2, 1999.

This particular form of the relationship was used in this case, rather than the more direct calculation of the product of soil volumetric water content and soil depth, since the saturation values were corrected to eliminate regions where estimated soil water storage exceeds estimated potential soil water storage.

The estimated average equivalent depths of water stored in the soil for each of the sampling occasions are shown in Table 4.3.

Examination of potential relationships between soil hydrologic parameters and soil moisture

Any one of the three measured soil hydrologic parameters could justifiably be assumed to have a distinguishable effect on soil volumetric water content: soil saturated hydraulic conductivity, representative of the infiltration rate upper limit or rate of soil drainage; soil porosity, a measure of maximum potential volumetric water content; and soil depth, which sets the location of soil moisture profile boundary conditions.

Since the 51 soil hydrologic parameter measurement sites were not coincidental with the 66 synoptic volumetric water content measurement sites, the interpolated soil

Table 4.3. Watershed average soil water storage

Sampling Date	Equivalent Depth (cm)	Volume (m³)
June 3, 1999	14.71	25,360
June 16, 1999	16.68	28,756
June 30, 1999	16.36	28,205
July 14, 1999	16.26	28,032
July 28, 1999	14.96	25,791
October 2, 1999	12.28	21,171
Potential Storage	19.49	33,601

saturated hydraulic conductivity, soil porosity, and soil depth maps were used to estimate these soil hydrologic parameters at each of the biweekly volumetric water content sampling sites. The results were plotted against the volumetric water content measurements for each of the six sampling dates. A list of the potential relationships examined is presented in Table 4.4. In addition to the three soil parameters listed, a typical topographic wetness index was estimated for each of the 66 soil moisture sampling sites, using the following equation:

$$Wetness\ Index = Ln\left(\frac{a}{Tan\beta}\right)$$

where “a” represents the upstream contributing area per unit contour width (A/b) for a given grid cell and β is the estimated topographic slope angle at the cell location. For grid data, unit contour width (b) is generally taken as grid cell size.

None of these potential relationships bore fruit in the sense that none of the plots of a given parameter against volumetric water content (on a given date) exhibited any distinguishable correlation. Scatter plots of the data are included as Appendix G.

Table 4.4. Potential relationships between soil hydrologic parameters and soil volumetric water content (VWC) investigated for the NDW

Potential Relationship	Result
Natural log of soil saturated hydraulic conductivity vs. VWC	No notable relationship
Soil porosity vs. VWC	No notable relationship
Soil depth vs. VWC	No notable relationship
Topographic wetness index vs. VWC	No notable relationship

The absence of notable relationships between soil moisture and these four parameters is somewhat surprising, since a physical argument in favor of such could conceivably be presented. This absence does not necessarily preclude any effect of these parameters on soil volumetric water content, but rather indicates an inability to isolate one of the variables as a strong predictive factor for soil moisture in the NDW.

In addition, as is apparent in Figures 4.21 through 4.26, significant portions of the watershed exhibited high degrees of saturation (i.e. greater than 0.5) on five of the six sampling days (discounting the areas just south of the service road where interpolated results lack supporting measured data). Correlation with any given parameter becomes difficult to detect with numerous data points approaching the maximum volumetric water content threshold. It should be noted, however, that in the absence of the effects of this porosity threshold (i.e. on the October 2 dry sampling day) there is still no apparent correlation between the parameters listed in Table 4.4 and soil volumetric water content, based on the data collected in the NDW. This result is especially significant in the case of topographic wetness index, since there is a physical basis for a correlation between soil moisture and topography, particularly during watershed drying cycles.

In fact, there is some evidence of correlation between elevation and volumetric water content (averaged across all depths at a single point and for all points along an approximate contour line) for the NDW (see Table 4.2) although the trend for the data, displayed in Figure 4.27, is weak. Volumetric water content appears to increase slightly with elevation in Figure 4.27. Note that the effects of the porosity threshold for volumetric water content are apparent on wet sampling days. Possible reasons for the slight trend of soil moisture with elevation might be:

1. lower vegetation density at higher elevations
2. greater precipitation at higher elevations due to orographic effects
3. lower temperatures at higher elevations resulting in lower evapotranspiration
4. slightly higher average porosities in the upper watershed, as compared with the lower watershed (see Figure 4.12).

As mentioned previously, there are three predominant species of trees in the watershed: red spruce, fraser fir, and yellow birch. The fir trees, which are more abundant at higher elevations, were killed in large numbers by an exotic insect (the balsam wooly aphid) beginning in the late 1980's. In addition, during the 1990's, two hurricanes downed large numbers of trees in the upper watershed. These factors suggest that vegetation density may be lower at high elevations which could lead to higher soil moisture due to lower evapotranspiration or lower interception losses.

It is not likely that the pattern displayed is associated with bias in the order of measurements, as discussed earlier in this Chapter. Were this the case, the trend observed on days when it was raining would presumably reverse for days when the watershed was drying, which is not reflected in Figure 4.27.

In the absence of evidence for any of the potential relationships presented in Table 4.4, the possibility of using a point or groups of point measurements of soil moisture to represent average watershed conditions was examined. The results of this analysis will be presented later in this chapter.

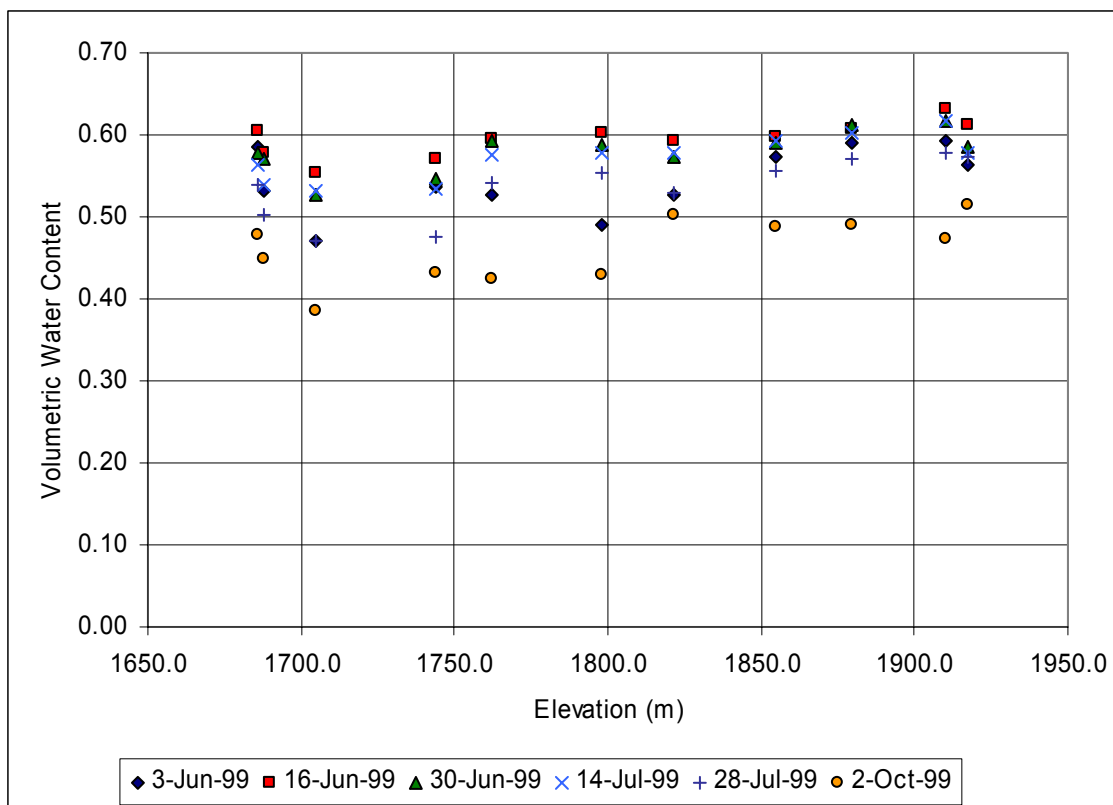


Figure 4.27. NDW elevation versus volumetric water content.

Variation of Soil Moisture with Depth

The biweekly sampling system of soil volumetric water content was designed to measure not only spatial variations but also variations of soil moisture with depth. In general, as the soil water profile drains and dries following precipitation, soil moisture would be expected to increase with depth. When examining volumetric water content data from each of the sampling sites in the NDW, this assumption was often but not always validated, due to the high degree of variability in measurements at any particular site. For this reason, the variation of volumetric water content with depth was examined based on averages of all sites. The installation of access tubes in 5-cm increments ranging from 5 cm to 30 cm facilitated averaging of measurements from all sites for each

depth increment.

Figure 4.28 summarizes the average soil moisture profile results for each biweekly volumetric water content sampling occasion. Single-site representative profiles for each of the 11 sample lines are included in Appendix H. Standard deviations corresponding to the results shown in Figure 4.28 are shown in Table 4.5.

The standard deviation of volumetric water content was nearly constant between five and 20 cm depth, and decreased at depths from 20 to 36 cm. This is consistent with expectation, since variability should decrease as volumetric water content approaches the porosity threshold at depth. It is also notable that the standard deviation of measurements in the upper soil profile on a dry day (October 2) is not significantly different from the standard deviation of measurements in the upper soil profile on wet days.

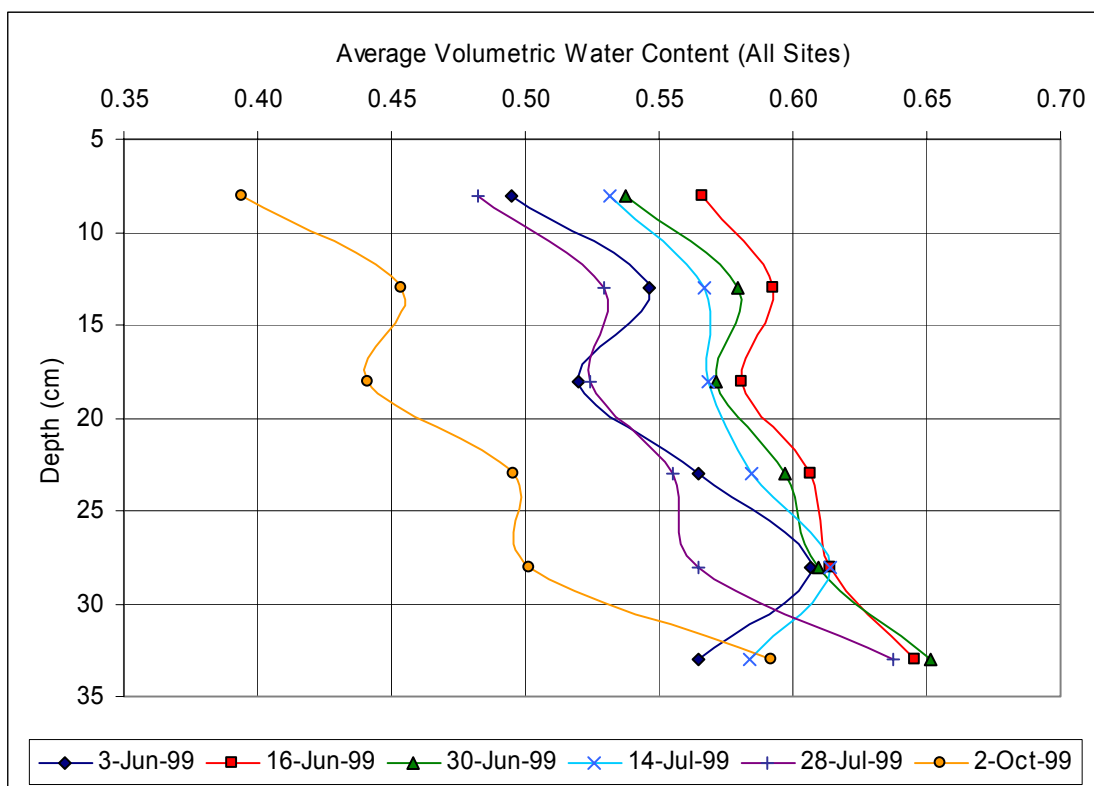


Figure 4.28. Average soil moisture profiles for the NDW.

Table 4.5. Standard deviation of volumetric water content measurements by depth

Soil Depth (cm)	Standard Deviation of Measurements (cm)					
	6/3/1999	6/16/1999	6/30/1999	7/14/1999	7/28/1999	10/2/1999
5 - 11	0.095	0.063	0.081	0.079	0.093	0.089
10 - 16	0.083	0.042	0.067	0.065	0.082	0.074
15 - 21	0.098	0.061	0.072	0.075	0.090	0.096
20 - 26	0.060	0.034	0.040	0.061	0.063	0.073
25 - 31	0.040	0.027	0.050	0.034	0.045	0.096
30 - 36	0.033	0.012	0.009	0.076	N/A	0.046

When the volumetric water content measurements for all sites on each sampling occasion are averaged, clear patterns of the distribution of soil moisture with depth emerge. For all sampling occasions, the uppermost soil moisture measurements are driest. The profiles become increasingly wet as depth increases, with two notable exceptions.

First, on all six days, a relatively wet layer is apparent at a depth between 10 and 16 cm. This could be due to larger fractions of high-porosity clay and organic matter near the surface, which would account for generally larger measured volumetric water content in this layer.

Second, on June 3 and July 14, a pronounced wet layer is apparent at a depth between 25 and 31 cm. A possible explanation for this could be preferential flow along an effective soil-rock interface near this depth. This is supported by the increasing amounts of large rock which were encountered beginning at approximately this depth during the excavation of the soil pits. Rain on both June 3 and July 14 occurred

overnight or during the previous evening, suggesting that the timing of infiltration to and initiation of preferential flow along the effective soil-rock interface is on the order of a half-day. Note that this effect is not observable on June 16, when rain also occurred the previous night; however, the observed wetness at depth on this occasion may be the residual result of rainfall events on prior days.

The relative wetness of each soil moisture profile with respect to the other profiles is consistent with the relative soil water storage estimates for each day. The soil water storage estimates for June 3 and July 28 were nearly the same, with a slightly higher estimate for July 28. The profile average volumetric contents on these days are also nearly equal, although the distribution along the profiles differ, most notably at the two deepest measurement locations. Results from June 3 and July 14 appear to reflect a profile wetting pattern or, as mentioned previously, preferential flow along the effective soil-rock interface, while results from July 28 and October 2 reflect a profile drying pattern.

Conceptually, it appears that the average soil moisture profile in the NDW generally remains near full saturation at depth, decreasing approximately linearly towards the surface. The soil moisture profile pivots about near-saturation at depth, ranging on the surface from field capacity during dry periods (i.e. October 2) to near-saturation during wet periods (i.e. June 16). Since overland flow was never observed in the watershed (even during periods of heavy rainfall) it can be concluded that the sandy-loam, shallow soil profile wets quickly in response to precipitation, and that the stormflow component of the hydrograph reaches the stream quickly, possibly as a result of preferential flow along the effective soil-rock interface. Note that the roughly linear

trend in the average soil moisture profiles lends support to the approach of averaging measured volumetric water content across all depths to represent mean single-site soil moisture.

Water Balance for the Noland Divide Watershed

The precipitation, streamflow, and soil moisture data collected for the NDW facilitated the estimation of a water balance for the watershed for the period beginning June 3, 1999 and ending October 2, 1999. An estimation of the inflows, outflows, and storage changes of water in the basin is based on the following conservation equation:

$$P - Q - ET = \Delta S$$

Precipitation is represented by P, while Q, ET, and ΔS represent streamflow, evapotranspiration, and groundwater storage, respectively. Rainfall and streamflow records were collected on an hourly basis during the field season. An hourly estimate of evapotranspiration for the watershed required calculation based on other available meteorological data for the area. The biweekly soil moisture measurements combined with soil depths provide a means for estimating soil water storage for the watershed on six occasions.

Precipitation

The precipitation record for the NDW for June through October 1999 was based on data collected at the Clingman's Dome climate station. A correction factor was applied to make that rainfall record consistent with measurements taken in the NDW during a portion of the field season, as described in Chapter 3 (see Figure 3.3). The

hourly precipitation records were added together for each period of interest (i.e. the time between successive soil moisture measurement occasions) and for the overall field season to obtain the values shown in the Table 4.6. These values represent the total amount of water arriving in the watershed during each time interval.

Streamflow

As detailed in Chapter 3, streamflow for the two streamlets which drain the watershed was obtained from a combination of datalogger and analog records. The results for the NE and SW weirs were added to estimate total runoff for each hourly time step. This volumetric time series was converted to a length scale by dividing by the total basin area (17.24 hectares). As with the rainfall data, these values were accumulated for each period of interest to obtain the final results shown in Table 4.6.

Evapotranspiration

The evapotranspiration (E^{forest}) values in the water balance were estimated using the following equation (Shuttleworth, 1993):

$$E^{forest} = 0.8E_{rc}^{forest} + \alpha_i P$$

The first term ($0.8E_{rc}^{forest}$) represents transpiration for well-watered forests, and was estimated using a specific implementation of the Penman-Monteith equation to calculate forest reference crop evaporation:

$$E_{rc}^{forest} = F_{rc}^1 A + F_{rc}^2 \overline{D}$$

The energy available for evaporation (A) was estimated using hourly measurements of temperature and solar radiation collected at the Clingman's Dome climate station for the

study period, and an assumed forest albedo of 0.14. A detailed description of the procedure used to estimate A using these data is given by Shuttleworth (1993). The vapor pressure deficit \bar{D} was estimated using saturated vapor pressure (derived from hourly measurement of temperature) and hourly measurements of relative humidity. The coefficients F_{rc}^1 and F_{rc}^2 are functions of temperature, wind speed, and site elevation. Note that measurements of temperature, wind speed, solar radiation, and relative humidity from the Clingman's Dome climate station were assumed to be representative of conditions in the NDW.

The second term in the equation used to estimate forest evapotranspiration ($\alpha_i P$) represents interception, estimated as a percentage of hourly rainfall (P). Recommended values for α_i range from 0.2 to 0.3 (Shuttleworth, 1993). An average value of 0.25 was assumed for NDW interception estimations. The precipitation values used in this estimation were based on the Clingman's Dome hourly record, adjusted for the NDW using the relationship shown in Figure 3.3. The results of the hourly evapotranspiration estimate, combined for time periods between successive soil moisture measurements, are shown in Table 4.6.

Soil water storage changes

Predicted changes in soil water storage (ΔS_{PRED} in Table 4.6) were calculated based on the measured precipitation and streamflow records and the estimated evapotranspiration record. Observed changes in soil water storage (ΔS_{OBS} in Table 4.6) were calculated using the differences in successive soil water storage measurements from Table 4.3. These differences, shown in Table 4.6, were compared with the predicted

storage changes to determine the error in the water balance relative to the total rainfall entering the basin.

There are three primary potential sources of error in the water balance. First, the rainfall estimate used was based on the apparent linear relationship (shown in Figure 3.3) between rainfall measured at Clingman's Dome and rainfall measured in the NDW.

When compared with actual measurements from the NDW rain gage for the period from June 30 to September 30, the error in the rainfall estimate used in the water balance was approximately 3 percent.

The second primary potential source of error in the water balance is infiltration into bedrock. Bedrock in the Blue Ridge Aquifer, which runs along the Tennessee-North Carolina border, is characterized as fractured and does allow for some infiltration.

Fractures are generally limited to within 300 feet of the surface, so groundwater

Table 4.6. Water balance results for the NDW

Time Period	Rainfall (mm)	Streamflow (mm)	ET (mm)	ΔS_{PRED} (mm)	ΔS_{OBS} (mm)	Error (mm)	Error (%)
6/3 – 6/16	99.6	16.4	51.0	32.1	19.7	12.4	12.5%
6/16 – 6/30	267.7	173.8	88.3	5.6	-3.1	8.8	3.3%
6/30 – 7/14	200.0	135.9	74.5	-10.3	-1.1	-9.2	4.6%
7/14 – 7/28	87.1	57.1	54.1	-24.1	-13.0	-11.1	12.8%
7/28 – 10/2	246.5	71.3	222.4	-47.3	-26.80	-20.5	8.3%
Balance for Entire Field Season:							
6/3 – 10/2	900.9	454.5	490.3	-43.9	-24.3	-19.6	2.2%

circulation is localized and follows relatively short, shallow flow paths (Lloyd and Lyke, 1995). Annual groundwater recharge for the Blue Ridge Aquifer, estimated as groundwater infiltration minus groundwater discharge to streamflow, is estimated as 10 cm per year, which is less than five percent of the 230-cm average annual precipitation for the NDW (Swain, Mesko, and Hollyday, 2004). Assuming approximately three to five percent of precipitation goes to groundwater recharge, the estimated overall error in the water balance would increase from two percent to approximately five to seven percent. It should also be noted that this localized groundwater circulation could account for a portion of the discrepancy between the subbasin areas delineated for the two watershed streamlets and the observed relative streamflow for the two streamlets. Tracer studies would be required to more accurately estimate the magnitude of this potential source of error.

The third and most significant potential source of error in the water balance is the estimate of evapotranspiration. This error is estimated to be on the order of 10 to 15 percent (Shuttleworth, 1993). While evapotranspiration was assumed to occur equally over the whole watershed, it is likely that this effect varies significantly across the watershed as a result of variations in vegetation type and density.

Given these potential sources of error as well as the potential error associated with spatial interpolations of porosity and soil depth, and the potential error associated with uncertainty in effective soil depth estimates, the water balance results shown in Table 4.6 are encouraging, considering that the errors in the balance for the five separate time intervals range from three to 13 percent of total precipitation. It is also significant to note that the temporal trend in the “predicted” storage results is generally consistent with the

temporal trend in the “observed” storage results.

The primary conclusion to be drawn from the results of the water balance is that nearly all of the water entering, being stored in, and leaving the watershed appears to be accounted for in rainfall, soil water storage, and streamflow and evapotranspiration, respectively. Although evapotranspiration estimation was not the focus of this study, the water balance (using “observed” changes in storage) could be used to check the validity of the evapotranspiration estimate. Results of such a comparison for the data presented in Table 4.6 are included in Appendix I. These results demonstrate that the evapotranspiration estimates were generally good approximations, but were overestimated for three of the five time intervals. It is also apparent from this comparison that the overestimation was more significant during a dry period (i.e. the period between July 28 and October 2).

To place the water balance results in Table 4.6 in the context of historical precipitation averages at the NDW, average rainfall in the NDW during the month of June is 18 cm, as compared with 36.7 cm for June 3 through June 30, 1999; average rainfall during July in the NDW is 21 cm, as compared with 28.7 cm for June 30 through July 28, 1999; and average rainfall during August and September in the NDW is 30 cm, as compared with 24.7 cm for July 28 through October 2, 1999. Relative to historical average precipitation in the NDW, June 1999 was very wet, July 1999 was wetter than average, and August and September 1999 were dryer than average.

Soil water residence time

Using the results of the water balance, a general approximation of average soil water residence time for the NDW can be made for each of the time periods between

successive soil moisture measurement occasions. Assuming perfect mixing, residence time can be approximated as:

$$\text{Residence Time} = \text{Average Soil Water Storage} / \text{Total Water Flux}$$

where residence time is in days, average soil water storage is in cm, and total water flux is in cm per day. Average soil water storage for each time period was estimated using the soil water storage values from Table 4.3. The total flux of water through the watershed for each time period was taken as total rainfall minus observed change in soil water storage, using the results presented in Table 4.6.

Average soil water storage estimates were refined to account for inactive storage in the soil profile, or water in the soil profile that will not drain under the force of gravity. Inactive storage was assumed to be constant for all time periods and was estimated the product of field volumetric water content (i.e. the volumetric water content at which water in the soil matrix against the force of gravity) and watershed average soil depth (28.1 cm). Field water content for the NDW was estimated as 0.17, using the average of the minimum volumetric water content measurement from the Theta probe (0.18) and the minimum volumetric water content measurement from the Campbell Scientific probes (0.15). The resulting estimate of inactive soil water storage for the NDW was 4.78 cm. The results of the residence time approximation are shown in Table 4.7.

The average weather conditions shown in Table 4.7 are based on the average precipitation in each time period relative to the average precipitation for the entire field season. A time series plot of rainfall and total streamflow for the NDW for May through October 1999 is included in Appendix D. A cumulative hourly time series plot of rainfall and streamflow, as well as the other elements of the water balance, is included as

Appendix J.

The average soil water residence time for the field season can be compared with travel time for water through the soil matrix roughly estimated by dividing the longest flow path for water in the soil to travel before reaching a stream (estimated as 200 meters) by the average soil water velocity estimated using Darcy's Law. The average velocity of water in the soil matrix was estimated to be approximately 16 cm/hr, based on an average soil saturated hydraulic conductivity for the watershed (1.05E-2 cm/s) and an average watershed slope of 23 degrees ($\tan(\beta) = 0.42$). The resulting approximate travel time of 52 days is estimated to be the upper bound for watershed soil water residence

Table 4.7. Approximate soil water residence times for the NDW

Time Period	Average Soil Water Storage (cm)	Active Soil Water Storage⁽¹⁾ (cm)	Total Flux Volume⁽²⁾ (cm)	Average Residence Time (days)	Average Weather Condition for Time Period⁽³⁾
6/3 – 6/16 (13 days)	15.70	10.92	7.99	17.8	Dry
6/16 – 6/30 (14 days)	16.52	11.74	27.08	6.1	Wet
6/30 – 7/14 (14 days)	16.31	11.53	20.11	8.0	Wet
7/14 – 7/28 (14 days)	15.61	10.83	10.01	15.1	Dry
7/28 – 10/2 (66 days)	13.62	8.84	27.33	21.3	Dry
Entire Field Season:					
6/3 – 10/2 (121 days)	15.21	10.43	92.52	13.6	--

(1) – Based on inactive storage estimate of 4.78 cm.

(2) – Total flux volume is divided by days in time period to estimate flux (cm/day).

(3) – Weather condition relative to overall weather conditions during field season.

time. The approximate residence times shown in Table 4.7 are consistent with this approximate upper bound noting that the watershed did not run dry during a sustained period of drought between late July and late September 1999.

Streamflow hydrographs for significant storm events during the study period are included as Appendix K. Hydrograph recession times for these storm events appear to range from approximately one day for a small storm event, to more than eight days for a moderate storm event. Based on this comparison, it can be concluded that residence times for the stormflow component of streamflow are on the order of one week or less (corresponding roughly to the wet period residence times estimated in Table 4.7), while residence times for the baseflow component of streamflow are on the order of two to three weeks (corresponding to the dry period residence times estimated in Table 4.7). Note that the residence times estimated in Table 4.7 rely on the assumption of perfect mixing, and are admittedly coarse approximations. Improved estimates of residence time could be achieved using isotope tracing studies.

Temporal Variation in Soil Moisture

In addition to the 66 soil moisture sampling sites at which measurements were taken every two weeks, continuously monitoring volumetric water content probes were installed in three locations in the NDW (see Figure 3.6). Measurements from three probes at Pits #1 and #2 and four probes at Pit #3 were recorded hourly. The results were ten continuous records of soil moisture for the field season.

As mentioned previously, the potential for using soil moisture measurements from a single point or a group of points to represent average watershed soil moisture conditions

was examined for the NDW. The concept of using a point measurement to represent basin average soil moisture response is treated extensively by Grayson and Western (1998). A statistical method for evaluating the potential for using any given measurement location in the watershed as representative of all measurement locations was developed by Vachaud et al. (1985) for watersheds of minimal relief and extended to watersheds of significant relief by Grayson and Western (1998), who termed representative measurement locations “CASMM” sites (catchment average soil moisture measurement). This method was used to perform a similar evaluation for the biweekly soil moisture sampling locations in the NDW. The method involves taking the average of all volumetric water content measurements at a given point in time (in this case, on a given day), quantifying the difference between each individual measurement (θ_i) and the basin average on that day, and normalizing this difference using the basin average. The result is identified as d_i , or the mean relative difference from the watershed average:

$$d_i = \frac{\theta_i - \bar{\theta}}{\bar{\theta}}$$

The mean and standard deviation of the results for each location across a number of sampling occasions is then estimated. A mean result near zero represents a location which on average, closely represents the basin average soil moisture condition. The standard deviation of the result measures what Vachaud terms the “temporal stability” of a site. That is, the smaller the standard deviation, the more closely a given site follows the overall trend of basin average soil moisture. Sites with mean results near zero and relatively small standard deviations across time are ideal potential CASMM sites. The results of this analysis for the NDW are presented in Figure 4.29.

In addition to the 66 biweekly soil moisture sampling locations, the three continuously-monitored soil pit locations were also included in the analysis. This was done by taking the average of all probe measurements at a given pit for the entire eight-hour period during which each of the biweekly soil moisture measurement collections was completed. The sites used in the analysis are identified by rank in Table 4.7. The CASMM results for the 66 biweekly soil moisture measurement locations are based on six sampling occasions. This is also true of Pit #1; however, the results presented for Pit #2 are based on five sampling occasions and the results for Pit #3 are based on only three sampling occasions. The small standard deviations for these two sites are due at least in part to fewer sampling occasions, and are not necessarily indicative of temporal stability.

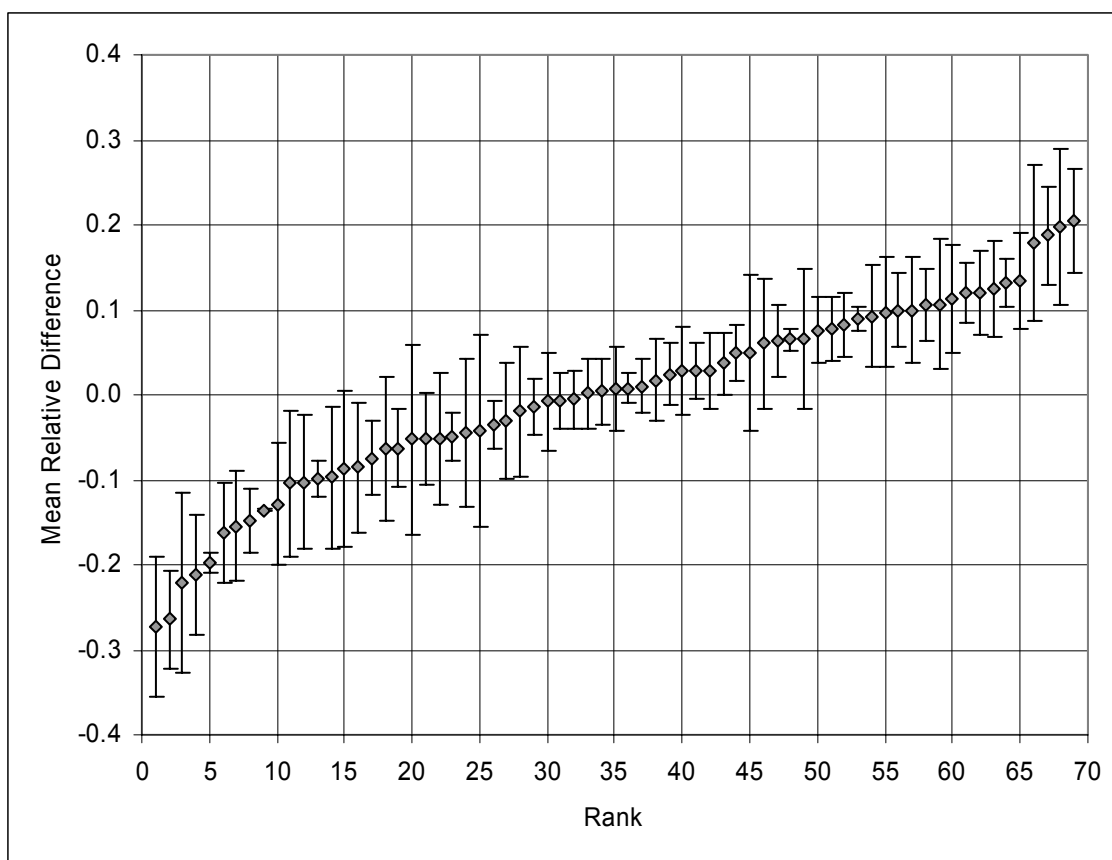


Figure 4.29. Results of CASMM analysis for the NDW.

Table 4.8. Results of CASMM analysis for the NDW

Site	Mean d_i	Standard Deviation of d_i	Rank
2.7	-0.273	0.082	1
3.2	-0.264	0.058	2
3.9	-0.221	0.105	3
3.7	-0.212	0.070	4
Pit 2	-0.197	0.012	5
4.11	-0.162	0.058	6
6.2	-0.154	0.066	7
4.1	-0.148	0.038	8
Pit 3	-0.136	0.001	9
5.14	-0.129	0.072	10
4.7	-0.104	0.086	11
5.11	-0.103	0.078	12
8.4	-0.099	0.020	13
3.5	-0.098	0.083	14
2.1	-0.087	0.092	15
4.8	-0.085	0.077	16
9.6	-0.074	0.044	17
5.16	-0.063	0.085	18
4.13	-0.063	0.045	19
3.6	-0.053	0.112	20
6.5	-0.052	0.054	21
5.3	-0.052	0.078	22
6.9	-0.049	0.028	23
4.3	-0.045	0.088	24
6.6	-0.043	0.113	25
5.15	-0.036	0.028	26
2.2	-0.031	0.068	27

Table 4.8. Continued

Site	Mean d_i	Standard Deviation of d_i	Rank
7.4	-0.019	0.077	28
3.10	-0.013	0.033	29
7.1	-0.008	0.058	30
4.9	-0.006	0.033	31
7.5	-0.005	0.034	32
5.7	0.002	0.041	33
8.6	0.004	0.038	34
7.2	0.007	0.049	35
4.2	0.008	0.018	36
3.1	0.010	0.031	37
5.9	0.017	0.048	38
6.8	0.025	0.037	39
4.6	0.027	0.052	40
3.8	0.028	0.034	41
1.1	0.029	0.044	42
5.2	0.037	0.036	43
5.13	0.049	0.032	44
5.4	0.050	0.092	45
2.5	0.061	0.077	46
5.1	0.064	0.043	47
8.1	0.065	0.014	48
7.3	0.065	0.083	49
1.2	0.076	0.038	50
5.10	0.078	0.039	51
6.7	0.082	0.037	52
10.2	0.090	0.015	53
4.12	0.092	0.060	54

Table 4.8. Continued

Site	Mean d_i	Standard Deviation of d_i	Rank
11.1	0.097	0.064	55
8.5	0.100	0.044	56
6.4	0.100	0.062	57
9.7	0.105	0.042	58
Pit 1	0.107	0.076	59
8.7	0.113	0.063	60
9.2	0.120	0.036	61
8.2	0.120	0.048	62
9.1	0.124	0.056	63
10.1	0.132	0.028	64
8.8	0.134	0.056	65
7.6	0.179	0.092	66
9.5	0.187	0.058	67
9.3	0.197	0.092	68
2.4	0.205	0.062	69

Sites with standard deviations of d_i smaller than 0.05, presumed to correspond to temporally stable potential CASMM sites, are shown in Figure 4.30 and are highlighted in bold in Table 4.8. As is apparent from the figure, there are several sites scattered across the watershed with high degree of temporal stability (a standard deviation less than 0.03). Two of these sites, site 4.2 and site 5.15, typically exhibit soil moisture near the mean value for all sites.

A site that is representative of the watershed average soil moisture is most useful if it can be identified without mapping the spatial distribution of soil moisture across the watershed on multiple occasions. While the two apparent best CASMM candidates are

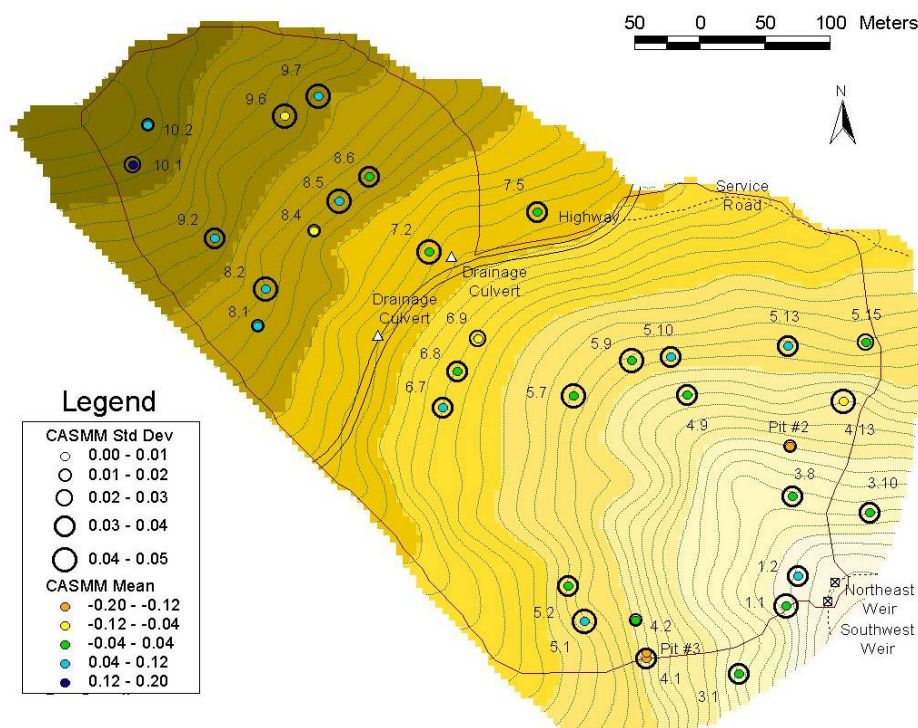


Figure 4.30. Potential CASMM sites for the NDW.

low in the watershed and near the watershed boundary, the sites in the mid-elevation range of the watershed with near watershed average volumetric water content and reasonable temporal stability are encouraging. This is consistent with the earlier observation of a potential correlation between volumetric water content and elevation for the watershed (see Figure 4.27). The relatively random distribution of temporally stable sites across the entire watershed, however, does not necessarily support the use of topography and aspect as predictors of CASMM locations.

As noted previously, the correlation between volumetric water content and elevation observed in the NDW is likely explained by differences in vegetation between the upper and lower watershed. For the NDW, average watershed vegetation characteristics may be a better predictor of CASMM locations than topography or aspect.

The continuously-monitored soil moisture pits locations were selected with the purpose in mind of testing the CASMM potential of these sites. Although they do not appear to be ideal CASMM candidates, the pit average volumetric water contents from all but the deepest probes at each site on each soil moisture sampling day were plotted against estimated watershed soil water storage from Table 4.3. The results are shown in Figure 4.31. Although the data shown is admittedly sparse for drawing meaningful conclusions, the apparent linear correlation for each pit does lend credence to the concept of deriving watershed soil water storage from point measurements.

For purposes of further exploring the possibility of using measurements at a single site to represent basin average soil moisture, the volumetric water content records for the two or three probes nearest the surface at each continuously-monitored pit (see Table 3.9) were compiled as a single average record for each pit. The reason for leaving the deepest

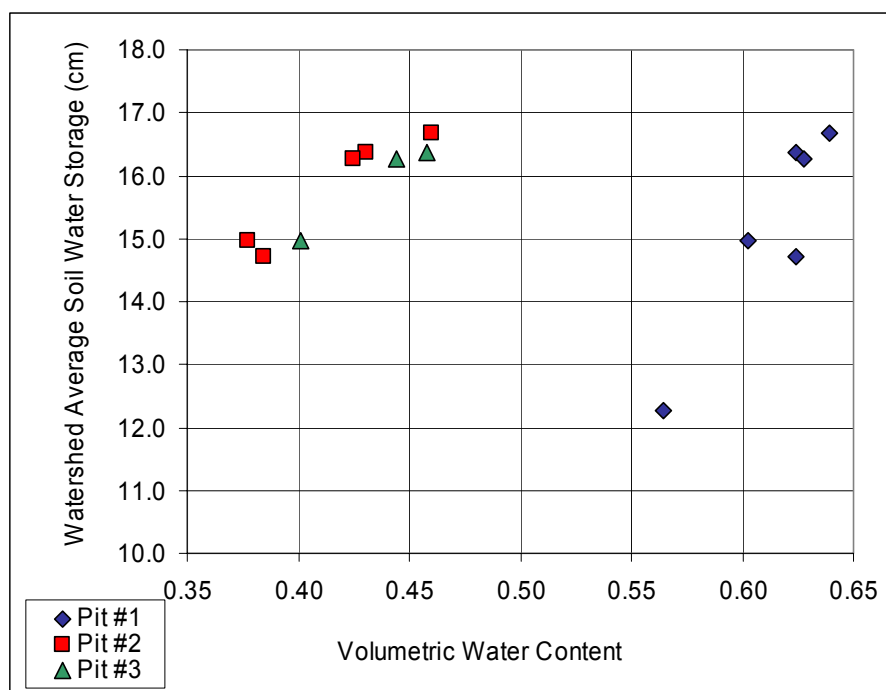


Figure 4.31. Pit volumetric water content versus estimated watershed soil water storage.

probe measurements at each pit out of this analysis was that the estimated depth to the effective soil-bedrock interface at each of the pits, based on the results shown in Figure 4.13, is less than 40 cm. The deepest probes at Pits #1, #2, and #3 were installed at 45, 57, and 50 cm, respectively. The soil-bedrock interface is not well-defined at these locations, as evidenced by the fact that probes were installed at depths greater than 40 cm. As explained previously, for the purposes of this work, the effective soil depth is the depth of the soil profile which actively stores and conveys infiltrating water. It is reasonable to assume that storage capacity and vertical infiltration are limited beyond a depth where significant amounts of rock are present. The conclusion that the effective interface is shallower than the deepest probes is supported by Figures 3.9, where soil moisture measured at the deepest probe is consistently the driest, and 3.10, where the soil moisture measured at the deepest probe is nearly equal to and at times drier than soil moisture measured at the shallowest probe.

Average volumetric water content records for each pit (excluding the deepest probe measurements) were converted to a continuous record of soil water storage for each pit location by multiplying the average volumetric water content record for each pit by the approximate effective soil depth (see Figure 4.13) at each pit location. Using a spreadsheet trial and error solve routine, the approximate soil depths at each pit location were adjusted to minimize the difference between the continuous soil water storage record for each pit and the six observed values of watershed soil water storage estimated from the six synoptic soil moisture measurement dates (see Table 4.3). The results are shown in Table 4.9, along with the estimates of effective depth for these locations taken from the soil depth map for the watershed (Figure 4.13).

The purpose of this is to compare, for each of the three pits, the effective soil depth resulting from interpolation with the effective soil depth resulting when the continuous record at each pit is fitted to observed synoptic data, under the assumption that a given pit is representative of watershed average soil moisture conditions.

The adjusted depth estimate for Pit #3 differs most significantly from the depth estimated based on watershed soil depth measurements. This is not surprising, since the length of the record for Pit #3 only allowed for the use of two of the biweekly storage estimates for adjustment. The closest correspondence is observable at Pit #2, lending support to the selection of this site as a potential surrogate for NDW average soil moisture conditions.

One of the products of the water balance estimation for the NDW was an hourly record of changes in soil water storage based on the difference between basin inflow (precipitation) and outflows (streamflow and evapotranspiration). This record of storage changes was converted to an hourly record of soil water storage by estimating the initial average depth of soil water stored in the watershed for the water balance period. In this case, the initial watershed soil water storage estimate was adjusted to minimize errors

Table 4.9. Soil effective depth estimates used to approximate continuous soil water storage records for Pits #1, #2, and #3

Pit ID	Adjusted Depth (cm)	Estimated Depth Based on Map Shown in Figure 4.13 (cm)
Pit #1	24.8	23.3
Pit #2	38.0	37.6
Pit #3	36.5	25.2

between the hourly water balance soil water storage estimate and the biweekly soil water storage estimates from Table 4.3. The hourly soil water storage record estimated based on the water balance is shown in Figure 4.32 (series labeled “Water Balance Result”). Also shown in this figure are the continuous records of soil water storage estimated using the adjusted soil depths listed in Table 4.9.

The biweekly soil water storage estimates from Table 4.3 (points labeled “Observed”) as well as the maximum potential soil water storage (calculated based on the measurements of soil porosity and soil effective depth) are shown in Figure 4.32 for reference. Based on these results as well as the results presented in Figure 4.30 and Table 4.9, it appears that Pit #2 has the greatest potential of the three in terms of representing average watershed soil water storage conditions, assuming the hourly record of soil water

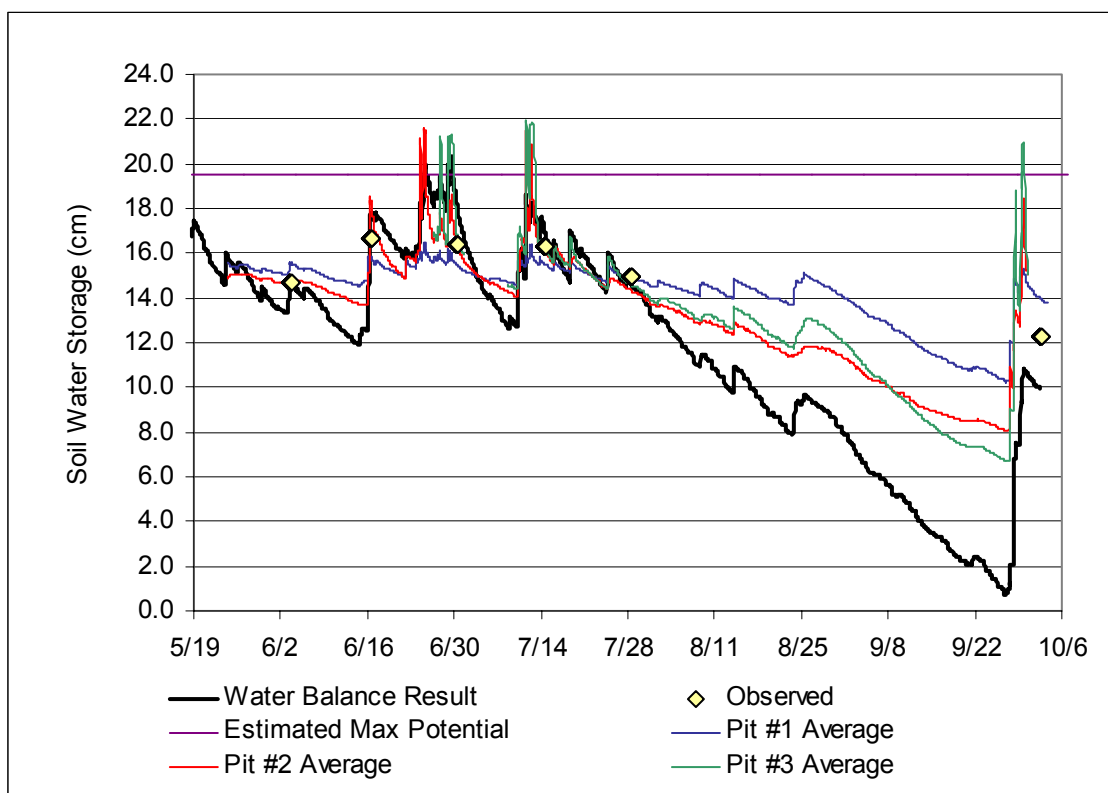


Figure 4.32. Estimated hourly soil water storage record for the NDW.

storage resulting from the water balance is a reasonable estimate of watershed average hourly soil water storage. That assumption is most notably called into question on the decreasing end of soil water storage hydrographs shown in Figure 4.32.

Evapotranspiration appears to be consistently overestimated during prolonged periods between successive rainfall events. One of the assumptions used in the method for evapotranspiration estimation was that water available for evapotranspiration was not limited. Although this is often a good assumption for the NDW, where frequent rainfall, shallow soils, a mulching litter layer, and an overstory tree canopy (particularly dense below the highway) combine to result in near-saturated soil profiles (see Figure 4.28), the assumption is not likely to be valid during prolonged dry periods.

Based on the CASMM analysis results shown in Figure 4.30 and the apparent linear relationship between volumetric water content measured at a point and watershed average soil water storage (Figure 4.31), Pit #2 was selected to estimate hourly changes in watershed average soil water storage using hourly volumetric water content measurements from all but the deepest probe at this site. Linear regression of the data shown in Figure 4.31 for Pit #2 was used to develop the following relationship:

$$\text{Watershed Average Soil Water Storage (cm)} = 25.04 * (\text{VWC}) + 5.39 \quad (R^2 = 0.92)$$

where VWC represents the average of the two water content reflectometer measurements (at depths of 15 and 35 cm) recorded at hourly intervals at Pit #2. A cumulative plot of the differences in successive hourly estimates of watershed average soil water storage (converted to units of mm) is shown in Figure 4.33. The other elements of the water balance are also shown in the figure for reference.

The trend in hourly changes in watershed soil water storage estimated using

volumetric water content measurements from Pit #2 agrees fairly well with the trend in hourly changes in soil water storage estimated from the water balance. Significant discrepancies in the two time series during periods of soil drying are not discouraging since, as noted previously, the evapotranspiration element of the water balance was likely overestimated during these periods.

In general, the results shown in Figure 4.33 demonstrate the potential for estimating average watershed soil water storage conditions based on soil moisture measurements taken at a single point. The distribution of potential CASMM sites across the watershed, however, (see Figure 4.30) seems to indicate that the demonstrated viability of the Pit #2 site, selected *a priori*, was more likely due to chance than the site selection criteria used.

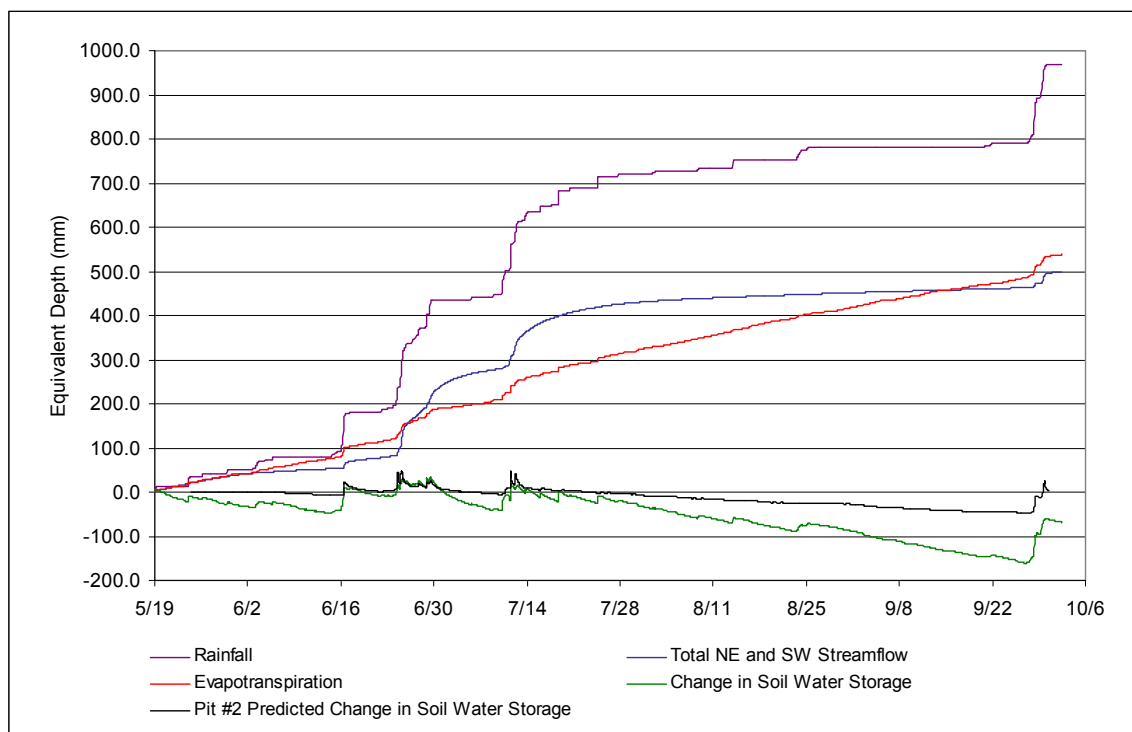


Figure 4.33. Cumulative plot of soil water storage predicted using volumetric water content measured at Pit #2.

In general, the results shown in Figure 4.33 demonstrate the potential for estimating average watershed soil water storage conditions based on soil moisture measurements taken at a single point. The distribution of potential CASMM sites across the watershed, however (see Figure 4.30), seems to indicate that the demonstrated viability of the Pit #2 site, selected *a priori*, was more likely due to chance than the site selection criteria used.

Relationship Between Soil Moisture and Streamflow

If it is assumed that the NDW behaves according to a partial contributing area conceptual model (Hewlett and Hibbert, 1967) then the watershed soil matrix acts as a reservoir and the magnitude and timing of the stormflow response should be a function of the reservoir level (i.e. the portion of the watershed area which is near saturation) or otherwise stated, the watershed soil water storage. This idea was explored using the soil moisture and streamflow data collected for the NDW. Since volumetric water content at a point and watershed soil water storage appear to be linearly related for the NDW (see Figure 4.31), volumetric water content (rather than soil water storage) was plotted against streamflow for the period from May 24, 1999 to September 30, 1999. The average of the two upper probe volumetric water content measurements from Pit #2 was used. The results are shown in Figure 4.34.

The results shown in Figure 4.34 demonstrate a soil moisture threshold above which streamflow response increases significantly. Similar results have also been documented by Woods et al. (2001). Siebert et al. (2003) further concluded that runoff was more tightly related to groundwater depth near the stream than upslope in the

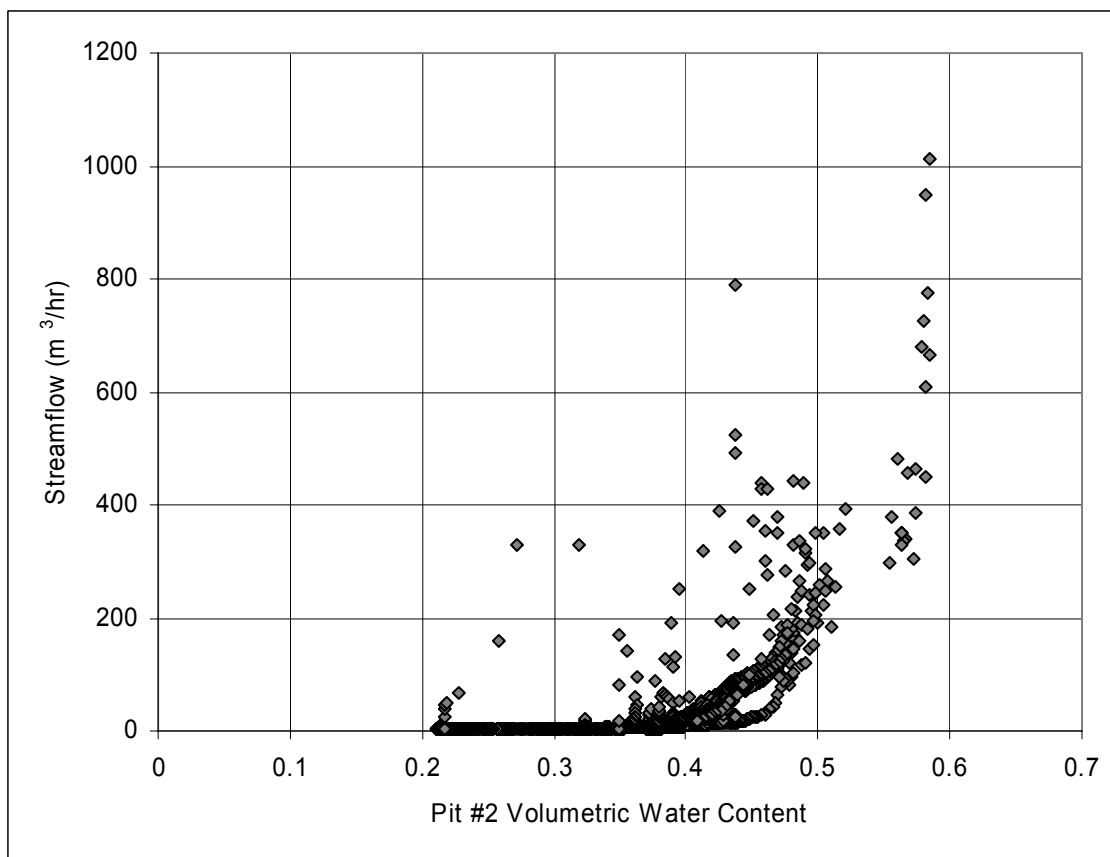


Figure 4.34. Plot of Pit #2 soil volumetric water content versus total streamflow for the NDW.

watershed. The latter conclusion may explain the few apparent large streamflow responses shown in Figure 4.34 at soil moisture levels below the threshold. This may be an indication that the Pit #2 site was outside of the watershed partial contributing area for some storm events.

Based on the results shown in Figure 4.34, the concept of partial contributing area as it applies to the NDW can be further refined. If the watershed soil matrix is considered to behave like a reservoir (such as a reservoir created by a man-made dam), then the baseflow component of streamflow is analogous to releases from a small low-level outlet, while the stormflow component of streamflow is analogous to a reservoir spillway.

When the soil water storage (represented by soil moisture at a point) reaches and exceeds a threshold comparable to the level of spillway, significant releases to the stream occur.

It should be noted that although the NDW appears to support the concept of partial contributing area in the reservoir sense, Figures 4.15 through 4.26 appear to indicate that the spatial distribution of the contributing area in the NDW does not adhere to the standard partial contributing area assumption of topographic control.

CHAPTER 5

SUMMARY AND CONCLUSIONS

The overall purpose of the work presented here was to form a conceptual and quantitative understanding of hydrologic processes in the NDW by collecting spatially distributed measurements of soil moisture and other hydrologically-pertinent soil properties, assembling a comprehensive hydrologic data set for a three-month field season in the NDW, and completing a water balance for the field season. The potential for use of point measurements of soil moisture as representative of average watershed soil water storage conditions was also examined, with the goal of contributing to a reduction in the extensive data requirements that tend to push engineering hydrology away from physically based analysis in favor of empirical methods.

Conceptual Understanding of NDW Hydrology

The following conclusions summarize the conceptual understanding of NDW basin hydrology gained from the collection and analysis of data described in the previous chapters:

1. The soil moisture profile is almost always at or near saturation at depth. The soil moisture profile pivots about this value approximately linearly from near saturation at the surface during frequent periods of rainfall to field water content at the surface during prolonged dry periods.
2. The sandy-loam, shallow soil moisture profile wets quickly in response to precipitation, evidenced by the rapid rise of continuously recorded soil moisture content at all depths and the lack of observed overland flow in the watershed

during periods of heavy precipitation.

3. Based on a comparison of stream hydrograph response times and estimated soil water residence times, hydrograph baseflow appears to be governed by flow through the soil matrix, while hydrograph response to precipitation (stormflow) appears to be governed by flow along the effective soil-rock interface.
4. The organic mulch layer and forest canopy inhibit evaporation of soil moisture from the profile and allow for continued storage of soil water during periods of drought, reflected in the observation that the streamlets seldom run dry.
5. It appears that the two gaged streamlets that drain the watershed draw from a common pool of soil water storage, based on inconsistencies between relative subbasin areas (delineated using a variety of methods) and the observed relative magnitude of streamflow responses.

Note that the basis for the last two conclusions could, to a minor extent, be accounted for by some amount of local groundwater circulation through the fractured sandstone bedrock.

Quantitative Description of NDW Hydrology

In addition to this conceptual understanding, a number of quantitative conclusions for NDW basin hydrologic response can also be drawn. The 17 ha NDW is composed of shallow (average depth to impenetrable layer of approximately 30 cm), sandy-loam soils (average saturated hydraulic conductivity of approximately $1.0E-2$ cm/s) with significant amounts of organic matter (average bulk density of 0.66 g/cm³ and average porosity of 0.69).

Potential soil water storage for the watershed is approximately 20 cm. Average estimated watershed soil water storage based on volumetric water content measurements taken during the study period ranged from 85 percent full on wet days to 65 percent full following a short period of precipitation that ended a prolonged drought. Note that the soil water storage condition at the driest point was regrettably not captured. The average soil water storage condition for the watershed during the study period was nearly 80 percent of maximum potential, consistent with the conclusion that the soil profile is nearly always saturated at depth. When compared with average monthly precipitation for the NDW, June and July 1999 were wetter than average, and August and September 1999 were drier than average.

No strong association was found between measured soil moisture and measured soil hydrologic properties, specifically soil saturated hydraulic conductivity, soil porosity, and soil depth, nor was any notable association found between measured soil moisture and a topographic index. The corollary to this conclusion is that variability in soil moisture measurements generally decreased as the watershed approached a saturated condition, consistent with the upper boundary for volumetric water content set by soil porosity.

Based on the comparison of estimated evapotranspiration and evapotranspiration calculated from the water balance, the streamflow, precipitation, and soil water storage elements of the water balance were well accounted for during the period from June to October 1999. For this overall period in general, rainfall entering the watershed was divided nearly equally between streamflow and evapotranspiration, noting that the method used to estimate evapotranspiration resulted in overestimation of this quantity

during dry periods, and also noting that the potential for a small amount of infiltration through fractured bedrock was not accounted for in the water balance.

Estimated residence time of water contributing to baseflow is on the scale of weeks to months, while observed stream hydrograph precipitation response times are on the scale of hours to days. Although the relationship between peak precipitation and corresponding peak streamflow was not examined in detail as part of this work, in general it appears that streamflow peak response seems to lag peak rainfall by anywhere from 30 minutes to four hours for the northeast stream weir, and from 30 minutes to six hours for the southwest stream weir. In addition, it appears that lag times are shorter for wetter antecedent conditions, and longer following dry spells. These estimates could potentially be improved by conducting tracer studies in the watershed.

Methods of Measurement and Analysis

A portable Delta-T Devices Theta probe was successfully used to measure the spatial and vertical distribution of soil volumetric water content in the steep, forested NDW. While field calibration of this impedance probe using gravimetric methods was unsuccessful, a subsequent laboratory gravimetric calibration using watershed soils produced a result closely associated to the manufacturer's standard calibration for soils containing organic matter. The most significant deviation from the manufacturer's standard calibration was at the high end of probe voltage output, where the specific laboratory calibration for NDW soils resulted in slightly smaller corresponding estimates of volumetric water content.

Campbell Scientific CS615-L water reflectometer probes were successfully used

to continuously monitor soil profile volumetric water content at three locations in the NDW, with measurement averages and ranges that correspond well to the portable impedance probe measurements. Maximum measurements of volumetric water content from both types of probes correspond well to average estimated watershed porosities, adjusted to account for soil organic content.

In general, the high degree of spatial variability in the watershed soils and the relatively small area of influence for the portable probe using 6-cm rod required the collection of a greater number of measurements than the longer water content reflectometer probes to capture trends in volumetric water content variation along the soil depth profile. Although measurements of volumetric water content using the manufacturer's calibration for the Campbell Scientific CS615 sensors, the portable Delta-T devices Theta probe, and gravimetric methods were shown to be consistent and mutually-validating for the work presented here, it is possible that minor improvements in the results could be achieved using a more rigorous calibration effort to account for potential sensor-to-sensor variability as well as variation in soil texture along the soil profile.

Potential for Using Point Measurements to Represent Average Watershed Soil Moisture Conditions

Results of an analysis of temporal stability and mean response relative to average watershed response for all of the soil moisture measurement locations in the NDW provides support for the use of point measurements of soil moisture to represent average watershed soil moisture conditions. A number of sites shown in Figure 4.30 display both temporal stability and near watershed average behavior. The potential catchment average

soil moisture measurement (CASMM) sites near the middle of the watershed (see Figure 4.30) also support the concept of selecting such sites *a priori*, although for the NDW, it appears that average watershed vegetation characteristics are an additional basis for surrogate site selection. The general correlation between soil volumetric water content and elevation for the NDW (see Figure 4.27) supports the idea of selection of representative sites based on average elevation in the watershed, noting that this correlation could be explained in large part by the difference in vegetation in the upper and lower portions of the watershed.

Despite the fact that the continuously monitored Pit #2 and #3 measurement locations generally exhibit drier conditions with respect to the watershed average, the temporal stability reflected in the analysis of these sites supports the potential for determination of a relationship between soil moisture at these sites and average watershed soil moisture. In fact, viable linear relationships between soil moisture and watershed average soil water storage are reflected in Figure 4.31 for all three continuously monitored soil moisture measurement locations.

Continuously monitored measurements of volumetric water content at a single site, combined with a local estimate of soil depth, can be used to construct a continuous record of soil water storage representative of average watershed soil water storage conditions, as shown in Figure 4.32. Correspondence between records resulting from measurements at Pits #1, #2, and #3 and the storage record resulting from the water balance (based on hourly measurements of precipitation and streamflow, and on estimation of hourly evapotranspiration) was improved in the case of Pit #2 by estimating and incorporating the linear relationship suggested in Figure 4.31. The resulting estimate

of hourly changes in watershed average soil water storage (see Figure 4.33) corresponds well with the hourly record of changes in watershed soil water storage derived from the water balance, noting that the evapotranspiration estimate used to calculate the water balance was likely overestimated during dry periods.

For the purpose of further examining and validating the suggested relationship between soil moisture measurements at a point and average watershed soil water storage for the NDW, it is recommended that at least one of the continuously monitored measurement locations be maintained. In addition, it is recommended that further soil moisture sampling be conducted at the established portable probe measurement sites to more firmly establish the statistical analysis of point temporal stability and behavior relative to watershed average.

Finally, it is recommended that future work include exploration of potential associations between watershed average soil water storage and streamflow, with the purpose of estimating a basin response function. A specific basin response function was not estimated as part of this work; however, results of a plot of Pit #2 volumetric water content versus total watershed streamflow for the period of May through September 1999 give indication of the potential viability of such a relationship and also support the concept of a soil moisture threshold above which streamflow response to rainfall increases significantly. In this sense the watershed soil matrix appears to operate in a manner similar to a man-made reservoir, where baseflow results from releases from a low-level outlet, while stormflow is the result of a threshold effect similar to the behavior of a dam spillway.

REFERENCES

- Alley, W.M. 1984. On the treatment of evapotranspiration, soil moisture accounting, and aquifer recharge in monthly water balance models. *Water Resources Research* 20(8): 1137-1149.
- Anderson, M.G., and T.P. Burt. 1990a. Process studies in hillslope hydrology: Overview, p. 1-8. In M.G. Anderson and T.P. Burt (Editors). *Process studies in hillslope hydrology*. John Wiley and Sons, New York.
- Anderson, M.G., and T.P. Burt. 1990b. Subsurface runoff, p. 365-400. In M.G. Anderson and T.P. Burt (Editors). *Process studies in hillslope hydrology*. John Wiley and Sons, New York.
- Bache, B.W. 1990. Solute transport in soils, p. 437-462. In M.G. Anderson and T.P. Burt (Editors). *Process studies in hillslope hydrology*. John Wiley and Sons, New York.
- Bathurst, J.C. 1986. Physically based distributed modeling of an upland catchment using Systeme Hydrologique Europeen. *Journal of Hydrology* 87: 79-102.
- Bear, J., 1972. *Dynamics of fluids in porous media*. Elsevier, Amsterdam. 764 p.
- Bell, J.P. 1973. Neutron probe practices. Institute of Hydrology Report No. 19. Institute of Hydrology, Wallingford, Oxon, UK.
- Beven, K.J., and M.J. Kirkby. 1979. A physically-based variable contributing area model of basin hydrology. *Hydrological Sciences Bulletin* 24: 43-69.
- Branson, J.L., G. Dunn, and J.T. Ammons. 1996. Noland Divide Watershed soils descriptions and soils chemical analysis report. Unpublished report, funded by Tennessee Valley Authority Technology Advancements Program. 13 p.
- Campbell Scientific, Inc. 1996. CS615 water content reflectometer instruction manual. Logan, Utah.
- Chiew, F.H.S., M.J. Stewardson, and T.A. McMahon. 1993. Comparison of six rainfall-runoff modeling approaches. *Journal of Hydrology* 147: 1-36.
- Creed, I.F., L.E. Band, N.W. Foster, I.K. Morrison, J.A. Nicolson, R.S. Semkin, and D.S. Jeffries. 1996. Regulation of nitrate-N release from temperate forests: A test of the N flushing hypothesis. *Water Resources Research* 32(11): 3337-3354.

- Creed, I.F., and L.E. Band. 1998a. Exploring functional similarity in the export of nitrate-N from forested catchments: A mechanistic modeling approach. *Water Resources Research* 34(11): 3079-3093.
- Creed, I.F. and L.E. Band. 1998b. Export of nitrogen from catchments within a temperate forest: Evidence for a unifying mechanism regulated by variable source area dynamics. *Water Resources Research* 34(11): 3105-3120.
- Delleur, J.W. 1971. General Discussion. *In* V.M. Yevjevich (Ed.). *Systems approach to hydrology, Proceedings from the First Bilateral U.S. Japan Seminar in Hydrology*. Water Resources Publications, Fort Collins, Colorado.
- Delta-T Devices, Ltd. 1998. ThetaProbe soil moisture sensor: Type ML-2 user manual. Cambridge, UK.
- Dunne, T., and R.D. Black. 1970a. An experimental investigation of runoff production in permeable soils. *Water Resources Research* 6(2): 478-490.
- Dunne, T. and R.D. Black. 1970b. Partial area contributions to storm runoff in a small New England watershed. *Water Resources Research* 6(5): 1296-1310.
- Famiglietti, J.S., J.A. Devereaux, C.A. Laymon, T. Tsegaye, P.R. Houser, T.J. Jackson, S.T. Graham, M. Rodell, and P.J. van Oevelen. 1999. Ground-based investigation of soil moisture variability within remote sensing footprints during the southern Great Plains 1997 (SGP97) hydrology experiment. *Water Resources Research* 35(6): 1839-1851.
- Fortin, J.P., R. Turcotte, S. Masicotte, R. Moussa, J. Fitzbeck, and J.P. Villeneuve. 2001. Distributed watershed model compatible with remote sensing and GIS data: I and II. *Journal of Hydrologic Engineering* 6(2): 91-108.
- Garbrecht, J., F. Ogden, P. DeBarry, and D. Maidment. 2001. GIS and distributed watershed models: I and II. *Journal of Hydrologic Engineering* 6(6): 506-523.
- Gaskin, G.J., J.D. and Miller. 1996. Measurement of soil water content using a simplified impedance measuring technique. *Journal of Agricultural Engineering Research* 63: 153-160.
- Germann, P., and K. Beven. 1981. Water flow in soil macropores: I, II, and III. *Journal of Soil Science* 32: 1-39.
- Grayson, R.B., I.D. Moore, and T.A. McMahon. 1992a. Physically-based hydrologic modeling 1. A terrain-based model for investigative purposes. *Water Resources Research* 28(10): 2639-2658.

- Grayson, R.B., I.D. Moore, and T.A. McMahon. 1992b. Physically-based hydrologic modeling 2. Is the concept realistic? *Water Resources Research* 28(10): 2659-2666.
- Grayson, R.B., and A.W. Western. 1998. Towards areal estimation of soil water content from point measurements: time and space stability of mean response. *Journal of Hydrology* 207: 68-82.
- Grayson, R.B., A.W. Western, and F.H.S. Chiew. 1997. Preferred states in spatial soil moisture patterns: Local and nonlocal controls. *Water Resources Research* 33(12): 2897-2908.
- Hendrickx, J.M.H. 1990. Determination of hydraulic soil properties, p. 43-92. *In* M.G. Anderson and T.P. Burt (Editors). *Process studies in hillslope hydrology*. John Wiley and Sons, New York.
- Hessen, D.O., A. Henriksen, A. Hindar, J. Mulder, K. Torseth, and N. Vagstad. 1997. Human impacts on the nitrogen cycle: A global problem judged from a local perspective. *Ambio* 26(5): 320-325.
- Hewlett, J. D., and J.R. Hibbert. 1967. Factors affecting the response of small watersheds to precipitation in humid areas, p. 275-291. *In* W. E. Sopper and H. W. Lull (Editors). *Forest Hydrology*. Pergamon Press, New York.
- Horton, R.E. 1933. The role of infiltration in the hydrological cycle. *Trans. American Geophysical Union* 14: 446-460.
- Hursh, C.R., and E.F. Brater. 1941. Separating storm hydrographs from small areas into surface and subsurface flow. *Trans. American Geophysical Union* 22: 863-870.
- Jones, S., J.M. Wraith, and D. Or. 2002. Time domain reflectometry measurement principles and applications. *Hydrologic Processes* 16: 141-153.
- Kalma, J.D., B.C. Bates, and R.A. Woods. 1995. Predicting catchment-scale soil moisture status with limited field measurements. *Hydrological Processes* 9: 445-467.
- Kirkby, M.J. (Ed.), 1978. *Hillslope hydrology*. John Wiley and Sons, New York. 389 p.
- Klemes, V. 1986. Dilettantism in hydrology: Transition or destiny? *Water Resources Research* 22(9): 177-188.
- Klemes, V. 1988. The modeling of mountain hydrology: The ultimate challenge. *In* L. Molnar (Ed.). *Hydrology of mountain areas, Proceedings of the Strbske Pleso workshop*. IAHS Publication No. 90, Czechoslovakia.

- Lamson, R.R. 1967. Response of soil moisture and litter flow to natural rainfalls in a forested New England watershed. M.S. thesis, University of Vermont, Burlington, Vermont. 172 p.
- Lloyd, O.B., and W.L. Lyke. 1995. Groundwater atlas of the U.S., Illinois, Indiana, Kentucky, Ohio, and Tennessee. U.S. Geological Survey. Hydrologic Investigations Atlas 730-K, Reston, Virginia. 30 p.
- McDonnell, J.J. 1990. A rationale for old water discharge through macropores in a steep, humid catchment. *Water Resources Research* 26(11): 2821-2832.
- McGlynn, B.L., and J.J. McDonnell. 2003. Quantifying the relative contributions of riparian and hillslope zones to catchment runoff. *Water Resources Research* 39(11): 1310.
- Miller, J.D., G.J. Gaskin, and H.A. Anderson. 1997. From drought to flood: Catchment responses revealed using novel soil water probes. *Hydrological Processes* 11: 533-541.
- Mulder, J., N. Christophersen, K. Kopperud, and P.H. Fjeldal. 1995. Water flow paths and the spatial distribution of soils as a key to understanding differences in streamwater chemistry between three catchments (Norway). *Water, Air, and Soil Pollution* 81: 67-91.
- Nelson, D.W., and L.E. Sommers. 1996. Total carbon, organic carbon, and organic matter, p. 539-579. *In* A.L. Page (Ed.). *Methods of soil analysis, Part 2, Chemical and microbiological properties*. American Society of Agronomy, Soil Science Society of America, Madison, Wisconsin.
- O'Callaghan, J.F., and D.M. Mark. 1984. The extraction of drainage networks from digital elevation data. *Computer Vision Graphics and Image Processing* 28: 328-344.
- O'Loughlin, E.M. 1990. Perspectives in hillslope research, p. 501-516. *In* M.G. Anderson and T.P. Burt (Editors). *Process studies in hillslope hydrology*. John Wiley and Sons, New York.
- Parkhurst, W.J., and B.L. Barnard. 1990. How clean is our air? A decade of change. Air quality in the Tennessee Valley Region. Tennessee Valley Authority. TVA/WR/AS--90/1, Knoxville, Tennessee. 24 p.
- Pauley, E.F., S.C. Nodvin, N.S. Nicholas, A.K. Rose, and T.B. Coffey. 1996. Vegetation, biomass, and nitrogen pools in a spruce-fir forest of the Great Smoky Mountains National Park. *Bulletin of the Torrey Botanical Club* 123(4): 318-329.

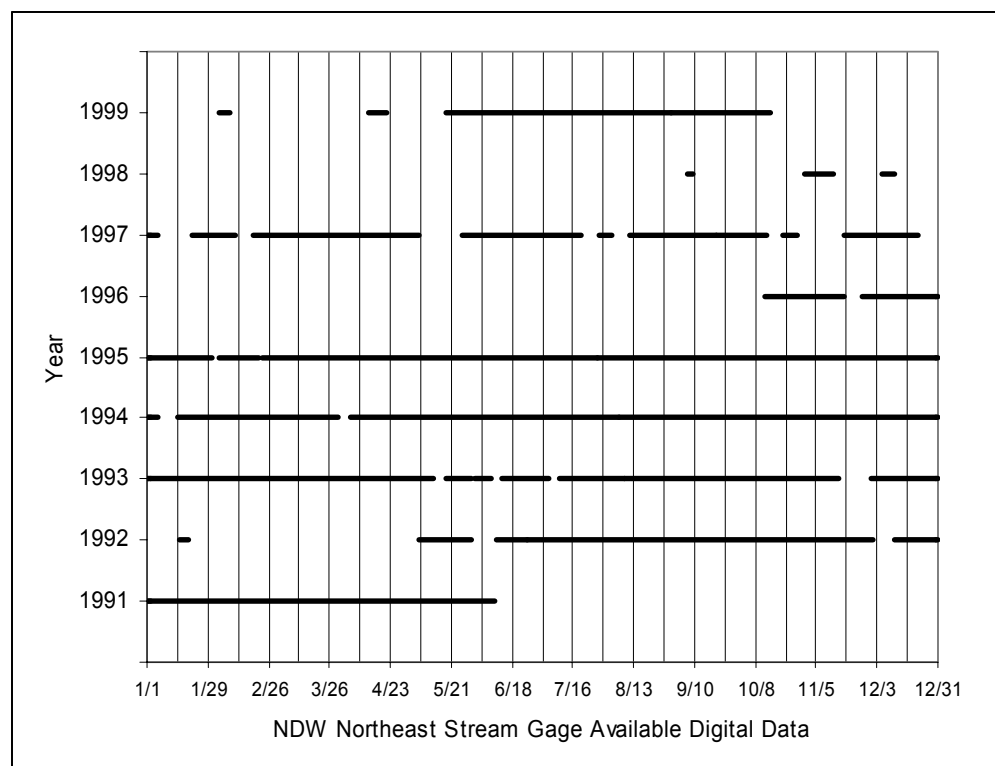
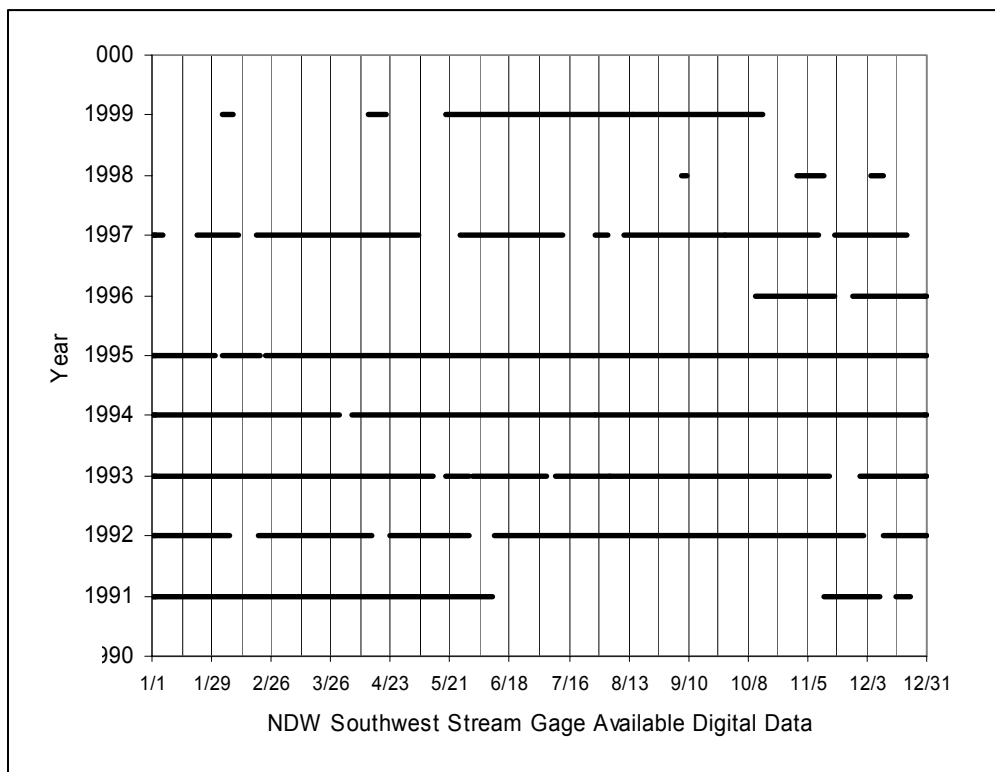
- Peters, D.L., J.M. Buttle, C.H. Taylor, and B.D. LaZerte. 1995. Runoff production in a forested, shallow soil, Canadian Shield Basin. *Water Resources Research* 31(5): 1291-1304.
- Philip, J.R. 1992. Hydrology and the real world, p. 201-207. *In* J.P. O'Kane (Ed.). *Advances in theoretical hydrology*. Elsevier, New York.
- Rawitz, E., E.T. Engman, and G.D. Cline. 1970. Use of the mass balance for examining the role of soils in controlling watershed performance. *Water Resources Research* 6(4): 1115-1123.
- Seyfried, M.S., and M.D. Murdock. 2001. Response of a new soil water sensor to variable soil, water content, and temperature. *Soil Science of America Journal* 65: 28-34.
- Shuttleworth, W.J. 1993. Evaporation, p. 4.1-4.53. *In* D.R. Maidment (Ed.). *Handbook of hydrology*. McGraw-Hill, New York.
- Siebert, J., K. Bishop, A. Rodhe, and J.J. McDonnell. 2003. Groundwater dynamics along a hillslope: A test of the steady state hypothesis. *Water Resources Research* 39(1): 1014-1029.
- Singh, V.P., and D.A. Woolhiser. 2002. Mathematical modeling of watershed hydrology. *Journal of Hydrologic Engineering* 7(4): 270-292.
- Sklash, M.G., M.K. Stewart, and A.J. Pearce. 1986. Storm runoff generation in humid headwater catchments 2: A case study of hillslope and low-order stream response. *Water Resources Research* 22: 1273-1282.
- Soilmoisture Equipment Corp. 1986. *Guelph permeameter 2800KI operating instructions*. Santa Barbara, California.
- Swain, A.S., T.O. Mesko, and E.F. Hollyday. 2004. Summary of hydrogeology of the Valley and Ridge, Blue Ridge, and Piedmont physiographic provinces in the Eastern U.S. U.S. Geological Survey Professional Paper 1422-A. 23 p.
- Sun, H., P.S. Cornish, and T.M. Daniell. 2002. Spatial variability in hydrologic modeling using rainfall-runoff model and digital elevation model. *Journal of Hydrologic Engineering* 7(6): 404-412.
- Tarboton, D.G. 1997. A new method for determination of flow directions and upslope areas in grid digital elevation models. *Water Resources Research* 33(2): 309-319.
- Tennessee Valley Authority . 2003. *How clean is our air? Air quality in the Tennessee Valley Region*. Tennessee Valley Authority, Knoxville, Tennessee. 29 p.

- Topp, G.C., J.L. Davis, and A.P. Annan. 1980. Electromagnetic determination of soil water content: Measurements in coaxial transmission lines. *Water Resources Research* 16(3): 574-582.
- Tuzinsky, L., and S. Gavenciak. 1988. Water budget of forest ecosystems in the Small Carpathians. In L. Molnar (Ed.). *Hydrology of mountain areas, Proceedings of the Strbske Pleso workshop*. IAHS Publication No. 90, Czechoslovakia.
- Vachaud, G., A.P.D. Silans, P. Balabanis, and M. Vauclin. 1985. Temporal stability of spatially measured soil water probability density function. *Soil Science Society of America Journal* 49: 822-827.
- Van Miegroet, H. 2000. Noland Divide Watershed soil carbon content data. Unpublished laboratory results, Utah State University College of Natural Resources, Department of Forest, Range, and Wildlife Sciences.
- Van Miegroet, H., I.F. Creed, N.S. Nicholas, D.G. Tarboton, D.G., K.L. Webster, J. Shubzda, B. Robinson, J. Smoot, D.W. Johnson, S.E. Lindberg, G. Lovett, S. Nodvin, and S. Moore. 2001. Is there synchronicity in nitrogen input and output fluxes at the Noland Divide Watershed, a small N-saturated forested catchment in the Great Smoky Mountains National Park? *The Scientific World* 1(S2): 480-492.
- Walker, J.P., G.R. Willgoose, and J.D. Kalma. 2004. In situ measurement of soil moisture: A comparison of techniques. *Journal of Hydrology* 293: 85-99.
- Wang, M., and A. Hjelmfelt. 1998. DEM based overland flow routing model. *Journal of Hydrologic Engineering* 3(1): 1-8.
- Whalley, W.R. 1993. Considerations on the use of time-domain reflectometry (TDR) for measuring soil water content. *Journal of Soil Science* 44: 1-9.
- Wood, E.F., M. Sivapalan, K. Beven, and L. Band. 1988. Effects of spatial variability and scale with implications to hydrologic modeling. *Journal of Hydrology* 102:29-47.
- Woods, R.A., R.B. Grayson, A.W. Western, M.J. Duncan, D.J. Wilson, R.I. Young, R.P. Ibbitt, R.D. Henderson, and T.A. McMahon. 2001. Experimental design and initial results from the Mahurangi River variability experiment: Marvex, p. 201-203. In V. Lakshmi, J.D. Albertson, and J. Schaake (Editors). *Observations and modeling of land surface hydrologic processes*. Water Resources Monographs, American Geophysical Union, Washington, D.C.

APPENDICES

APPENDIX A

Available Digital Steamflow Data for the
Noland Divide Watershed
1991 to 1999



APPENDIX B

Method for Conversion of Analog Streamflow Data to
Digital Streamflow Data for NDW Stream Gages

The items required to complete digitization of NDW streamflow data from analog charts were as follows:

1. Analog streamflow charts for the study period
2. Manufacturer's official ruler
3. Chart reading to stage relationship, in this case **Stage = 0.166 * (Chart Reading)**
4. Stage to discharge relationship, in this case **Discharge = 2.57 * (Stage)^{1.99}**

The method used for converting chart data to discharge data is described in detail below:

1. Each chart represents a one-week period. The date and time when the chart was changed as well as a corresponding staff height were recorded at the beginning and end of each period. These staff heights represent a manual stage reading at the beginning and end of the chart record period.
2. The bold vertical lines on the chart represent daily time steps; the smallest chart increment is two hours.
3. The official ruler has a scale from 0.0 to 12.0. This scale is not linear so the official ruler must be used.
4. The two staff readings were used to establish the datum for each chart. This was accomplished as follows:
 - The beginning staff height was converted to a chart reading using the inverse of the relationship given above.
 - The calculated chart reading corresponds to a reading made using the official ruler. The ruler was used to mark the datum (baseline) at the beginning of the chart.

- The former two steps were repeated for the staff height at the end of the chart.
 - A straight edge was used to connect the start and end points, establishing the baseline for the chart. It should be noted that this baseline would ideally be approximately parallel to the horizontal lines on the chart. Often this is not the case due to inaccuracies associated with taking a stage reading with the staff. A second option would be to establish the baseline as exactly horizontal while balancing the errors in the beginning and end points.
5. The official ruler was used to take readings at each time increment (1-hour increments in this case, half the smallest increment on the chart). Dates, times, and readings for the entire chart (one week) were noted.
 6. Readings were converted to stage heights using the given relationship.
 7. Stage height was converted to instantaneous discharge using the given equation.
 8. Volumetric discharge per hour was obtained by integrating the instantaneous data using the trapezoidal rule.

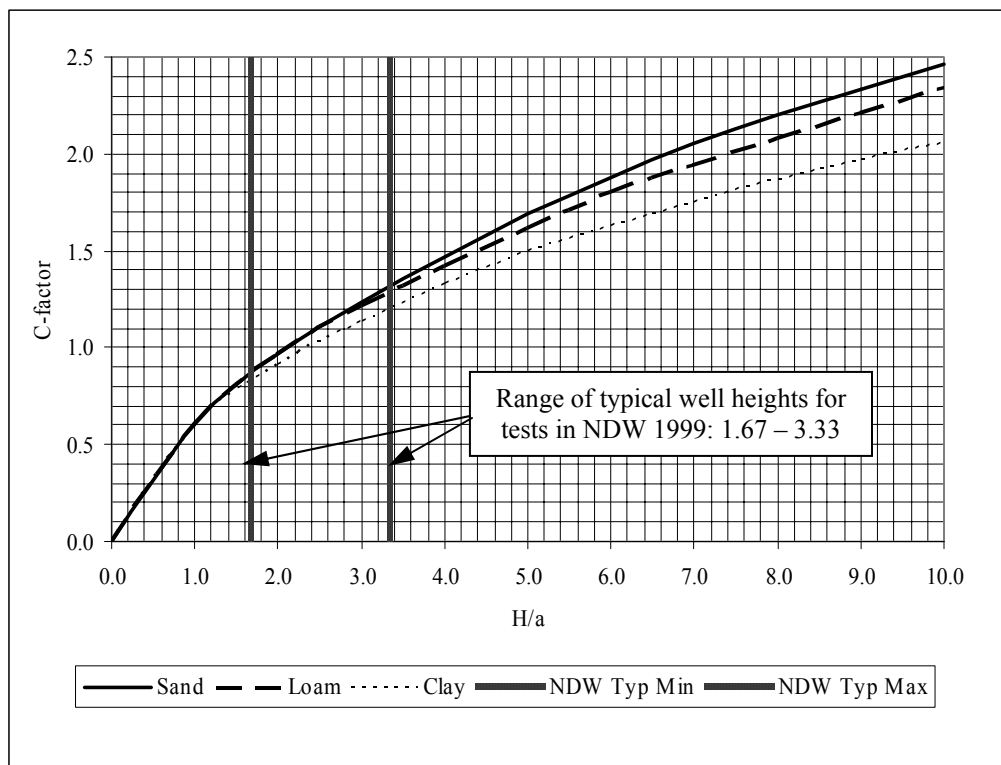
Care was taken during the digitization process to maintain smooth transitions between data recorded by the datalogger and analog chart data. Slight adjustments in the baseline were necessary to achieve this in some cases.

In addition, missing analog data made it necessary to estimate discharge from the southwest weir for the week of July 14 to July 21, 1999. A recorder pen malfunction during this period prevented collection of reliable data. As a basis for this estimation, the relationship between the discharge at the two weirs was examined. Recorded streamflow

at the northeast weir was plotted against recorded streamflow at the southwest weir using all available data from 1999. Different lag times between the two datasets were examined. A linear relationship was discovered at lag six (southwest (SW) response six hours after northeast (NE) response, $SW = 0.60 * NE + 3.24$, $R^2 = 0.85$). This relationship was improved by limiting the dataset to the month of July, maintaining the six-hour lag ($SW = 0.61 * NE + 3.30$, $R^2 = 0.97$). This latter equation was used to estimate discharge in the southwest streamlet for the week in question. In using this estimation it is recognized that a more rigorous statistical analysis would be necessary to develop a general empirical relationship between the discharges in the two streamlets. This estimation method was only deemed useful in this particular case inasmuch as few other alternatives were present given the available data.

APPENDIX C

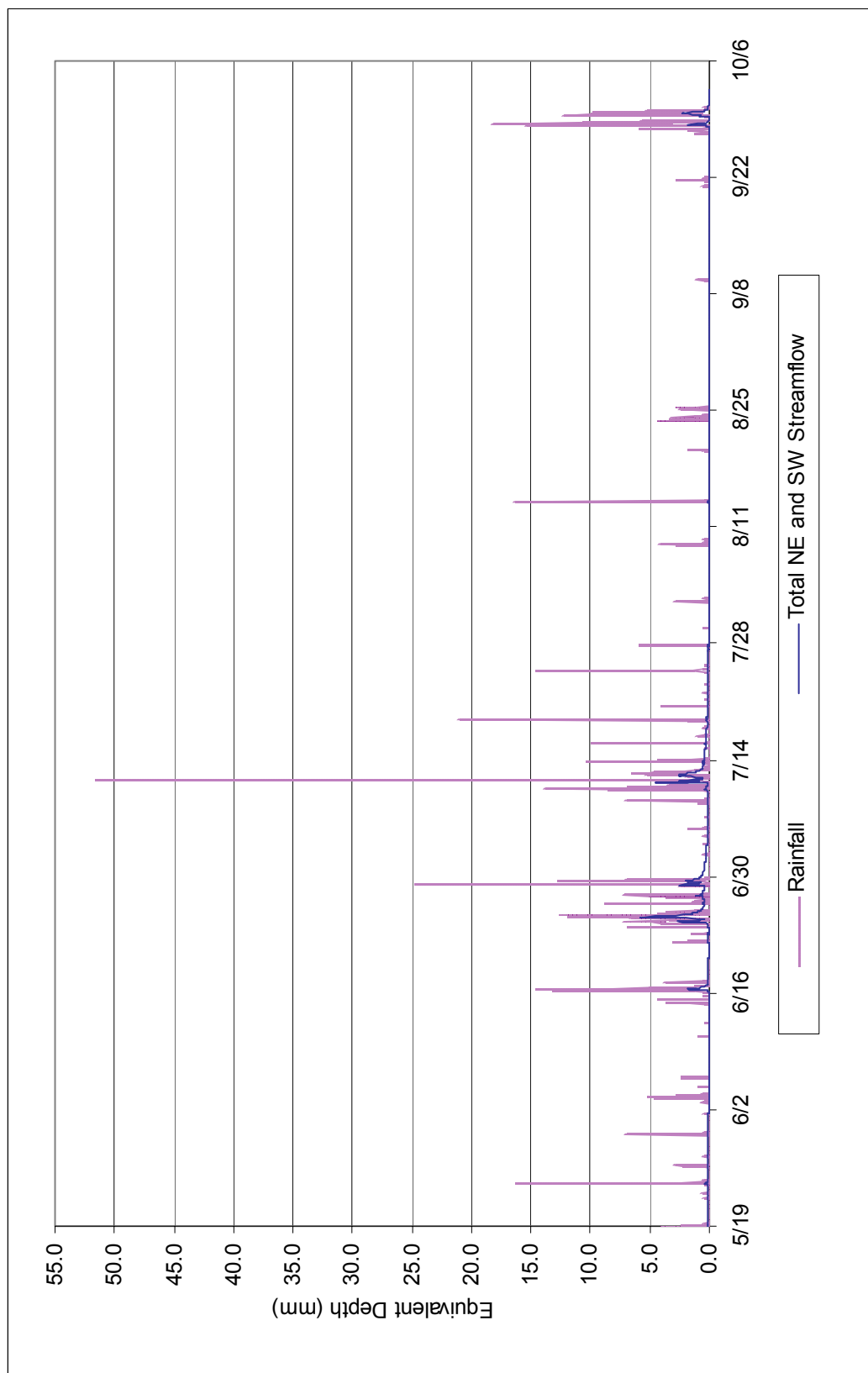
Guelph Permeameter C-Factor Based on Soil Type



Soilmoisture Equipment Corp. (1986).

APPENDIX D

Rainfall and Total Streamflow Records for the NDW
for May through October 1999



APPENDIX E

Description of Portable Soil Moisture Probe Laboratory Calibration
Using NDW Soils

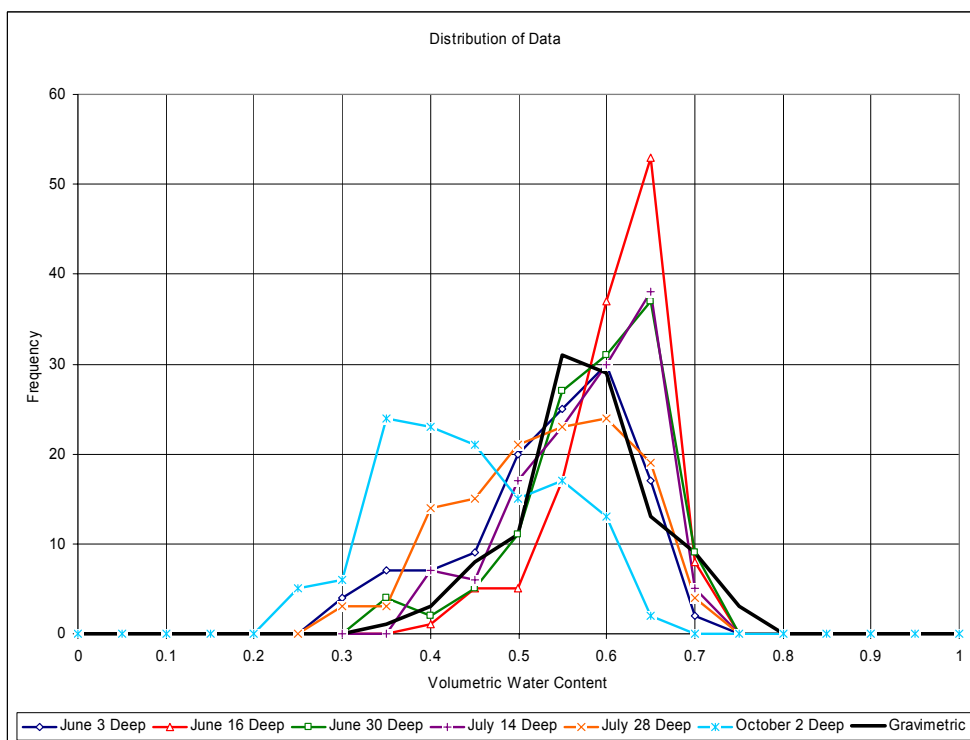
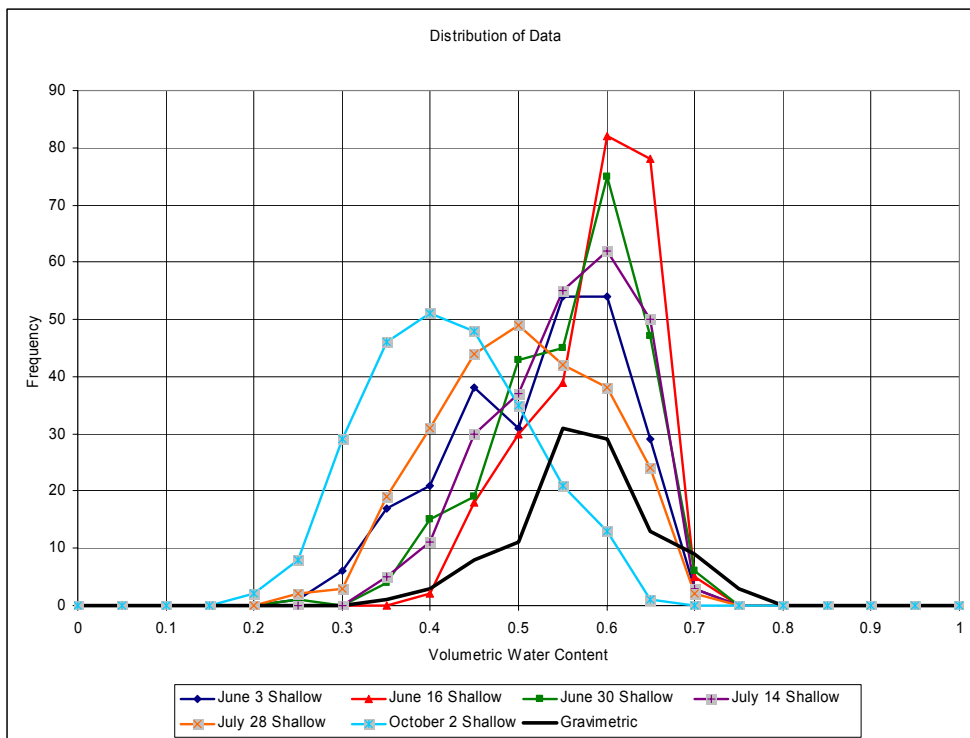
Tasks associated with laboratory calibration of a portable Theta probe used in NDW soil moisture measurements are described below. Results of these tasks were used with information provided by the probe manufacturer to achieve calibration, as described in Chapter 3.

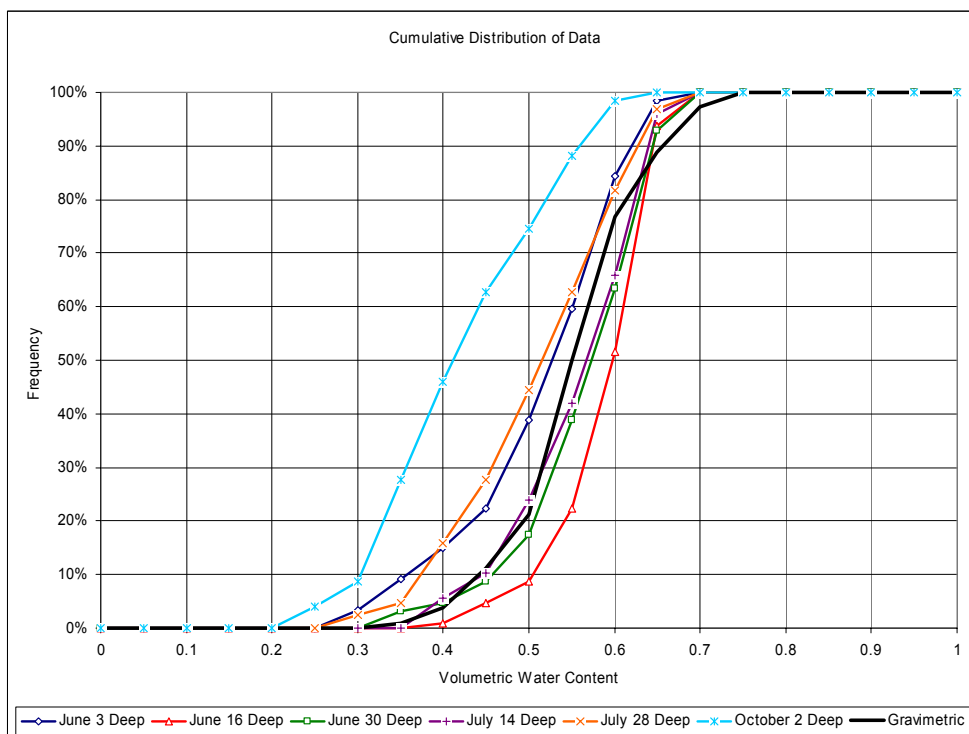
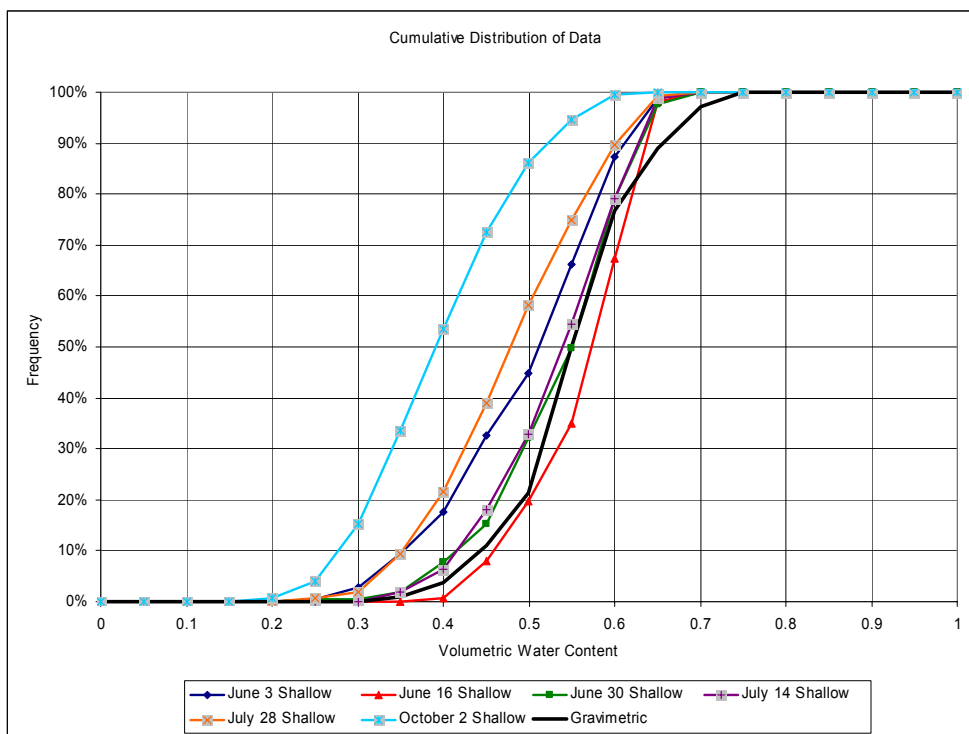
1. An approximately equal amount of soil was placed in each of fifteen 32-oz plastic cups. Individual samples had to be relatively large to accommodate full insertion of the Theta probe rods.
2. Water was gradually added to the first sample, in small volume increments to allow for infiltration. The volume of water required to approach saturation was recorded. This value was scaled down in approximately equal increments across the fifteen samples (no water was added to the final sample). Cups were numbered from wettest to driest.
3. All samples were covered to avoid excessive evaporation and allowed to equilibrate for about a day and a half.
4. Samples were compacted firmly and evenly (attempting to maintain a reasonably level soil surface) using a large pestle.
5. A thumbtack was used to mark the soil sample level in each cup.
6. Each sample (cup and soil) was weighed and recorded.
7. The Theta probe was inserted into each soil sample and a voltage reading was recorded.
8. Soil was carefully emptied from each cup into a large drying tin (disposable bread tins were used to accommodate the relatively large volume of each sample). Each tin weight was recorded prior to this.

9. Each sample (tin and soil) was weighed and recorded.
10. All samples were placed in a drying oven at 105 °C overnight.
11. Each cup was weighed. The difference between the wet soil + cup and this result gives the initial wet soil mass. This was checked against the wet soil mass obtained by subtracting the tin weight from the wet soil + tin. The average discrepancy in these results was between 2 and 3 grams, an error of approximately 0.3 to 0.4 percent given an average wet soil mass of 745 g.
12. A graduated cylinder was used to fill each cup with water to the level previously occupied by the soil sample. The volume of water added was recorded as an estimate of the soil sample volume.
13. After drying, soil samples were removed from the oven and weighed. The tin weight was subtracted from this result to arrive at dry mass of soil.
14. Volumetric water content was estimated as dry soil mass subtracted from wet soil mass, divided by sample volume and the density of water (1.0 gm/cm³). The wet soil mass as determined by subtracting tin weight from combined soil and tin weight was used.

APPENDIX F

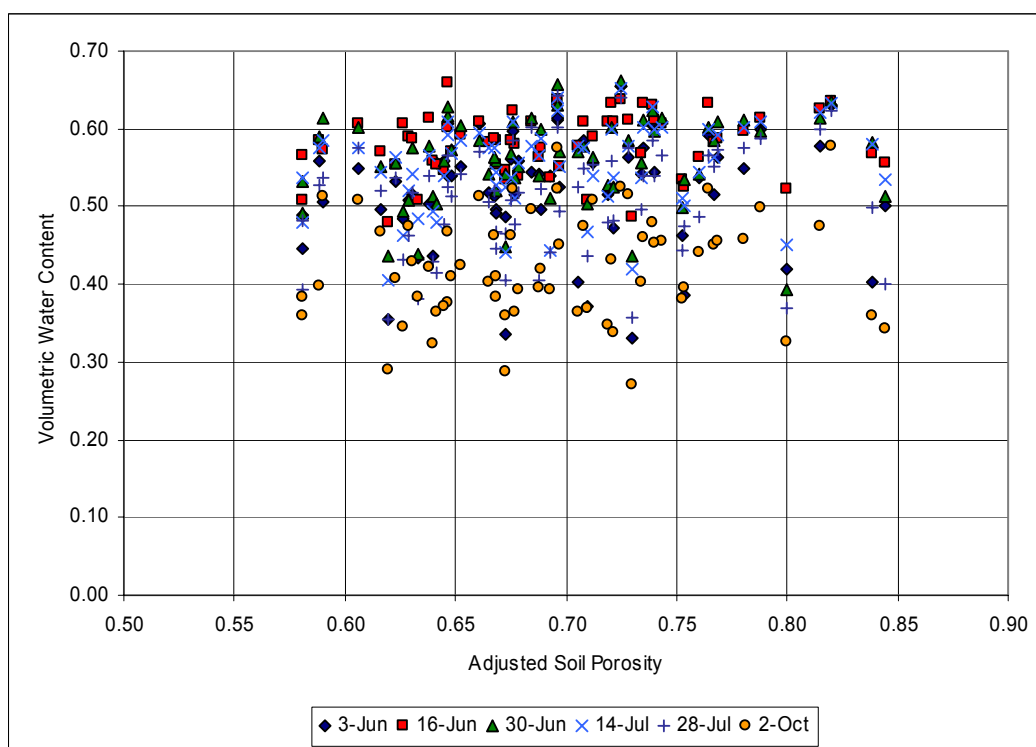
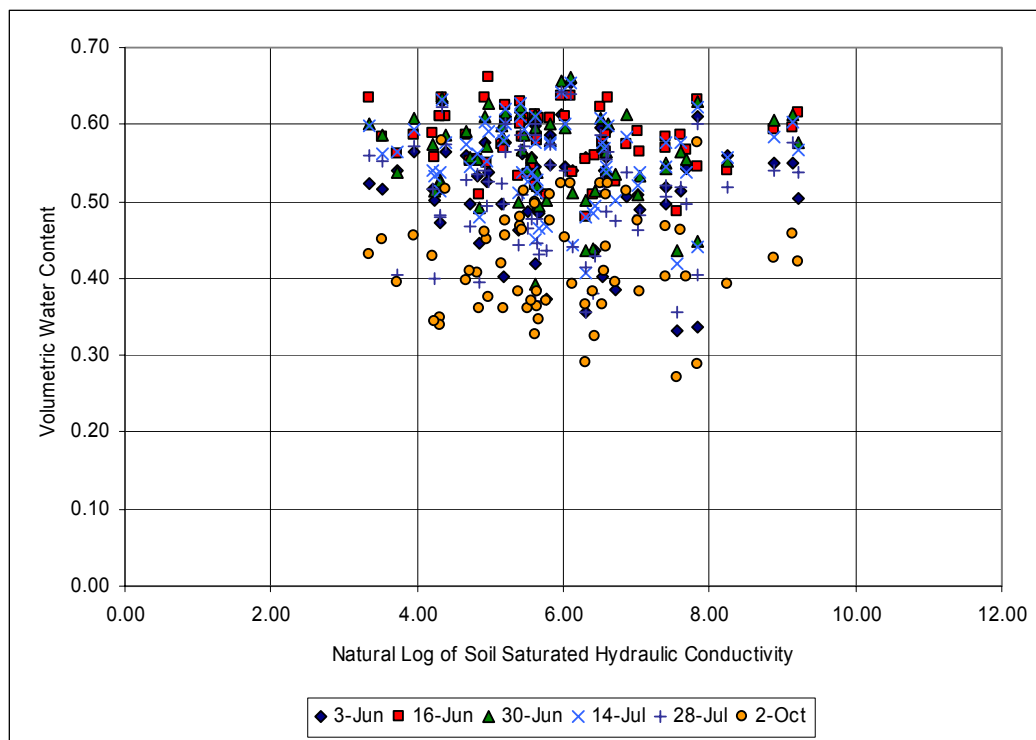
Statistical Comparison of Portable Probe, Static Probe, and
Gravimetric Measurements of Volumetric Water Content

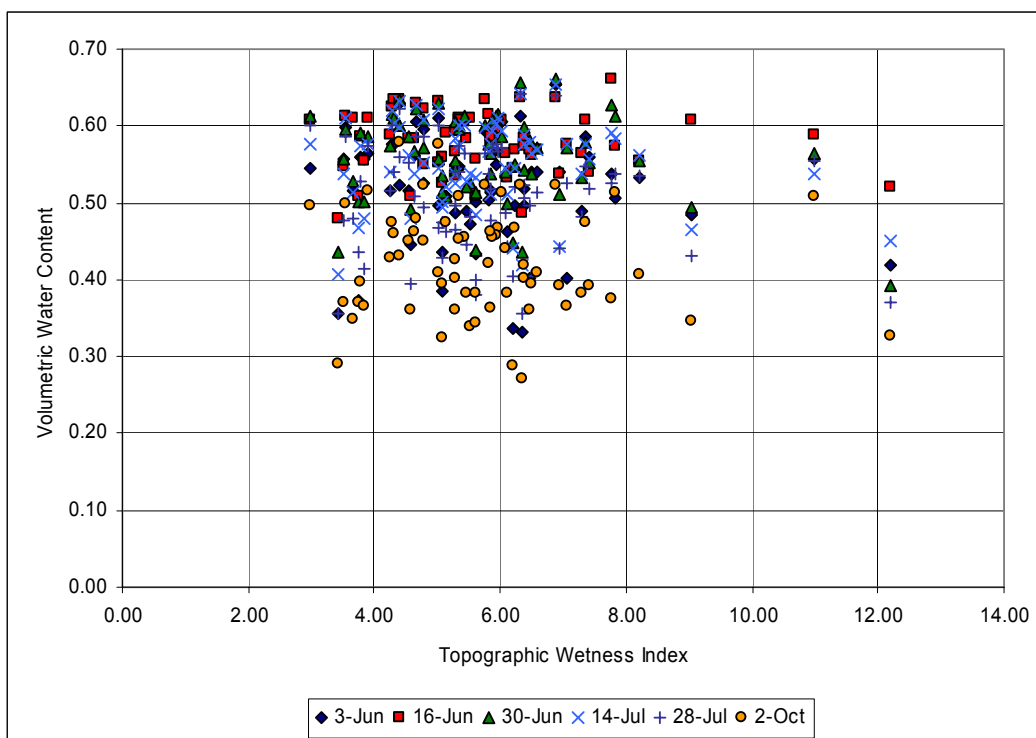
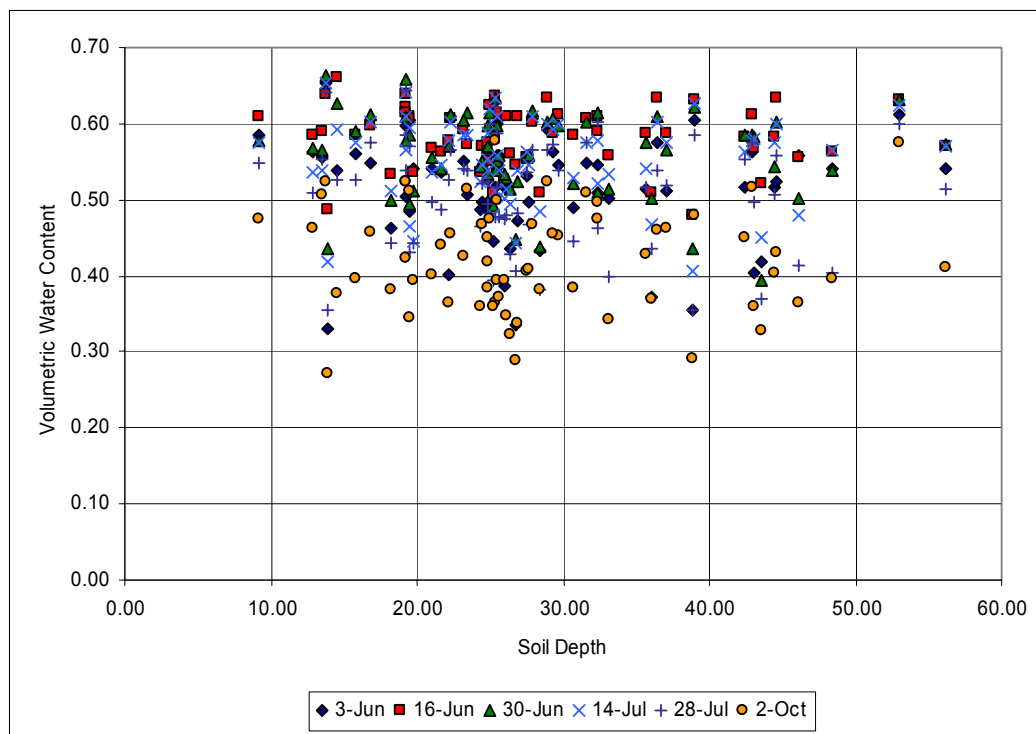




APPENDIX G

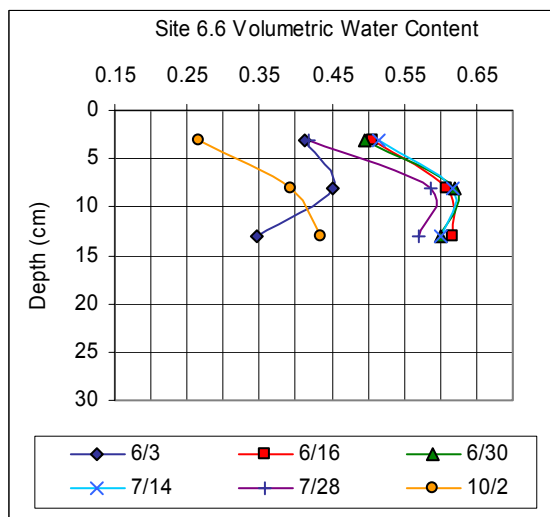
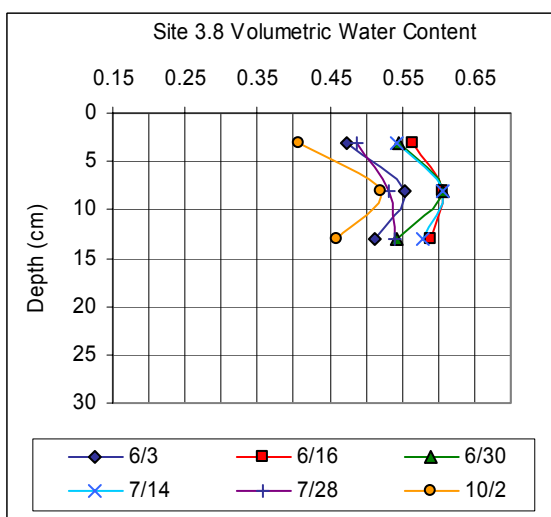
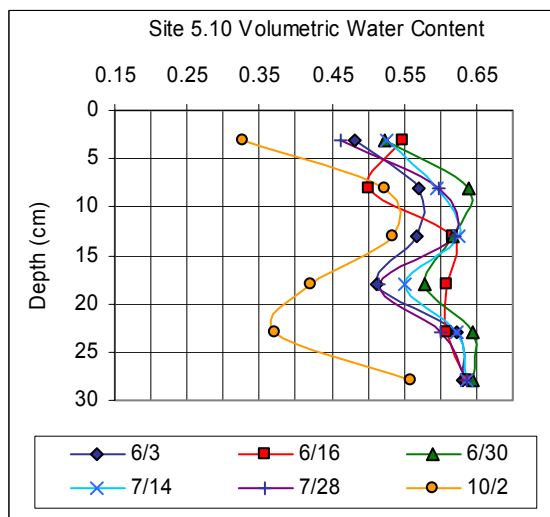
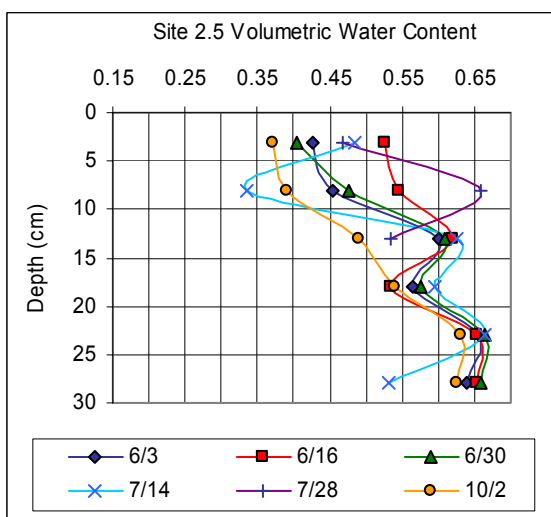
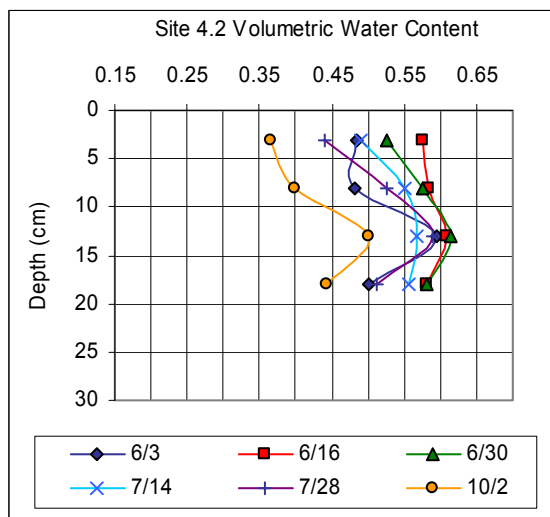
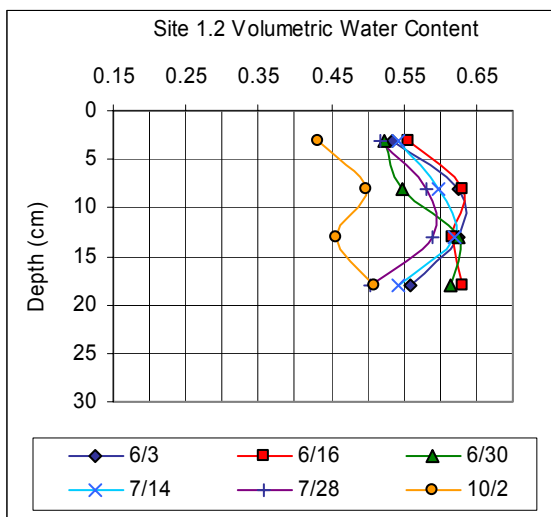
Scatter Plots of Biweekly Soil Moisture Measurements
Versus Various Soil Hydrologic Parameters

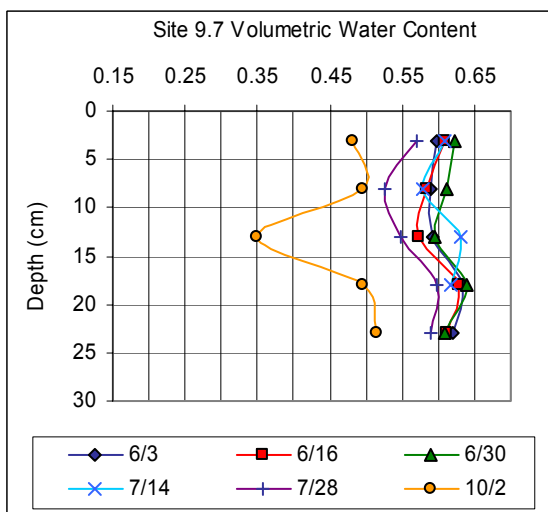
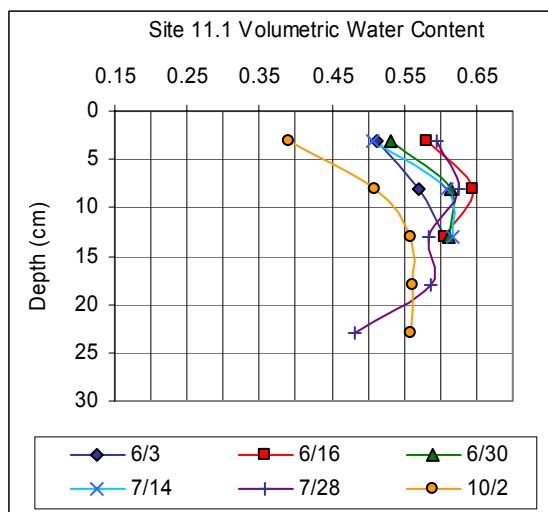
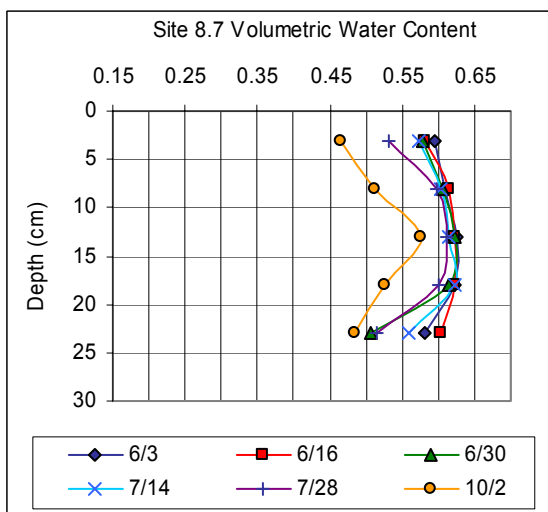
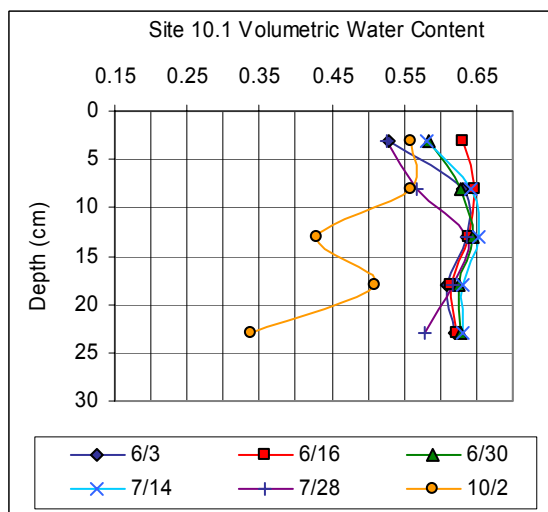
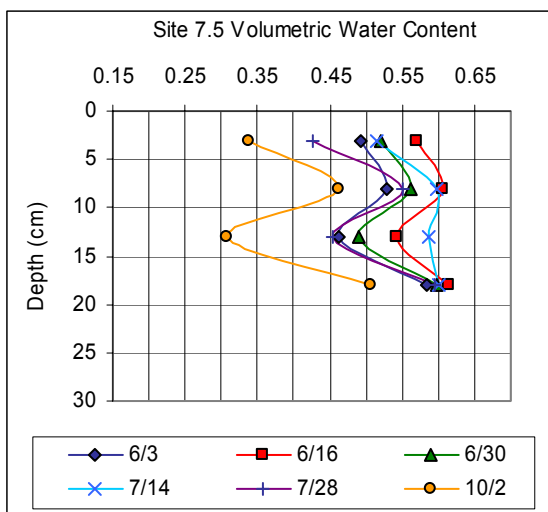




APPENDIX H

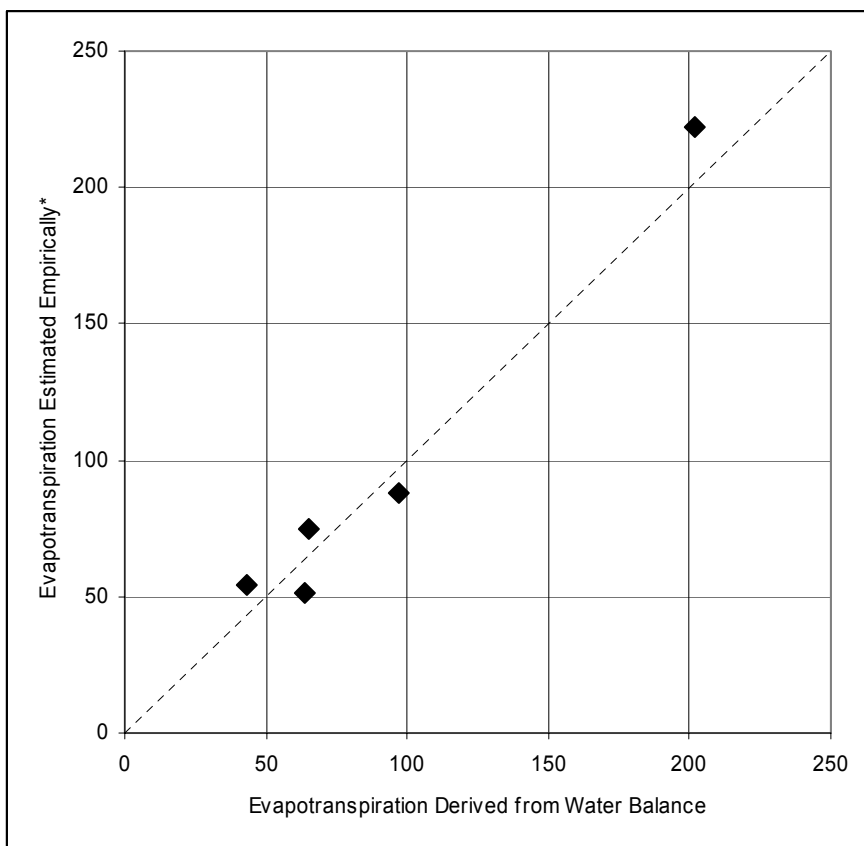
Representative Biweekly Measurement Site
Soil Moisture Profiles





APPENDIX I

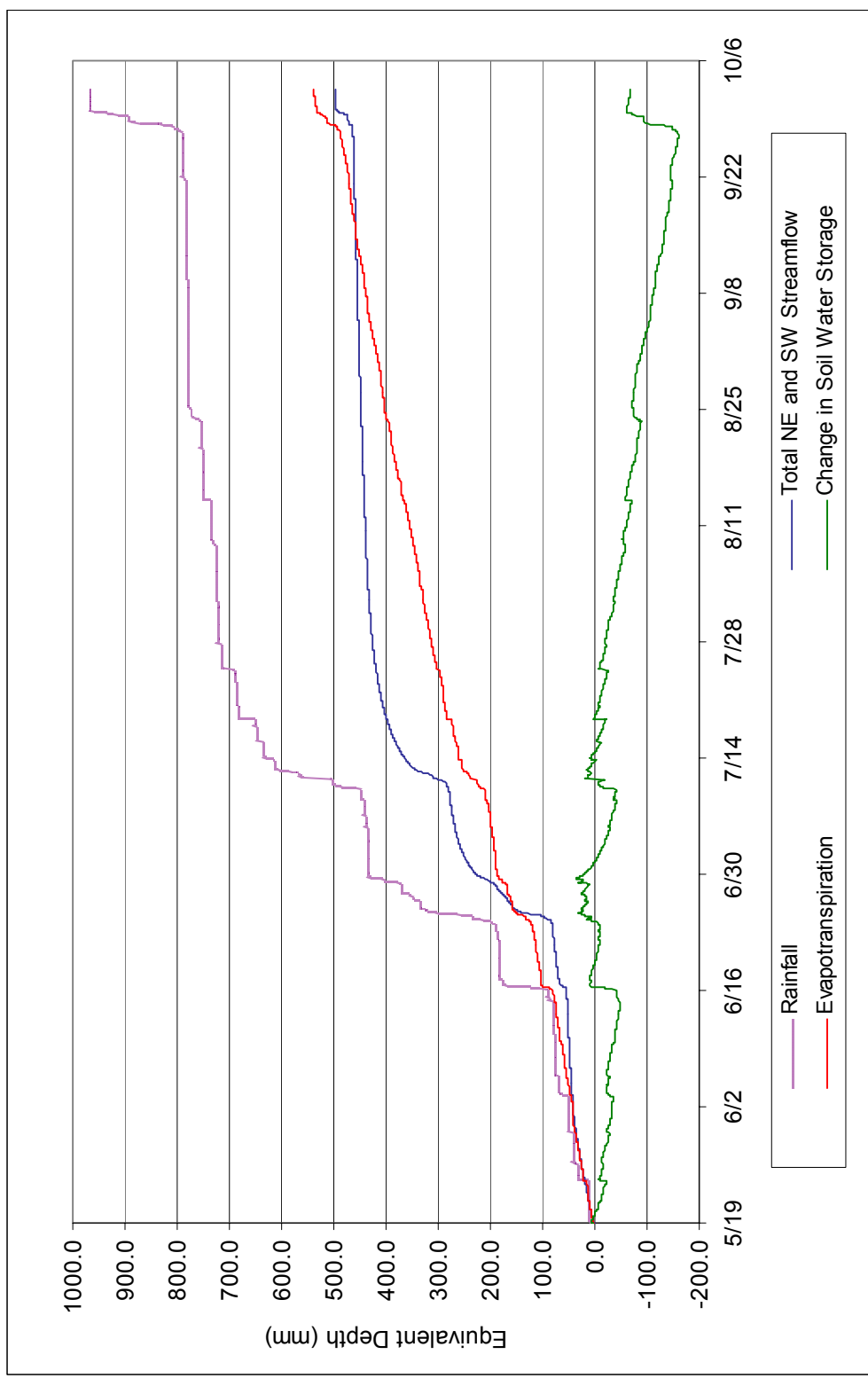
Comparison of Estimated Evapotranspiration and Evapotranspiration
Derived from NDW Water Balance



- Forest evapotranspiration estimated per Shuttleworth (1993)

APPENDIX J

Cumulative Rainfall, Streamflow, Evapotranspiration,
and Soil Water Storage Changes for the NDW
for May through October 1999*



* Measured rainfall and streamflow. Evapotranspiration estimated per Shuttleworth (1993). Change in soil water storage derived from water balance.

APPENDIX K

Streamflow Hydrographs from Selected NDW Storm Events
During the May through October 1999 Study Period

